AD-A151 580 THE IN-FLIGHT ESTIMATION AND INDICATION OF CUMULATIVE FATIGUE DAMAGE TO HELICOPTER GEARS(U) AERONAUTICAL RESEARCH LABS MELBOURNE (AUSTRALIA) K F FRASER MAR 84 1/2

UNCLASSIFIED ARL/AERO-PROP-164 F/G 13/9 NL

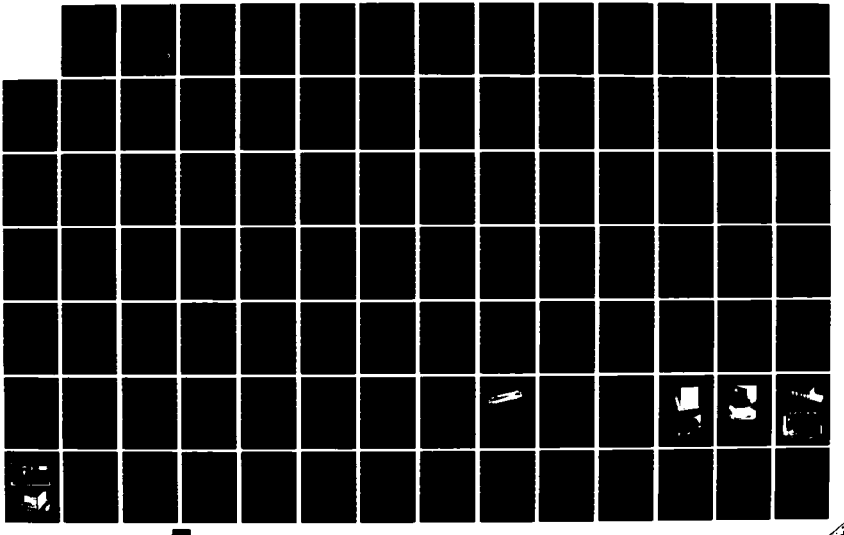

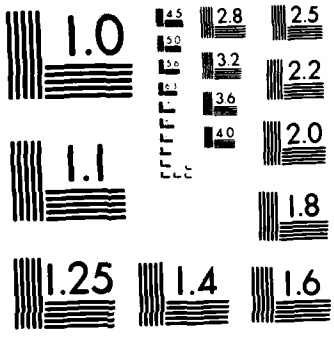

(2)

ARL-AERO-PROP-REPORT-164

AR-003-013

DEPARTMENT OF DEFENCE

DEFENCE SCIENCE AND TECHNOLOGY ORGANISATION

AERONAUTICAL RESEARCH LABORATORIES

MELBOURNE, VICTORIA

AERO PROPULSION REPORT 164

THE IN-FLIGHT ESTIMATION AND INDICATION OF CUMULATIVE FATIGUE DAMAGE TO HELICOPTER GEARS

by

K. F. Fraser.

APPROVED FOR PUBLIC RELEASE

MARCH 1984

COPY No

AR-003-013

DEPARTMENT OF DEFENCE
DEFENCE SCIENCE AND TECHNOLOGY ORGANISATION
AERONAUTICAL RESEARCH LABORATORIES

AERO PROPULSION REPORT 164

THE IN-FLIGHT ESTIMATION AND INDICATION OF CUMULATIVE FATIGUE DAMAGE TO HELICOPTER GEARS

by

K. F. Fraser.

SUMMARY

Estimates of the safe fatigue life of helicopter transmission components may be made if in-service load data together with transmission fatigue data, represented as the number of cycles to failure as a function of tooth load, are available. Instrumentation has been developed to provide in-flight estimation and indication of the proportion of safe fatigue life expended for critical gears in single or twin-engine helicopter transmission systems. In addition, basic transmission load data in the form of totalized times spent in a number of contiguous torque bands are continually updated and stored during flight. The basic load data together with values of life expenditure for critical gears for the current flight can be automatically printed out after flight. This technique opens the way towards fatigue life monitoring of individual transmissions.

The special demands of the life estimating system are evaluated and in particular the very significant effects of errors in mean torque estimation are assessed.

POSTAL ADDRESS: Director, Aeronautical Research Laboratories,
Box 4331, P.O., Melbourne, Victoria, 3001, Australia

CONTENTS

NOMENCLATURE

A_1, B_1, A_2, B_2, C_1	gear fatigue curve shape constants
f	torque readings per second
G	width of torque band
K_1, K_2	constants for hypothetical torque band spectra
N	gear endurance (used for cycles to failure and "safe" cycles)
N_i	safe cycles corresponding to torque band T_i
P	torque transmitter pressure
q	proportion of operating time torque T is exceeded
r	gear rotational speed
S	tooth root bending stress
t	elapsed time
T	torque corresponding to failure at N cycles
T_i	specified torque band
T_{EF}	highest torque for infinite life (corresponding to endurance limit)
T_{ES}	factored highest torque for infinite life
T_H	maximum torque transmitted during gear operation
u	life usage per torque reading
u_i	life usage per torque reading for torque developed in band T_i
U	fraction of safe fatigue life expended
v_i	rationalized mean amplitude of noise signal element i
W	mean rate of fatigue life usage
X	normalized amount by which torque endurance limit is exceeded
Y	analogue-to-digital converter reading
α	proportional change in indicated rate of fatigue life usage due to measurement inaccuracy
β	square wave noise amplitude factor
ε	fractional torque measurement error referred to T_{ES}
θ	instantaneous phase of alternating signal component
σ	maximum value of X achieved
τ	total operating time of gear
ω	radian frequency

1. INTRODUCTION

Components subject to high amplitude fluctuating stresses may eventually undergo fatigue failure if a sufficiently high number of load cycles is applied before the component is replaced. In the simple arrangement of two gears in mesh, each tooth will experience one load cycle per revolution of that gear. Under load, a bending stress proportional to the torque transmitted will be developed at the gear root. For any given gear tooth the number of load cycles experienced per unit time is given by the gear rotational speed. A fatigue failure is evidenced by a tooth crack or breakage. If gears are not subject to high stresses there will be no tendency for fatigue failure to occur and life will then be limited by wear considerations.

Fatigue failures of transmission components are generally referred to as High Cycle Fatigue (HCF) failures. HCF is characterized by the large number (typically greater than 10^7) of load cycles to produce failure. In contrast, components prone to Low Cycle Fatigue (LCF) failure, for example gas turbine discs, are subject to much higher stresses than those which fail due to HCF. In such cases peak stresses result in local plastic deformation of the material, with failure occurring typically after 10^3 to 10^5 load applications.

Usually the lives of certain critical gears in helicopter transmission systems are limited by fatigue considerations. Prediction of the safe life of such transmission components is of particular concern to aircraft operators as components must be replaced before failure occurs. Valid estimates of the safe life of helicopter transmission systems, apart from being vital for operational safety, are necessary for the formulation of an economic maintenance policy.

For fatigue life estimation of transmission compponents, two basic sets of data are required. Firstly, gear fatigue data in the form of the number of cycles to failure as a function of stress level (S/N curve) are required together with a suitable stress or safety factor to define a "safe" curve. Secondly, load spectra (giving proportion of flying time above various torque levels) must be available for the transmission under normal operating conditions. For helicopter transmissions computation of load cycles is simplified because gear rotational speed can be assumed to be constant.

Load spectra for a given helicopter may vary significantly according to the type of use and hence it is usually necessary for each operator to establish his own spectra.

ARL research[1,2,3] into the life of helicopter transmissions is being conducted at the request of the Royal Australian Navy (RAN) which currently operates Wessex Mk 31B and Sea King Mk 50 helicopters. The ARL work, initially on the Wessex helicopter, had its origin in a UK study in which the latest available data were used to re-estimate the safe fatigue life of the crown-wheel and pinion in the main rotor gearbox. This study yielded a safe life figure much lower than the 2500 hours previously promulgated. As the RN (Royal Navy, UK), RAF (Royal Air Force, UK) and RAN Wessex fleets had at that stage been operated well beyond the revised safe life, the figure was clearly suspect. The gear fatigue data, upon which the new estimates were based, had been obtained by the manufacturer in tests to failure of a sample of main rotor gearboxes, and was judged to be valid, at least for the specific items tested. Doubts were therefore cast on the validity of the torque spectra used. It was essential that these doubts be resolved with particular emphasis on the Australian operating environment.

Internationally very little work had been done in the area of in-flight measurement of torque loading of helicopter transmission components. As no suitable instrumentation was available to measure load history it was decided to develop it locally. First generation torque spectrum indicating equipment[4] was fitted in two Wessex helicopters in 1975. Torque data from over 700 flights were gathered and, with data on the usage of all aircraft in the fleet, were used to estimate the mean safe life. A statistical analysis[3] was developed whereby a tolerance limit on life, defined as 95% confidence that 95% of the population will exceed the stated life, was estimated for the appropriate aircraft usage pattern. As a result of this work a replacement life of 2400 hours (equal to three overhaul periods) was adopted by the airworthiness authority.

Following the successful program with Wessex a similar program was initiated for Sea King. Second generation torque spectrum indicating equipment[5] was fitted in a Sea King helicopter in 1978. The indicating equipment was similar to that fitted in Wessex but included improved circuits and changes necessary to meet the demands of the twin-engine Sea King.

Application of microcomputing technology has made it feasible to incorporate the gear fatigue data in read-only-memory programs and to estimate and indicate fatigue life expenditure of gears during flight. Third generation equipment exploits the new technology to estimate and indicate expenditure for up to four gears in the main rotor gear box for the Sea King helicopter. In addition basic load data are stored during flight and automatically printed out after flight. The basic load data can be used with the aid of a ground based computer to predict the safe fatigue life of each gear in operating hours.

Currently accepted aircraft maintenance practice involves replacement of fatigue-critical gears after estimated life is expended. The development, described in this report leads the way towards fatigue life monitoring of individual transmissions and replacement according to indicated life usage.

2. ESTIMATION OF FATIGUE LIFE OF TRANSMISSION COMPONENTS

Three main variables influence the fatigue life of a component:

(i) Component geometry.

(ii) Properties of the component material or materials.

(iii) Level and nature of the service loads.

The effects of the first two may be described by a suitable curve (Section 2.1) and the information for (iii) must be obtained from in-service load measurements (Section 2.2).

2.1 Analytical Representation of Gear Fatigue Data

A "safe" S–N curve for the transmission component of interest must be established before any estimates of safe fatigue life can be considered. Usually it is more convenient to consider torque (T) in lieu of stress (S) as the tooth root bending stress is proportional to applied torque and the T–N curve includes component geometry effects. Initially the standard T–N curve, defining mean cycles to failure at various torque levels, must be established by testing a sufficient number of gears to failure. By applying a suitable scatter factor to the standard relationship a "safe" T–N relationship can be formulated.

Tests were performed by the manufacturer (Westland Helicopters Limited) on a small sample of main rotor gear boxes (MRGB's) for the Wessex[6,7] and Sea King[8] transmission systems respectively. Insufficient gear tests were performed in these instances to establish the shape of the T–N curve but previous tests[9] on a sample of 47 Wessex Tail Rotor Gearbox bevel gears at various steady load levels in a closed circuit gear testing rig were used to establish a mean failure curve for the tail gears. A similar curve shape was assumed to apply for Wessex and Sea King MRGB components as these gears were of similar gemoetry, material and underwent similar heat treatment to the Wessex tail rotor gears.

Failures for the Wessex tail rotor gears occurred in the endurance range 5×10^4 to 2×10^7 cycles. Tests were performed at constant gear rotational speed and hence both torque and tooth root bending stress were proportional to power transmitted. Results of these tests are reproduced in Fig. 1. The shape of the failure curve in this case was established by the manufacturer by drawing a best-fit curve through the medians of the logarithms of the endurances at each test torque level. The curve was given the mathematical form:

$$T \quad T_{LL}(1 + A_1 N^{-1/B_1}) \tag{1}$$

Values of A_1 and B_1, and a nominal value for T_{LL} were computed using three points on this best-fit curve. Estimated values for parameters A and B, 48·9 and 2·58 respectively, are used in this report. Using experimental values of transmitted power (proportional to torque T assuming constant rotational speed) and N corresponding to each of the 47 failures, and the values of A_1 and B_1 estimated as above, the mean and standard deviation of the computed T_{LL} values

were established. A coefficient of variation (ratio of standard deviation to mean) of 0·068 resulted. The distribution of T_{EF} was only moderately skewed and, within the restraints of the limited number of test points, approximated the normal distribution (a χ^2 test applied to the test data shows that at 95% confidence level the data are consistent with the hypothesis that they conform to a Normal distribution). Values of T_{EF} for critical Sea King gears were estimated from a smaller number of failure tests in a similar manner to that used for the Wessex tail rotor gears.

Westlands[9] state "It has been suggested by many sources that a value three standard deviations below the mean provides a safe estimate of the extremes of scatter". A "safe" working relationship may be derived by applying such a factor to the computed mean endurance limit. Analytically the safe curve may be expressed as

$$T = T_{ES}(1 + A_1 N^{-1/B_1}) \tag{2}$$

The three-standard-derivation safe curve illustrated in Fig. 1 represents a stress or safety factor (T_{EF}/T_{ES}) of about 1·25. At this value of scatter factor the probability of premature gear failure occurring is approximately one in 1000 (as predicted by the Normal distribution).

The endurance relationship may be expressed in normalized form as

$$X = \frac{T}{T_{ES}} - 1 = A_1 N^{-1/B_1} \tag{3}$$

where

A_1 is a constant of value 48·9

and

B_1 is a constant of value 2·5846

$$\left(\frac{1}{B_1} = 0{\cdot}3869\right)$$

From equation 3 the endurance N may be expressed explicitly

$$N = \left(\frac{A_1}{X}\right)^{B_1} \tag{4}$$

This normalized relationship, upon which the safe life estimations for Wessex and Sea King MRGB components are based, is plotted in Curve 1 of Fig. 2. For convenience the N axis has been made logarithmic.

From tests[7] to failure of five crownwheels in the Wessex MRGB, an unfactored endurance limit of 41677 lb. in. was established by Westlands. A scatter factor of 1·3 was then applied to establish the safe curve for the Wessex MRGB studies.

However Westlands used a slightly modified curve as indicated in Curve 2 of Fig. 2 in their studies on the Wessex MRGB. This latter curve, which is based on Curve 1, exhibits an endurance limit at the value of load (or of X) which yields a life of 10^8 cycles for Curve 1. For Curve 2 the endurance limit specified in this manner is considered to apply beyond 2×10^7 cycles (hence the portion of Curve 2 parallel with the X axis extending from $N = 2 \times 10^7$ cycles to ∞ and passing through Curve 1 at N 10^8 cycles). A line drawn from the 2×10^7 cycles point to meet Curve 1 tangentially provides the next segment of Curve 2. The two curves meet at a value for N of about 3×10^6 cycles. For applied loads greater than that corresponding to a life of 3×10^6 cycles, Curve 2 is made to coincide with Curve 1.

Analytically the relationship of Curve 2 can be expressed:

$$X \quad A_2 \quad B_2 \ln N \tag{5}$$

$$N \quad e^{(A_2 \quad X)/B_2} \tag{6}$$

in the range $2{\cdot}9145 \times 10^6 \geq N \geq 2 \times 10^7$ or $0{\cdot}1542 \geq X \geq 0{\cdot}0393$, where A_2 is a constant of value 1·04246 and B_2 is a constant of value 0·05967.

For $A < 0{\cdot}0393$ N is considered to be infinite.

Some of the normalized torque values applicable for selected values of N are compared in the following table.

N	A	
	Curve 1	Curve 2
1×10^8	0·0393*[1]	0·0393
2×10^7	0·0732	0·0393*[1]
1×10^7	0·0957	0·0807
$2{\cdot}9145 \times 10^6$	0·1542	0·1542
1×10^6	0·2333	0·2333
3×10^5	0·3717	0·3717
1×10^5	0·5686	·05686

*[2]

*[1] These are made equal as indicated above.

*[2] Curve 2 is made coincident with Curve 1.

For the range $0{\cdot}039 < A < 0{\cdot}154$ Curve 2 predicts more life usage than Curve 1 and thus Curve 2 is more conservative in that range. *However Curve 1 does predict some fatigue life usage* for $0 < A < 0{\cdot}039$, whereas Curve 2 predicts no usage in that range. While conservative within the above range, Curve 2 represents a relationship that no physical system could obey by virtue of the abrupt change from infinite to finite life that the relationship implies for an infinitesimal change in torque loading.

From the data derived from life substantiation tests[8] carried out on Sea King MRGB gears, the values of endurance limit applicable to all critical gears were computed. In cases where no failures occurred in tests involving at least three gears a "safe" endurance limit was obtained by applying a scatter factor of 1·24 to the test torque. In tests where failures occurred a scatter factor of 1·30 was applied if results for four or more gears were available. Specific details on the endurance limits used for computations on the safe lives of critical gears are given in Section 4.3.

The safe life curves of Fig. 2 have been adopted initially for use in life studies on transmission components in Sea King helicopters operated by the RAN.

2.2 Fatigue Life Usage Estimation

From the gear fatigue data discussed in Section 2.1 it can be assumed that the relationship between torque load T and safe cycles at that torque is known. At this point it is worth defining a life usage term L which indicates the current proportion of total fatigue life used. Consider the torque range to be divided into a number of narrow bands of mean torque value $T_1, T_2, \ldots$ etc. If the gear is subject to n_1 cycles within the T_1 band, n_2 cycles within the T_2 band etc., then it is common practice to apply Miner's summation law[10] to quantify the cumulative damage.

$$L = \frac{n_1}{N_1} + \frac{n_2}{N_2} + \cdots + \frac{n_k}{N_k}$$

$$L = \sum_{i=1}^{k} \frac{n_i}{N_i} \qquad (7)$$

where N_i represents the safe life cycles corresponding to torque band T_i.

When $U = 1$ or any other selected value safe life is considered to be totally expended. Westlands[11] have summed the life fraction to 0·75 rather than 1·00 "to allow for the known uncertainty of the cumulative damage hypothesis. It has been found that the damage sum is about 1·0 under fully random loading conditions but greater and lower values have been obtained with sequential loading tests, depending on the sequence. However the loading of many helicopter components may be considered to be nearly random and this value represents a justifiable conservation".

Alternative gearbox maintenance policies, with quite distinct measurement and computation demands, can be adopted for gears subject to high cycle fatigue damage:

(i) Replace critical gears at the completion of a specified number of operating hours.

(ii) Replace critical gears when the indicated safe lives for the particular gears have been expended.

2.2.1 Fixed Interval Replacement—Estimation of Safe Replacement Interval

It is current practice to replace fatigue-critical helicopter transmission components within a specified number of operating hours based on safe fatigue life estimations. To establish the safe replacement interval it is first necessary to determine the applicable torque load spectrum (a graph indicating the proportion of total flying time spent above specified torque levels). If a statistical pattern emerges so that there is a correlation between sortie type and life expenditure, then by measuring torque loads for a small sample of aircraft the load spectra and fatigue damage which apply for the various types of sortie can be established. In such cases statistical methods can be used to estimate the safe replacement interval for all critical gears. If most fatigue damage arises during transient over-torquing incidents which cannot be correlated with sortie types the above approach is unsatisfactory. In such instances it is not unusual for gearboxes to be overhauled as a result of a single over-torquing event, particularly if considerable fatigue damage is possible.

For illustration purposes a hypothetical torque spectrum graph for Sea King total torque (Section 4.2) is drawn in Fig. 3. Only the shaded portion of the graph for which the torque is above the "safe" endurance limit is relevant for fatigue life usage computations.

One way to establish the shape of the torque spectrum curve would be to continuously record torque (on magnetic tape for instance) during flight and subsequently totalize times spent above specified torque levels at the ground station data reduction facility. Such a method would result in the need to handle large quantities of basic data and its adoption was not considered to be justified.

Indicating equipment (Section 5) developed at these laboratories and installed in two Sea King helicopters totalizes the time spent in each of 10 contiguous torque bands and prints the totals after each flight. To establish the shape of the torque spectrum curve (Fig. 3) it is essential that torque be measured in bands below the endurance limit as well as above it. Because the high torque loads only are relevant for fatigue life usage considerations, the bands have been made narrower at the high torque end of the spectrum. Bands chosen for Sea King MRGB torque measurement are indicated in Fig. 3.

To compute fatigue life usage a finer resolution of torque is required than that represented by the 10 torque bands (for which there is generally virtually no contribution from the upper two bands). A computer program[3] has been developed to interpolate at 1% rated torque intervals between the broadly separated data points illustrated in Fig. 3.

Define q (Fig. 3) as the proportion of time for which torque exceeds value T. The proportion of the time for which torque has value between T and $T + \Delta T$ is Δq (see inset of Fig. 3).

At torque T the rate of life usage is given by $r\,N$ where r is gear rotational speed and N is the safe cycles at torque T.

The fatigue life usage ΔU which results due to torque developed in the range T to $T+\Delta T$ is given by

$$\Delta U = \tau r \frac{\Delta q}{N}$$

where τ is total operating time for the gear and N is the mean "safe" cycles within the torque interval.

By summing contributions to fatigue life usage resulting from torque in excess of the endurance value T_{ES} the current value of life fraction used U can be computed.

$$U = \tau r \sum_{T=T_{ES}}^{\infty} \frac{\Delta q}{N} \tag{8}$$

The above summation can be performed numerically by adding contributions for specified torque increments (say 1% rated torque) above the endurance limit. Such a method was used in the prediction of the safe life of Wessex gears. If q is known analytically as a function of torque T the above summation may be expressed more conveniently by the following integral.

$$U = \tau r \int_{T_{ES}}^{\infty} \frac{1}{N}\left(-\frac{dq}{dT}\right) dT \tag{9}$$

The "$-$" sign ahead of dq/dT is necessary since dq/dT is always negative (or zero).

The safe replacement interval τ_R is the value of τ for $U = 1$ (or any other nominated value such as 0·75 used by Westlands). For replacement at $U = 1$,

$$\tau_R = \frac{1}{r \sum_{T=T_{ES}}^{\infty} \frac{\Delta q}{N}} \tag{10}$$

$$= \frac{1}{r \int_{T_{ES}}^{\infty} \frac{1}{N}\left(-\frac{dq}{dT}\right) dT} \tag{11}$$

2.2.2 On-Condition Replacement—Indication of Safe Life Expended in Individual Transmissions

With the ever increasing cost of ownership there is a growing impetus in the aircraft industry to look towards a maintenance policy which involves on-condition replacement of critical components. Replacement of a transmission component subject to high cycle fatigue damage when the indicated safe life for that component has been expended can be considered loosely as an "on-condition" replacement although there is, of course, no observable change in the component behaviour. Torque load data can be handled in various ways to make possible a maintenance policy for which fatigue life usage of individual transmissions is monitored:

(i) Torque spectrum indicators can be fitted in each helicopter in the fleet and a subsequent ground station computer analysis along the lines indicated in Section 2.2.1 can be used to estimate the current value of life usage U for the particular transmission components of interest.

(ii) An on-board computing system in each aircraft can be used for in-flight storage of the total time spent in various torque bands above the endurance limit and at the termination of the flight the fatigue life usage for that flight can be computed. To eliminate the need for complex curve fitting techniques required in the ground station analysis the torque bands can be made quite narrow (say 1 % rated torque or less). If an electromechanical counter readout of the current value of fatigue life usage is required, this method has significant limitations as all the counters would have to be updated at the end of the flight. Alternatively a printer or other device can be used to output the fatigue life usage incurred for critical transmission components during the current flight.

(iii) An on-board computer in each aircraft can be used to estimate fatigue life usage during flight and provide real-time indication of usage, with an electromechanical counter readout for instance. A life increment computation can be performed at the data sampling frequency. Complex curve fitting techniques required in (i) are not needed.

Approach (i) requires a maximum of airborne instrumentation and a maximum of ground station support when compared with approaches (ii) or (iii). Approach (ii) can provide faster in-flight data handling than (iii) but it requires significantly more data to be stored during flight than approach (iii). Approach (iii) represents the simplest and most desirable solution. Adequate dynamic response has been demonstrated for this approach so it has been used in the Fatigue Life Usage Indicator (Section 5) for Sea King.

Computation requirements for approach (iii, will now be considered in general analytical terms. Assume that the incremental fatigue life usage u is to be computed each time the relevant transmission component torque T is measured.

$$u = \frac{s}{fN} \tag{12}$$

where

s is gear rotational speed,
f is number of torque readings taken per unit time (sampling frequency),

and

N is the "safe" cycles at torque T.

For values of torque below the endurance limit N has infinite value and hence u is zero. The current value of fatigue life usage U is given by

$$U = \sum_{r=1}^{n} u_r \tag{13}$$

where

r is a sample number suffix which has initial value 1 for a new gear with zero value of fatigue life usage,

and

n is the current sample number.

When U 1 (or other specified value) full life is considered to be expended. To take account of significant variations in indicated life usage which could occur due to measurement errors (Section 3) the value of U for which full life is considered to be expended can be suitably down rated. However the individual gearbox indicated-life replacement scheme should yield greater average lives for fatigue-critical gears than the fixed-interval scheme since, to be conservative, the latter must be based on extreme rather than typical load excursions. The use of an individual gearbox indicated-life replacement scheme could allow the fatigue lives of critical gears to be increased to such an extent that other factors such as wear effectively limit the component life.

In situations where significant fatigue damage is likely to occur during transient overtorquing excursions the individual transmission monitoring scheme would be most appropriate. Without such monitoring there is currently no acceptable way of assessing fatigue damage under such circumstances and hence gear replacement is sometimes undertaken.

To take into account the effects of finite resolution of the measuring system some refinements to the relationship expressed in equation 12 of this section are necessary. These refinements are considered in detail in Section 3.3.

3. GENERAL CONSIDERATIONS APPLYING TO TORQUE LOAD MEASUREMENT FOR FATIGUE LIFE ESTIMATION

There is a number of considerations applicable to any helicopter transmission system for which there is a need to measure in-service loads for fatigue life studies on critical components. Of particular significance is the overall measurement precision as the indicated rate of fatigue life usage can be significantly modified by measurement inaccuracies. Some aspects of the torque load measurement which have significant bearing on the estimated rate of fatigue life usage are considered in the following sections.

3.1 Effect of Absolute Measurement Inaccuracy on Indicated Rate of Fatigue Life Usage

The rate of fatigue life usage increases non-linearly as a function of applied torque in excess of the endurance limit. In Fig. 4 the life usage per stress cycle (equal to the reciprocal of N) is plotted on a linear scale as a function of applied torque for the Curve 1 and Curve 2 relationships (Section 2.1). Multiplying the life usage per stress cycle by gear rotational speed yields the instantaneous rate of fatigue life usage. It is of interest to examine the amount by which the measured rate of fatigue life usage (henceforth to be called the "indicated" rate of fatigue life usage) is changed due to absolute or mean torque measurement inaccuracies. A simple relationship does not apply as the difference in rate will be a function of the torque load spectrum applicable to the helicopter transmission system. However the order of the difference to be expected can be appreciated by assessing the differences which apply when some very simple torque spectra are used as test examples.

To perform the required assessment the safe cycles versus torque relationships represented by Curve 1 and Curve 2 (Fig. 2) or equations 4 and 6 (Section 2.1) will be considered. The relationships may be rewritten:

Curve 1:

$$\frac{1}{N} = \left(\frac{X}{A_1}\right)^{B_1} \tag{14}$$

for $X \geqslant 0$.

Curve 2:

$$\frac{1}{N} = e^{(X - A_2)/B_2} = c_1 e^{X/B_2} \tag{15}$$

in the range $0{\cdot}1542 \geqslant X \geqslant 0{\cdot}0393$ and corresponds with Curve 1 for $X \geqslant 0{\cdot}1542$. c_1 is a constant of value $2{\cdot}5879 \times 10^{-8}$.

Two simple torque spectra (Fig. 5) which can be readily represented analytically will be considered. For the first spectrum the time spent in equal width torque bands within the torque range extending from just below the endurance limit T_{ES} to a value $(1+\sigma)\ T_{ES}$ is the same for all bands. For the second spectrum the time spent in equal width torque bands within the torque range extending from just below the endurance limit T_{ES} to a value $(1+\sigma)\ T_{ES}$ decreases linearly to zero at the high torque limit.

If T_H represents the maximum torque transmitted during aircraft operation then

$$T_H = (1+\sigma)\, T_{ES}$$

and

$$\sigma = \frac{T_H}{T_{ES}} - 1$$

i.e. σ is the maximum value of X achieved.

Analytically the hypothetical spectra defined above can be represented by the relationships given below.

Spectrum 1:

$$\frac{dq}{dX} = -K_1 \tag{16}$$

where

X represents the normalized amount by which the endurance limit is exceeded (Section 2.1),

q is the proportion of time for which the normalized torque exceeds the specified value X (Section 2.2.1)

and

K_1 is a constant.

Spectrum 2:

$$\frac{dq}{dX} = -\frac{K_2}{\sigma}(\sigma - X) \tag{17}$$

where

dq/dX has zero value at $X = \sigma$ and has value $-K_2$ at $X = 0$.

Note that by definition $0 < X < \sigma$ for the torque range of interest.

From equation 9 the mean rate of fatigue life usage W may be written:

$$W = \frac{U}{\tau}$$

$$= r \int_{T_{ES}}^{\infty} \frac{1}{N}\left(-\frac{dq}{dT}\right) dT$$

$$W_{X_H} = r \int_{X_L}^{X_H} \frac{1}{N}\left(-\frac{dq}{dX}\right) dX \tag{18}$$

where X_L and X_H represent the true bounds of the integration.

For Curve 1 $X_L = 0$ and for Curve 2 $X_L = 0{\cdot}0393$ (Section 2.1). For both torque spectra considered (equations 16 and 17) the maximum torque corresponds to $X_H = \sigma$. Thus

$$W_\sigma \quad r \int_{X_L}^{\sigma} \frac{1}{N}\left(-\frac{dq}{dX}\right) dX \tag{19}$$

If true torque T is read as $T + \varepsilon\, T_{ES}$ where ε represents the fractional measurement error referred to the endurance limit T_{ES} then the maximum torque will appear to shift from $T = (1+\sigma)T_{ES}$ to $T = (1+\sigma+\varepsilon)T_{ES}$ or from $X = \sigma$ to $X = \sigma + \varepsilon$.

The proportional change α in the indicated rate of fatigue life usage due to absolute measurement inaccuracy is given by

$$\alpha = \frac{W_{\sigma+\varepsilon} - W_\sigma}{W_\sigma} = \frac{W_{\sigma+\varepsilon}}{W_\sigma} - 1 \tag{20}$$

Using the relationships presented above, expressions for the proportional change α in the indicated rate of fatigue life usage due to absolute torque measurement error ε have been derived in Appendix 1 for Curve 1 and Curve 2 relationships (equations 14 and 15) and for both torque spectra (equations 16 and 17) considered.

As indicated earlier the Curve 2 relationship of equation 15 applies only in the range $0{\cdot}1542 > X > 0{\cdot}0393$. At the value $X = 0{\cdot}1542$, represented more generally in Appendix 1 by the symbol X_M, Curve 2 meets Curve 1 tangentially and follows the Curve 1 relationship thereafter. To take account of the abrupt change in the analytical expressions required to define Curve 2 as the X_M value is passed it is necessary to define α separately for normalized maximum torque below and above X_M respectively.

The various expressions derived for α in Appendix 1 are summarized below.

Curve 1: Torque Spectrum 1

$$\alpha = \left(1 + \frac{\varepsilon}{\sigma}\right)^{B_1+1} - 1 \tag{21}$$

Curve 1: Torque Spectrum 2

$$\alpha = \left(1 + \frac{\varepsilon}{\sigma}\right)^{B_1+2} - 1 \tag{22}$$

Curve 2: Torque Spectrum 1

For $\sigma \leqslant X_M$ and $(\sigma+\varepsilon) \leqslant X_M$

$$\alpha = \frac{e^{(\sigma+\varepsilon-X_L)/B_2} - 1}{e^{(\sigma-X_L)/B_2} - 1} - 1 \tag{23}$$

For $\sigma \geqslant X_M$ and $(\sigma+\varepsilon) \geqslant X_M$

$$\alpha = \frac{(\sigma+\varepsilon)^{B_1+1} + L_3}{\sigma^{B_1+1} + L_3} - 1 \tag{24}$$

where

$$L_3 = X_M^{B_1+1}\left\{\frac{B_2(B_1+1)}{X_M}\left(1 - e^{-(X_M-X_L)/B_2}\right) - 1\right\} \tag{25}$$

When the value of σ is in the immediate vicinity of X_M neither equation 23 nor 24 applies, but α can be calculated using equations A16 and A17 derived in Appendix 1.

Curve 2: Torque Spectrum 2

For $\sigma \leqslant X_M$ and $(\sigma+\varepsilon) \leqslant X_M$

$$\alpha = \frac{e^{(\sigma+\varepsilon-X_L)/B_2} - \left(1 + \dfrac{\sigma+\varepsilon-X_L}{B_2}\right)}{e^{(\sigma-X_L)/B_2} - \left(1 + \dfrac{\sigma-X_L}{B_2}\right)} - 1 \tag{26}$$

For $\sigma \geqslant X_M$ and $(\sigma+\varepsilon) \geqslant X_M$

$$\alpha = \frac{\left(\frac{\sigma+\varepsilon}{X_M}\right)^{B_1+2} + L_6\left(\frac{\sigma+\varepsilon}{X_M}\right) - L_7}{\left(\frac{\sigma}{X_M}\right)^{B_1+2} + L_6\left(\frac{\sigma}{X_M}\right) - L_7} - 1 \tag{27}$$

where

$$L_6 = \left(B_1+2\right)\left\{\frac{B_2(B_1+1)}{X_M}\left[1-e^{-(X_M-X_L)/B_2}\right]-1\right\} \tag{28}$$

and

$$L_7 = \left(B_1+1\right)\left\{\frac{B_2{}^2(B_1+2)}{X_M{}^2}\left[\left(1-\frac{X_L}{B_2}\right)e^{-(X_M-X_L)/B_2} + \frac{X_M}{B_2}-1\right]-1\right\} \tag{29}$$

When the value of σ is in the immediate vicinity of X_M neither equation 27 nor 28 applies, but α can be calculated using equations A28 and A29 derived in Appendix 1.

The change α in the indicated rate of fatigue life usage due to absolute measurement inaccuracy, as given by equations 21, 22, 23, 24, 26 and 27, has been expressed numerically in Tables 1 and 2 for various values of σ in the range $0 < \sigma < 0{\cdot}3$ and for ε having values $+0{\cdot}01$, $-0{\cdot}01$, $+0{\cdot}02$ and $-0{\cdot}02$. Numerical values for constants L_1 to L_7 (Appendix 1) have been calculated and are given in Table 2. The α relationships have been presented graphically in Figs 6 and 7.

The graphs serve to indicate that small errors in torque measurement result in very significant changes in the indicated rate of fatigue life usage. In all cases the resultant changes are very high for low values of σ. For any given gear train subject to high torque loading the normalized endurance limit will be lowest for the most critical gear and hence that gear will have the highest value of σ. In practical terms this means that variations in indicated rate of fatigue life usage resulting from absolute torque measurement inaccuracies will be lowest for the most critical gears which have the shortest fatigue life.

The graphs of Figs 6 and 7 indicate that the change α in the indicated rate of fatigue life usage due to torque measurement inaccuracy is very nearly the same for the Curve 1 and Curve 2 relationships at high values of maximum torque ($\sigma > 0{\cdot}2$). At intermediate values of maximum torque ($0{\cdot}05 < \sigma < 0{\cdot}2$) the magnitude of the differences between the two Curves tends to be higher but the differences are not always in the same sense (sometimes Curve 1 yields a higher value for α than Curve 2 and sometimes the opposite occurs). At very low values of maximum torque ($\sigma < 0{\cdot}05$) the errors for Curve 2 are definitely higher than for Curve 1 (refer to Tables 1 and 2).

The changes in the indicated rate of fatigue life usage due to torque measurement inaccuracy are higher for Torque Spectrum 2 than for Torque Spectrum 1 over the full range of torque considered ($0 < \sigma < 0{\cdot}3$) for both Curve 1 and Curve 2 relationships. The differences become very significant as the value of maximum torque is reduced (i.e. as $\sigma \to 0$). It is normal for the actual torque spectrum for a helicopter transmission system to be characterized by progressively less time being spent within any specified width torque band as the torque is increased above the endurance limit T_{ES}. Thus the absolute torque measurement error curves for Torque Spectrum 1 represent unrealistically favourable conditions, so in practice the errors will be closer to those given using Torque Spectrum 2.

For the RAN Sea King torque excursions above the endurance limit are rare. Under worst conditions the value of σ is not likely to exceed $0{\cdot}15$ for the most critical gear. According to the graphs of Figs 6 and 7 a 1% torque measurement error is likely to produce a change in excess of 20% in the indicated rate of fatigue life usage at that value of σ. Consequently there is a need for fairly precise measurement of torque so that results obtained for different gear boxes and possibly by different operators can be meaningfully compared. Furthermore a knowledge of

the accuracy of the torque measurement is required so that an adequate factor can be applied to the total summation limit, especially when the fatigue life usage for individual transmissions is monitored.

Alternatively, if the maximum measurement inaccuracy has been established the working endurance limit can be lowered to take account of the measurement system inaccuracy. Under such conditions higher accuracy will obviously allow higher average values of safe operating life and thus reduce maintenance costs if a policy of replacement of individual transmission components after service corresponding to the indicated fatigue life is adopted.

Significant inaccuracies in the measurement of transmission torque (after appropriate sensing via the aircraft torque measuring system) would mean, in effect, that two instruments monitoring the same torque data would be likely to indicate very different amounts of fatigue expenditure. Any differences would, of course, have to be absorbed using whatever operating method is adopted. However, it must be stressed that the inherent uncertainties of the estimated T–N relationship together with the inaccuracies of the hydraulic torque sensing system may have far greater bearing on the attainable gear life than any inaccuracies introduced in the estimation of torquemeter pressure.

The analyses carried out in this Section can be applied to assess the effect of a change in stress factor on the indicated rate of fatigue life usage. If T_H is the maximum torque transmitted in aircraft operation then

$$\sigma = \frac{T_H}{T_{ES}} - 1$$

$$T_{ES} = \frac{T_{EF}}{\gamma}$$

where γ is the stress factor applied. Hence

$$\sigma = \gamma \frac{T_H}{T_{EF}} - 1$$

If γ is changed to a value $(1+\beta)\gamma$ then

$$\sigma_2 - \sigma_1 = \beta \gamma T_H / T_{EF} \tag{30}$$

where σ_1 and σ_2 are the initial and final values of σ respectively. In practice the term $\gamma T_H/T_{EF}$ is likely to be very close to unity (has been taken nominally as 1·15 for RAN Sea King).

The change in value of σ computed via equation 30 can be substituted for ε in equations 21, 22, 23, 24, 26 and 27 to provide the effect on the mean rate of indicated fatigue life usage due to a fractional change β in stress factor.

Any error in the estimation of the number of stress cycles which occur per unit time will be reflected as a change in the indicated rate of fatigue life usage. Such an error could arise from two causes:

(i) Absolute error in the estimation of helicopter gear rotational speed.

(ii) Absolute timing inaccuracy in the measuring system which has the same effect as an error in the estimation of gear rotational speed.

However the speed or timing errors reflect only a linear change in the indicated rate of fatigue life usage (a 1% speed or timing error will produce a 1% change in the mean indicated rate of fatigue life usage). Hence the accuracy demands for gear rotational speed and for torque duration timing are not stringent.

As an example of the order of speed variations to be expected the relevant range is about 4% for the Sea King Mk 50 helicopter in normal operation.

3.2 Effect of Noise on Indicated Rate of Fatigue Life Usage

Any unfiltered alternating signal components which do not reflect true torque variations will be referred to as "noise". Such components will have an effect on the indicated mean rate of fatigue life usage. Because the rate of fatigue life usage increases with increasing torque, the effect of noise (which by definition is assumed to have a mean value of zero) will always be to

increase the indicated rate of fatigue life usage to a value above that which applies when no noise is present. It follows that any estimates of safe life based on torque spectra established by "noisy" measuring systems will be conservative.

The net effect of noise on the indicated mean rate of fatigue life usage will be a function of the waveshape and amplitude of the noise, and of the torque spectrum which applies. To obtain some analytical assessment of the order of change in rate to be expected as a result of the presence of noise the analysis of the previous section relating to mean torque measurement errors can be used to advantage. Hypothetical torque spectra (Fig. 5) as used previously will be considered again here.

Any noise signal which is repetitive can be approximated as the sum of a number n of rectangular elements (Fig. 8*a*) of different amplitudes. For convenience the elements can be made of equal width $\Delta\theta$ (equal to $2\pi/n$). Angle θ is the phase of the alternating signal and is equal to ωt where ω is the radian frequency and t is the elapsed time. Consider initially just the ith element (Fig. 8*a*) representing a torque deviation $v_i T_{ES}$ relative to the mean torque value. The proportion of time for which the torque deviation from the mean value falls within the range of element v_i is $\Delta\theta/2\pi$ or $1/n$. The change in the mean rate of fatigue life usage due to the ith element will be $1/n$ times the change which would result if level v_i were applied continuously.

Using equation 20 and introducing the suffix N to indicate the change in the indicated rate of fatigue life usage due to the presence of noise the following expression results for the th element.

$$\Delta\alpha_N = \frac{1}{n}\left(\frac{W_{\sigma+v_i}}{W_\sigma} - 1\right)$$

The net effect for the composite noise signal is obtained by summing the effect of all n elements in the range $0 < \theta < 2\pi$.

$$\alpha_N = \frac{1}{n} \sum_{i=1}^{n} \left(\frac{W_{\sigma+v_i}}{W_\sigma} - 1\right) \tag{31}$$

The above relationship may be expressed in integral form.

$$\alpha_N = \frac{1}{2\pi} \int_0^{2\pi} \frac{W_{\sigma+v_i}}{W_\sigma} d\theta - 1 \tag{32}$$

To obtain some analytical appreciation of the effect of noise a square wave noise signal (Fig. 8*b*) of amplitude βT_{ES} (peak to peak amplitude $2\beta T_{ES}$) will be considered. Such a noise waveshape, although most unlikely in practice, represents the worst case waveshape for noise of that amplitude. Using equation 31 the following expression results.

$$\alpha_N = 0{\cdot}5\left(\frac{W_{\sigma+\beta} + W_{\sigma-\beta}}{W_\sigma}\right) - 1 \tag{33}$$

$$= 0{\cdot}5(\alpha_{\sigma,+\beta} + \alpha_{\sigma,-\beta}) \tag{34}$$

where $\alpha_{\sigma,+\beta}$ and $\alpha_{\sigma,-\beta}$ represent the values of α according to equations 21, 22, 23, 24, 26 and 27 for $\varepsilon = +\beta$ and $\varepsilon = -\beta$ respectively. $\alpha_{\sigma,+\beta}$ is always positive and $\alpha_{\sigma,-\beta}$ is always negative

For the two T–N curves and for the two torque spectra considered in the previous section, the increase in the indicated rate of fatigue life usage due to the presence of square wave noise has been presented numerically in Tables 1 and 2 and graphically in Fig. 9 for $\sigma \leqslant 0{\cdot}3$ and for $\beta = 0{\cdot}01$ and $0{\cdot}02$. Clearly the effect of noise becomes less significant as σ is increased. In practical terms this means that the fractional increase in the indicated rate of fatigue life usage will be lowest for the most critical gears which have the shortest fatigue life.

The effect of sinusoidal noise may be estimated using the relationship of equation 32. Consider sinusoidal noise (Fig. 8*c*) of amplitude βT_{ES}.

$$v_i = \beta \sin \theta$$

$$\alpha_N = \frac{1}{2\pi} \int_0^{2\pi} \frac{W_{\sigma+\beta \sin \theta}}{W_\sigma} d\theta - 1 \tag{35}$$

Applying this relationship to equations 21, 22, 23, 24, 26 and 27 yields

Curve 1: Torque Spectrum 1

$$\alpha_N = \frac{1}{2\pi} \int_0^{2\pi} \left(1 + \frac{\beta \sin \theta}{\sigma}\right)^{B_1+1} d\theta - 1 \tag{36}$$

Curve 1: Torque Spectrum 2

$$\alpha_N = \frac{1}{2\pi} \int_0^{2\pi} \left(1 + \beta \frac{\sin \theta}{\sigma}\right)^{B_1+2} d\theta - 1$$

Curve 2: Torque Spectrum 1

For $(\sigma + \beta) \leqslant X_M$

$$\alpha_N = \frac{\left\{\frac{1}{2\pi} \int_0^{2\pi} e^{(\sigma - X_L + \beta \sin \theta)/B_2} d\theta\right\} - 1}{e^{(\sigma - X_L)/B_2} - 1} - 1 \tag{38}$$

For $(\sigma - \beta) \geqslant X_M$

$$\alpha_N = \frac{\frac{1}{2\pi} \int_0^{2\pi} (\sigma + \beta \sin \theta)^{B_1+1} d\theta + L_3}{\sigma^{B_1+1} + L_3} - 1 \tag{39}$$

Curve 2: Torque Spectrum 2

For $(\sigma + \beta) \leqslant X_M$

$$\alpha_N = \frac{\left\{\frac{1}{2\pi} \int_0^{2\pi} \left[e^{(\sigma - X_L + \beta \sin \theta)/B_2} - 1/B_2(\sigma - X_L + \beta \sin \theta)\right] d\theta\right\} - 1}{e^{(\sigma - X_L)/B_2} - 1/B_2(\sigma - X_L) - 1} - 1 \tag{40}$$

For $(\sigma - \beta) \geqslant X_M$

$$\alpha_N = \frac{\left\{\frac{1}{2\pi} \int_0^{2\pi} \left[\left(\frac{\sigma + \beta \sin \theta}{X_M}\right)^{B_1+2} + L_6\left(\frac{\sigma + \beta \sin \theta}{X_M}\right)\right] d\theta\right\} - L_7}{\left(\frac{\sigma}{X_M}\right)^{B_1+2} + L_6\left(\frac{\sigma}{X_M}\right) - L_7} - 1 \tag{41}$$

When the value of σ is in the immediate vicinity of X_M the Appendix 1 equations A16, A17, A28 and A29 can be applied as appropriate.

Numerical integration methods can be used to evaluate the increase α_N in the indicated rate of fatigue life usage (as indicated by equations 36 to 41) resulting from superimposed sinusoidal noise. As the increase in each case will be less than that applicable for square wave noise of equivalent amplitude the integrals of equations 36 to 41 have not been evaluated. The effect of noise of any arbitrary waveshape can be conservatively rated by assessing the effect of square wave noise of equivalent amplitude.

The author has been involved in the measurement of torque in Wessex Mk 31B and Sea King Mk 50 helicopters both of which are fitted with hydraulic torque sensing systems.

In the case of Wessex the torquemeter signal was validated[12] by comparing it with a direct measurement on a special main drive shaft fitted with strain gauge transducers. When rated 100% torque was developed, dynamic components of true torque amounted to almost 2% RMS maximum whereas noise components were as high as 14% RMS. The maximum signal frequency of interest was considered to be blade passing frequency as the higher order harmonics had insignificant amplitude.

It was not possible to perform a similar validation for the torque pressure signal for Sea King. However when rated 100% torque was applied the component of torque at blade passing frequency (17 Hz) was found to be less than 1% RMS for all aircraft tested. There were no components of significance at multiples of blade passing frequency present in the oil pressure signal. The maximum level of alternating components observed in the aircraft tested was about 6% RMS when rated 100% torque was being developed. Based on the Wessex work it was assumed that most of the alternating signal was noise. High attenuation of such noise components was considered an essential requirement of instrumentation used in fatigue life studies.

Because the amplitude of the noise signals can be quite high it is desirable that the measuring system be linear to prevent such signals giving rise to an apparent change in mean torque.

The analysis of this section serves to indicate that superimposed noise transferred through the measuring system can produce a significant increase in the indicated rate of fatigue life usage. It is therefore desirable that alternating components which do not reflect true torque be attenuated as much as possible in the measuring system.

3.3 Dynamic Response Requirements

In all helicopters there will be alternating or vibratory components of true torque which are transferred through the transmission system. In contrast the "noise" components discussed in the previous section do not arise from true alternating torque. Attenuation of the alternating components of true torque, either due to limitations in the response of the measuring system or due to deliberate filtering, will cause the indicated mean rate of fatigue life usage to be lower than the true value. Quantitatively the reduction in rate can be assessed in exactly the same way that the increase in rate due to superimposed noise was assessed in the previous section.

A component of torque at blade passing frequency (equal to rotor speed multiplied by number of blades) will always be present in helicopter transmission systems. For example, the passing frequency for Wessex is about 15 Hz and for Sea King about 17 Hz. All three generations of equipment developed at these laboratories for torque spectrum or fatigue life usage indication pass the fundamental component at this frequency without attenuation but to minimize the transfer of extraneous noise through the system low pass filters are used to attenuate any signals above this frequency. The justification for this approach was given in Section 3.2.

From the above discussion it follows that a system bandwidth typically of the order of 20 Hz is required for instrumentation used in helicopter transmission fatigue studies. It is to be emphasized that the dynamic response need arises only because of the non-linear relationship between torque and rate of fatigue life usage. If a linear relationship were to apply, the changes in fatigue life usage rate due to positive and negative excursions of the alternating torque component would tend to cancel over a long period thus yielding a value of life usage which would be the same as that which would result if the alternating component were completely removed.

To digitize the measured value of torque some form of analogue to digital conversion with associated signal sampling must be used. Wherever the question of specifying a minimum sampling frequency to guarantee some value of signal bandwidth arises, it is normal to take heed of Shannon's sampling theorem[13] which states "Given a band limited signal $f(t)$ containing no frequency components beyond F Hz, $f(t)$ may be recovered completely from the infinite sequence

of impulse samples of $f(t)$ separated by time intervals no greater than $1/2F$ second". Thus for proper recovery of the alternating signal the sampling frequency must, in theory, be not less than twice the highest signal component frequency. However special techniques must be used to recover the signal if the minimum sampling frequency is adopted.

"Recovery" of the alternating torque is a requirement only if it is necessary to respond to instantaneous variations in fatigue life usage rates. If the alternating component amplitude at any given level of mean torque tends to remain fairly constant over the life of the gear then a sampling frequency much lower than the highest component frequency of interest can be used. Provided a large number of samples are taken over the relevant torque range the deviation relative to any given mean value should follow a sinusoidal distribution (assuming any harmonics of the blade passing component are removed by filtering) and over a long period should give the same net life usage which would result if a much higher sampling frequency were used.

The minimum acceptable value of sampling frequency cannot be clearly defined; it will be a function of the torque spectrum applicable and of the requirement in relation to torque transient response. Generally if much of the gear life usage occurs due to relatively few transient excursions to high torque levels, for which the usage rate becomes very high, there may be insufficient samples to obtain an accurate indication of usage if a low sampling rate is used. Clearly there is no merit in deliberately reducing the sampling frequency if a higher value can be accommodated without penalty. Broadly it may be stated that a sampling frequency of 100 Hz should accommodate any application regardless of the torque spectrum applicable and should place no special demands for signal recovery. On the other hand a sampling frequency of 1 Hz say, would place significant restrictions on the torque spectrum which could be accommodated and may be too low to allow high level transients, which may account for significant fatigue life usage, to be followed.

In-flight measurements of the torque pressure signal on a sample of three RAN Sea King helicopters revealed considerable variation in the value of alternating torque at blade passing frequency. Differences were observed between the various helicopters tested, and between port and starboard engine torques for each helicopter. In all cases the amplitude of the component at blade passing frequency increased as the mean torque value was increased. The maximum value of mean test torque used was 110% rated torque and at this test torque the measured range of peak to peak values of alternating component at blade passing frequency was 0·8 to 2·6% rated torque.

The analysis of this section shows that attenuation and neglect of real components of alternating torque can give results which are less conservative than those which take account of these components. Life estimating systems must employ a sampling rate high enough to allow transient excursions to high torque to be followed.

3.4 Considerations Relating to Measurement Resolution

All instrumentation developed at these laboratories for torque spectrum or fatigue life usage indication digitize the value of torque measured using a voltage analogue to digital converter (ADC). If the torque corresponding to a particular ADC reading i is T_i then the system resolution can be defined as $T_{i+1}-T_i$ where i is an integer. If an ADC reading of i is obtained then all that can be deduced is that the true torque value T lies in the range $T_i \leqslant T < T_{i+1}$ assuming that the ADC is aligned in the normal manner such that a true torque input T_i results in the ADC output being just on the switching point $i-1 \rightarrow i$. It follows that on the average the torque will be underestimated by an amount equal to $1/2(T_{i+1}-T_i)$ (i.e. half the resolution). Thus the magnitude of the mean underestimate is proportional to the system measurement resolution.

For torque spectrum indication as implemented in the first[4] and second[5] generation indicators developed at these laboratories, the full torque range is divided into only 10 bands. Totalized times for all bands are thereby readily handled by front panel mounted electromechanical counters. In these instances the measurement resolution is much coarser than that provided by the ADC. Since there is no need to accurately measure instantaneous values of torque but there is a need to accurately measure the proportion of time above specified band limits, the low resolution measurement is quite satisfactory in this case. Basically it is essential that sufficient points be obtained on the $q-T$ graph (Fig. 3) so that a curve can be accurately

fitted to establish the relationship which applies at intermediate values of torque between the band limits. Once an adequate resolution to satisfy this condition has been established, no improvement in measurement precision can be provided by increasing the resolution. However any lack of precision in establishing the band changeover points will result in errors as discussed in Section 3.1 being introduced. Hence for torque spectrum indication, high measurement precision is worth striving for but high resolution is not.

For fatigue life usage estimation during flight much higher resolution is necessary if the complex $q-T$ curve fitting techniques which can be readily applied in a ground based analysis are to be avoided. However it is desirable that account be taken of the mean underestimate which is a fundamental characteristic of the conversion process. For a narrow torque band it can be assumed that, when considered over a long period, there will be equal probability that the true torque have any value within the band. Consider the band bounded by T_i and T_{i+1} which is applicable for an ADC reading of i. A better estimate for the fatigue life usage u_i per sample is obtained by averaging as follows:

$$u_i = \frac{1}{T_{i+1}-T_i} \int_{T_i}^{T_{i+1}} u\, dT \tag{42}$$

$$= \frac{s}{f(T_{i+1}-T_i)} \int_{T_i}^{T_{i+1}} \frac{1}{N} dT \tag{43}$$

where

$$u = \frac{s}{fN}$$

using equation 12.

Because of the non-linearity of the $T-N$ relationship the above provides a better estimate of fatigue life usage than a computation based on mean torque $(T_i+T_{i+1})/2$.

For a linear torque measuring system the width of all torque bands will be equal and in such cases equation 43 may be re-written.

$$u_i = \frac{s}{fG} \int_{T_i}^{T_i+G} \frac{1}{N} dT \tag{44}$$

where G is the torque band width.

To take account of an endurance limit T_{ES} which has some intermediate value between T_0 and T_1 the fatigue life usage per sample for an ADC reading corresponding to T_0 is computed as follows.

$$u_0 = \frac{s}{f(T_1-T_0)} \int_{T_{ES}}^{T_i} \frac{1}{N} dT \tag{45}$$

If the T N Curve 2 (Section 2.1) is used $1{\cdot}0393\ T_{ES}$ is substituted in the above equation in lieu of T_{ES}.

The general relationships developed in this section may be used for estimating life usage from torque readings taken using a torque measuring system with finite resolution. These relationships are further developed in Appendix 2. Specific details on the procedure employed for on-board estimation of fatigue life usage in Sea King transmission components are given in Appendix 2.

4. SPECIAL DEMANDS FOR ESTIMATING TRANSMISSION FATIGUE LIFE IN SEA KING HELICOPTERS

The torque load measurement requirements for the single-engine Wessex Mk 31B helicopter have been discussed elsewhere.[4] As this report deals more specifically with transmission fatigue life estimation for the twin-engine Sea King Mk 50 the demands relevant to that helicopter will be considered in this section.

4.1 System of Torque Sensing

Engine torque is a parameter of vital significance to helicopter operators and is always displayed via cockpit meters to the pilots. Usually it is feasible to develop very high levels of torque and pilots are required to maintain torque below prescribed limits. Because torque has to be displayed to pilots a method of torque sensing is always included as part of the helicopter transmission design. This is convenient for life estimation purposes as torque is a very difficult quantity to sense as an 'after-thought'.

The Sea King is a twin-engine aircraft which employs a hydraulic system to sense the torque developed by each engine. In principle helical gear axial loading, which is proportional to applied torque, is supported by a 'cushion' of oil the pressure of which is proportional to torque. Torque pressure transmitters convert the pressure signals to analogue electrical signals in the form of synchro angles which are taken to the cockpit torquemeters.

To optimize the accuracy of torque measurement for use in the estimation of the safe fatigue life of critical gears the basic pressure signal has been adopted as the input to the specially installed measurement system. High performance strain gauge pressure transducers inserted in the hydraulic torque transmitter lines are used to convert the pressure signals to analogue voltage signals. An added advantage which accrues because of the use of the pressure signal as input, is that the complete measuring system can be readily calibrated away from the aircraft.

Earlier measurements on Wessex[12] were used to validate the hydraulic torque sensing system in that helicopter for both mean and dynamic components of applied torque. In that validation program, a special strain gauged main drive shaft was used to transmit measured torque to receiving equipment. The accuracy of in-flight measurement of main drive shaft torque and of torquemeter pressure were each assessed as being better than 1%. Torquemeter pressure equivalent mean torque was found to exceed the directly measured shaft torque by an average of 1·1% rated torque and by a maximum of 2·4% rated torque. Very good agreement between the two sensing systems was realized for the measurement of dynamic components of torque, but low pass filtering of high frequency noise components in the hydraulic system was considered necessary.

It was not possible to assess the accuracy of the Sea King hydraulic torque sensing system by an independent measurement of torque as was done for Wessex. Figures released by the aircraft manufacturer on the calibration accuracy of the torque system tends to suggest a long term accuracy figure not better than ±3%. However, based on the Wessex measurement, it is unlikely that the long term accuracy will be better than 2%. Bossler[14] suggests a ±2% accuracy for a similar hydraulic torque sensing system for a T53 engine.

The transducer originally chosen for measuring the torque transmitter pressure for each engine is a Bell and Howell Model 4-800 (Fig. 10) which is a strain gauge type with special vented gauge option (the pressure of interest is torquemeter pressure relative to ambient pressure). This transducer has the following salient characteristics:

(i) 10 VDC nominal excitation (15 VDC maximum).

(ii) 350 ohm nominal bridge resistance.

(iii) 30 mV nominal full scale output (for 10 bar pressure).

(iv) Natural frequency above 10 kHz.

(v) Non-linearity not greater than 0·3% of nominal full scale output.

(vi) Hysteresis less than 0·1% of nominal full scale output.

(vii) Compensated temperature range −54 to +120°C.

(viii) Operating temperature range −54 to +150°C.

(ix) Thermal zero shift within 0·009% full scale per °C over compensated range.

(x) Thermal sensitivity shift within 0·009% full scale per °C over compensated range.

(xi) Designed to operate in severe airborne environment (high vibration, shock or steady acceleration).

Based on the manufacturer's worst case drift figures, 0·5% shift in zero and 0·5% shift in sensitivity could occur over a 55°C temperature range. Two transducers of the above type fitted in a Sea King helicopter for torque spectrum measurement revealed shifts in calibration as tabulated below after 18 months operation.

Transducer	Zero shift		Sensitivity shift
	Relative to full scale transducer output	Relative to 100% rated torque	
Port engine	−0·43%	−0·56%	−0·11%
Stbd engine	−0·24%	−0·33%	−0·07%

The shift in calibration, particularly the zero shift has been significant for these strain gauge transducers over the specified interval. To reduce the effect of long term drifts, re-calibration could be performed more frequently (perhaps half yearly).

It is appreciated that quartz resonator transducers with analogue frequency outputs could have provided considerable improvement in long term stability and simplified the realization of a high performance signal conditioner but the cost of these units was considered to be prohibitive, at least during the prototype evaluation phase.

Normally torque is expressed in normalized form as per cent rated value, 100% rated torque being a somewhat arbitrary figure which can be exceeded. For Sea King, torque transmitter pressure is related to engine torque by the relationship:

$$150\%\ \text{Rated Torque} \equiv 110\ \text{p.s.i. (pound per square inch)}$$

Symbollically the relationship can be written:

$$P = 0{\cdot}7333\,T \tag{46}$$

where

P = torque transmitter pressure (p.s.i.)

T = engine torque (per cent rated value)

The relationship between torque and pressure is very closely linear. Accurate calibration of the pressure transducers is performed using a dead weight calibration. Because of the high linearity of the strain gauge transducer relationship, transducer output voltage can be taken to be linearly related to applied pressure. A computer program is used to establish the line of best fit to the calibration points. The overall relationship between transducer output and torque can be expressed:

$$e_T = mT + e_z \tag{47}$$

where

e_T = transducer output in millivolt (mV)

T = normalized torque (per cent rated value)

m = sensitivity factor (mV per % rated torque)

e_z = transducer zero offset in mV.

For the transducers initially used for in-flight fatigue life usage indication the following constants apply for the initial calibration.

Transducer	Sensitivity factor m	Zero offset e_z
Port	+0·1457	+0·129
Stbd	+0·1338	+0·082

Because the overall system of converting torque to voltage for Sea King is linear, considerable simplifications result in the calibration of torque spectrum or fatigue life usage indicators. However, in general, a linear relationship is not necessary but the nature of any non-linearities must be known and account taken of them. Other helicopter torque sensing systems (e.g. that used in Chinook helicopter) provide relationships which are definately not linear.

Some early problems were experienced with the ingestion of corrosive contaminants into the vented sections of the Bell and Howell transducers which are mounted in the Sea King transmission compartment. The transducers were subsequently modified by the manufacturers to include an integral vent plus cable which extends into the cabin area. For comparison purposes a second Sea King aircraft used in the transmission fatigue life estimation and evaluation program has been fitted with the alternative Druck PDCR120/WL/C transducers of similar type to the Bell and Howell ones. The Druck transducers are differential types which are purported by the manufacturer to be designed to tolerate corrosive fluids in either pressure input. In this case one of the lines is vented to the cabin as for the Bell and Howell transducer. Both transducer systems are being used to gather Sea King transmission load data at present and are performing satisfactorily.

4.2 Load Spectra Required for Estimating Safe Life of All Gears

For the Sea King transmission system (Fig. 11) comprising the main rotor gearbox and associated gears there are three torque spectra which must be measured to allow estimations to be made on the safe fatigue life of all relevant gears.

(i) Spectrum of torque developed by port engine for gears at the output of that engine.

(ii) Spectrum of torque developed by starboard engine for gears at the output of that engine.

(iii) Spectrum of total torque for gears in the main rotor gearbox.

Individual engine torques are not necessarily equal, although it is normal practice to keep them fairly well balanced. Single-engine flying is possible and indeed pilots are required to regularly execute single-engine flying. Maximum permissible engine torque is different for twin and single-engine operation. Absolute maximum ratings[15] which apply for Sea King Mk 50 helicopters operated by the RAN are reproduced below.

Twin/Single Engine operation	Condition	% Rated Engine torque	% Rated Total torque
Twin	Maximum steady indication	111	111
	Transient for not more than 5 second	120	120
Single	Contingency rating for continuous use on failure of opposite engine	123	61·5
	Contingency rating for 2·5 minutes on failure of opposite engine	135	67·5
	Transient for not more than 5 second	150	75

High levels of torque developed during single-engine operation produce high loads on the gearing at the output of the associated engine but produce low loading on gears in the main rotor gearbox. Normalized total torque is equal to the mean of the port and starboard engine torques.

Torquemeters (Fig. 11) allow the torque output from each engine to be measured separately. To establish the required spectra, the times spent in 10 selected bands for each torque are totalized. Torque band limits for individual engine torque have been made different from those applicable to total torque. The limits which have been used in the Torque Spectrum Indicators[5] and in the Fatigue Life Usage Indicator (described in this report) are tabulated below:

Band Number	Individual Engine Torque Band Limits (% Rated Torque)	Total Torque Band Limits (% Rated Torque)
1	30·2–65	*15·2–47
2	65–83	47–71
3	83–95	71–83
4	95–107	83–95
5	107–119	95–101
6	119–128	101–107
7	128–137	107–113
8	137–146	113–119
9	146–155	119–125
10	>155	>125

* This lower limit is chosen such that zero time is totalized when rotor power is not applied (such as when electrical power is applied during ground tests without rotor power).

To measure the required torque spectra, three Torque Spectrum Indicators each fitted with 10 counters were used initially. More recently the Fatigue Life Usage Indicator has been used to totalize the contributions in all 30 torque bands for the current flight and print these out after each flight.

4.3 Particular Gears Selected for In-Flight Fatigue Life Usage Monitoring

In the Fatigue Life Usage Indicator (FLU Indicator) four gears, designated G1 to G4 (Fig. 11), have been selected for in-flight fatigue life usage monitoring. Normalized torques applicable to each of these gears are different and these gears represent the most critical ones

for the particular torque loads. G3 used for summing the two engine torques is special in that each tooth is subject to two load cycles per revolution. Information relevant to the selected gears is given in the following table.

Gear Designation	Description	Rotational Speed Rev/min Average Values for Normal Operation (103·0% Rated Speed)	Factored Endurance Limit T_{ES} Used for Fatigue Curve 1 (Section 2.1)	Factored Base Endurance Limit T_{BS} ($T_{BS} = 1{\cdot}0393\ T_{ES}$) Used for Fatigue Curve 2 (Section 2.1)	Torque Loading
G1	Spur Pinion S.6137.23051/2	19525	118·3	123·0	Port Engine Torque
G2	Spur Pinion S.6137.23051/2	19525	118·3	123·0	Stbd Engine Torque
G3	Helical Gear (Summing) S.6137.23050/1	3291	114·0	118·5	Two load applications per revolution —Port and stbd engine torques in sequence
G4	Spiral Bevel Pinion S.6137.23053/1	3291	104·9	109·0	Total torque

Endurance limits for the above table have been calculated from the basic gear test data[8] provided by the manufacturer. Some minor differences relative to the manufacturer's calculations resulted.

Fatigue life usage for G1 to G3 will occur only during single-engine operation (Section 4.2). Single-engine operation is expected to occur for only about 0·8% of total flying time.

5. REAL TIME INDICATION OF FATIGUE LIFE USAGE

The fatigue life usage indicator, which represents the most recent instrumentation development carried out at these laboratories for use in fatigue life studies on helicopter transmission components, is described in this Section.

5.1 Background

As indicated previously two generations of helicopter torque load spectrum measuring instrumentation have been developed by these laboratories for gathering data on Wessex[4] and Sea King[5] transmissions respectively. Basically the second generation equipment, called

Torque Spectrum Indicator, is very similar to the first but includes necessary changes for twin-engine torque measurement and some notable improvements which are summarized below.

(i) Incorporation of pressure transducers with improved long term stability.

(ii) Addition of excitation sense leads in the transducer cables so that system calibration is unaffected by the length of the transducer cables which of necessity form a fixed wiring addition to the aircraft.

(iii) Incorporation of a programmable read-only-memory method of selecting torque band limits.

(iv) Replacement of 10 individual torque duration pre-counters with a single time-shared counter with subsequent saving in component count.

(v) Provision of alternate link connection to allow the instrument to be used for counting level excursions rather than totalizing time.

One major drawback of the second generation equipment is that three instruments are required to indicate the three requisite torque spectra (Section 4.2) for the twin-engine Sea King. Because each spectrum requires the totalized times spent in each of 10 torque bands (Section 2.2.1) to be displayed via eight-digit electromechanical counters, the whole of the front panel of the instrument was effectively taken up by these counters. Hence there seemed little point in combining the operations in a single instrument. Because of rapid advances in microcomputer technology which occurred since the second generation equipment was developed it became possible to combine the following operations in a single instrument.

(i) Provide in-flight estimation and indication of fatigue life expended for critical gears.

(ii) Store information on the requisite three torque spectra for post-flight readout.

Broadly the following general requirements must be met by instrumentation intended for in-flight fatigue life usage computation.

(i) The mean or steady component of torque should be measured fairly accurately for reasons discussed in Section 3.1. Ideally indicated life usage should be independent of the specific indicating unit used. As stated earlier (Section 3.1) significant variations from one instrument to the next will occur unless good measurement precision is attained.

(ii) Alternating components of torque, at least up to blade passing frequency (17 Hz for Sea King), should be passed without attenuation (Section 3.3) to the analogue-to-digital converter input. While it is possible to achieve a system bandwidth of this value using a low sampling frequency, (Section 3.3) a sampling rate of 100 Hz has been adopted as that rate can be achieved without any hardware or software penalty.

(iii) Because system noise will increase the indicated rate of fatigue life usage (Section 3.2) it is important that alternating components which do not reflect true torque be significantly attenuated.

(iv) Paradoxically, although it is desirable that mean torque be accurately measured, comparably high measurement resolution is not a requirement (Section 3.4). A resolution, referred to the analogue-to-digital converter of 0·6% rated torque per bit (as used in the second generation equipment) is considered to be quite adequate.

Requirements special to the program conducted at these laboratories in relation to the safe life of Sea King transmission components are summarized below.

(i) In-flight (real time) estimation and indication of the current value of safe fatigue life expended for four gears is required (Section 4.3).

(ii) Print-out at the termination of each flight of totalized times spent in each of 10 torque bands for the three requisite spectra is required. For convenience the torque bands should agree with those used in the second generation equipment.

In addition, to provide compatibility with existing aircraft fittings installed in Sea King for the second generation equipment, and also to minimize the resources necessary to realize the new instrumentation, minimum hardware changes relative to the second generation system were considered to be very desirable.

Third generation instrumentation, called a Fatigue Life Usage Indicator, developed to meet the above requirements is described in the following sections.

5.2 Fatigue Life Usage Indicating System

System instrumentation units installed in Sea King for fatigue life usage estimation and indication are shown schematically in Fig. 12. The strain gauge pressure transducers (Fig. 10) are mounted in the port and starboard transmission compartments respectively. The other units which comprise the aircraft installation are the Transmission Fatigue Life Usage Indicator (Fig. 13), the Printer (Fig. 14) and the Terminator (Fig. 15). These units are mounted in the port-side cabin compartment below the transmission compartment.

The Terminator provides convenient interconnection of system cables. Except for a small relay circuit (Section 7) associated with the post-flight automatic print command, it contains only wire connections between chassis mounted connectors.

The Transmission Fatigue Life Usage Indicator is the system unit developed at these laboratories for in-flight estimation and indication of fatigue life usage for up to four gears. More detailed information is given later in this section and in Sections 5.3 to 5.6.

The Printer comprises a Datel Model APP-20 printer slightly modified for airborne use. At the termination of each flight when the aircraft is on the ground and fuel to either the No. 2 (starboard) or No. 1 (port) engine is switched off, a 28 VDC signal is transferred to the Indicator to signify an automatic print request. At this time values of basic torque spectrum data, gear fatigue life usage and flying time for the current flight are automatically printed. If printing of these data were not required the printer could be omitted with no variation required to the rest of the system. Alternatively the printer could be omitted from the aircraft installation and a portable printer unit could be plugged in after the flight (before power is switched off) to extract the data for the current flight. A cockpit-mounted 'Print' button allows the aircrew to initiate manually an 'early' printout as soon as the aircraft has landed.

The Flight-Line Function Tester (Fig. 16) is used for ground functional tests of the system and is therefore not required for airborne use. A description of the Tester is given in Section 6.

Approximate dimensions and mass of the system units are given in the following table.

System Unit	Approx. Dimensions (mm)	Mass (kg)
Transmission Fatigue Life Usage Indicator	320 × 145 × 127	6·10
Printer	310 × 145 × 150	4·34
Transducer	140 × 25 × 25	0·15
Terminator	120 × 57 × 188	0·65
Airborne System Cables		1·85
Tester	240 × 145 × 236	3·13

The Fatigue Life Usage Indicator and the Printer can be directly substituted for two second generation Torque Spectrum Indicators without any further change in the aircraft mounting hardware. Similarly the Terminator, although electrically different from the equivalent second generation unit, is of identical size and has compatible mounting arrangements to that used in the earlier unit. Transducers and associated cables are identical to those used with the second generation instrumentation. However other system cables are different.

Basically the Transmission Fatigue Life Usage Indicator, for which a functional block schema is drawn in Fig. 17, comprises the following hardware items.

(i) Five front panel-mounted electromechanical counters (four to indicate total fatigue life usage for four gears and one to indicate total flying time).

(ii) Four external connectors for power input, transducer input, printer output and tester output.

(iii) Five printed circuit card slots, four of which are presently utilized for circuits.

(iv) Power supply.

The printed circuit cards have dimensions 118×125 mm approximately and plug into 44-pin edge connectors (22 per side). These circuits which are described in Sections 5.3 to 5.6 will be referred to by the functional names (Fig. 12) listed below.

(i) Transducer Excitation Generator.

(ii) Analogue Signal Conditioner.

(iii) Microcomputer.

(iv) Reset Signal Generator and Output Driver.

Except for the electromechanical readouts which make use of aircraft 28 VDC, all circuits in the Transmission Fatigue Life Usage Indicator draw basic power from the aircraft 115 VAC 400 Hz supply (one phase only). Regulated supply units provide ± 15 V for the analogue circuits and $+5$ V for the digital circuits (Fig. 12). The Tester which plugs into the Indicator draws current from the $+5$ V supply in the Indicator.

The Datel printer incorporates its own power supply capable of direct operation from aircraft 115 VAC 400 Hz.

Power requirements for the various units in the fatigue life usage indicating system are tabulated below.

Unit		Demand from Aircraft Supplies	
		Current from 115 VAC 400 Hz	Current from 28 VDC
FLU Indicator	Without Tester	113 mA	665 mA peak max.
	With Tester	150 mA	810 mA peak max.
Printer	When printing	100 mA	Nil
	Not printing	30 mA	
Terminator		Nil	Nil
Tester		See Indicator above	

Current drawn from the regulated supplies in the Indicator are summarized in the following table.

Regulated Supply	Current Demand
+ 15 V	135 mA
- 15 V	120 mA
+ 5 V (Without Tester)	505 mA
+ 5 V (With Tester)	880 mA

Complete details on circuits, components and system wiring are given by Krieser[16] in a complementary publication. A summary of the contents of that publication is given in the Addendum.

5.3 Transducer Excitation Generator

Because the strain gauge transducer sensitivity (millivolt output per unit change in pressure) is directly proportional to the bridge excitation voltage, it is essential that a highly stable supply be used.

A voltage regulating circuit as shown in Fig. 18 is used to generate the required 10 V excitation. Input power is extracted from the ±15 V supplies (Section 5.2).

To reduce the common mode voltage to zero (approximately) separate supplies of +5 V and −5 V relative to signal common are generated. Such an arrangement has the advantage that any changes in common mode signal rejection with temperature in the following amplifier (Section 5.4) do not translate as zero shifts.

The highly stable LM 723 is used as the basic regulating device. Excitation voltage level for both +5 V and −5 V outputs is set via R_{V1} and balance of the two supplies via R_{V2}. Complimentary transistors provide output drive power for the transducers. Excitation current for the 350 ohm (nominal) transducer is approximately 30 mA from each supply.

To allow the transducer excitation voltage to be precisely set, independently of the length of transducer connecting cable used, sense leads from each supply have been taken right to the transducer. Because the transducer manufacturers have provided compensation to improve the performance over a wide temperature range when constant voltage excitation is used, the use of constant current excitation (and hence deletion of sense leads) was not considered to be a viable alternative.

Independent excitation generator circuits conforming to the arrangement of Fig. 18 are used for the port and starboard transducers respectively. If a common excitation circuit were used there would have been a conflict with respect to the remote sensing of the transducer excitation voltage. The excitation voltage of one transducer only can be sensed by a single circuit.

5.4 Analogue Signal Conditioner

Transducer output signal amplification and conversion to digital form is achieved using the circuit configuration depicted in Fig. 19.

As no external pre-amplification is employed the incoming signal has a full scale range of 0–20 mV approximately (Section 4.1). Instrumentation pre-amplifier *U1* is a differential input type having low drift and excellent common mode rejection characteristics. Gain A_1 for the pre-amplifier is set by the value of external resistance R_G and is given by

$$A_1 = -\left(1 + \frac{200\,000}{R_G}\right) \tag{48}$$

where R_G is expressed in ohm.

The 200 000 ohm value of an internal resistance gives rise to the constant term in the above relationship. One major advantage of this type of pre-amplifier is that setting of the gain determining resistance R_G is not further complicated by the need for precise resistance balancing to maintain high common mode rejection, as applies for the more conventional differential amplifier. Pre-amplifier gain has been set to about 200 for the present application.

Initially it had been decided that to maintain best common mode performance, no signal filtering would be incorporated in the pre-amplifier stage. However it was later found that some high frequency (1 MHz for fundamental component) noise due to digital circuit switching was picked up on the incoming +SIG and −SIG lines from the transducer. As the frequency

band for such noise was well outside the pass-band of the pre-amplifier (having cut-off frequency of about 1·5 kHz at the above gain setting) it was first thought that such noise could have no effect on the performance of the signal conditioner. Further tests indicated that although the high frequency noise did not pass through the pre-amplifier, it did give rise to a small DC offset, apparently due to some internal non-linearity. To eliminate this offset, bypass capacitors (Fig. 19) had to be incorporated in the input signal lines right at the pre-amplifier input.

For reasons discussed in Section 3.3, limiting of the signal bandwidth to just above blade passing frequency 17 Hz was considered essential. The output amplifier comprising *U2* and associated components forms a low pass filter having 3 dB bandwidth of 25 Hz approximately.

If the effect of the zero adjusting circuit is ignored the transfer function A_2 (filter voltage output divided by filter voltage input) for the filter can be expressed as the ratio of feedback and input impedances:

$$A_2 = -\frac{R_3}{R_1+R_2}\left\{\frac{1}{1+j\omega\dfrac{C_1 R_1 R_2}{R_1+R_2}}\right\}\left\{\frac{1}{1-\dfrac{\omega^2 C_2 C_3 R_3 R_4}{1+j\omega(C_2+C_3)R_4}}\right\} \tag{49}$$

where ω is the radian frequency.

The two frequency dependent terms in the above equation define the responses of the input and feedback filter sections respectively. Hence the response of each filter section may be considered separately and the overall response obtained by multiplying the individual responses together.

The overall rationalized gain modulus A_R (considered to be unity at DC) is given by:

$$A_R = \frac{1}{\sqrt{\left\{1+\left(\dfrac{\omega C_1 R_1 R_2}{R_1+R_2}\right)^2\right\}}}\sqrt{\left\{\frac{1+\{\omega(C_2+C_3)R_4\}^2}{(1-\omega^2 C_2 C_3 R_3 R_4)^2+\{\omega(C_2+C_3)R_4\}^2}\right\}} \tag{50}$$

It is of interest to define the frequency at which the second term peaks and the relative amplitude of the peak.

Define

$$\alpha = \{(C_2+C_3)R_4\}^2 \tag{51}$$

and

$$\beta = C_2 C_3 R_3 R_4 \tag{52}$$

It can be shown that the radian frequency ω_0 of the peak is given by:

$$\omega_0{}^2 = \frac{1}{\alpha}\left\{\sqrt{\left(1+\frac{2\alpha}{\beta}\right)}-1\right\} \tag{53}$$

and the amplitude of the peak by:

$$A_{RO} = \sqrt{\left\{\frac{1+\alpha\omega_0{}^2}{(1-\beta\omega_0{}^2)^2+\alpha\omega_0{}^2}\right\}} \tag{54}$$

If it can be assumed that $\alpha \ll \beta$ then the following approximate expressions apply:

$$\omega_0{}^2 \approx \frac{1}{\beta} \tag{55}$$

$$A_{RO} \approx \sqrt{\left(1+\frac{\beta}{\alpha}\right)} \tag{56}$$

Using the values indicated in Fig. 19 and substituting in the above equations yields the values indicated in the following table.

	Frequency (f_0) of peak*	Relative amplitude of peak
Exact Solution (Eqns. 53–54)	21·6 Hz	1·97
Approx. Solution (Eqns. 55–56)	23·3 Hz	2·28

* Where $f_0 = \frac{\omega}{2\pi}$

It is to be noted that the approximate solution provides figures very close to those yielded by the exact solution.

In Fig. 20 the measured response of the individual filter sections together with that for the composite filter are drawn. It is to be observed that the measured characteristic of the bridged-T filter agrees closely with the exact solution predicted above.

Filter response is only slightly affected by adjustment of the gain trim resistance R_1. Gain of the filter stage has been set to 2 approximately in the present application.

The zero adjusting circuit takes care of any zero offset from the transducers and allows the system zero to be accurately set to correspond, in the present instance, to $+2{\cdot}6\%$ rated torque. Because of the need for very high zero stability, the well regulated EXCIT SENSE outputs from the Transducer Excitation Generator (Section 5.3) are used to provide stable reference voltages for the zero adjusting circuit as shown in Fig. 19.

Identical pre-amplifier and filter configurations are used for handling port and starboard input channels.

Sequential selection of port and starboard channels is performed using the CMOS (complementary-metal-oxide-semiconductor) analogue switch U3.

Analogue voltage to digital conversion is performed using U4 which has the following salient features:

(i) Conversion is performed using the successive approximation technique and takes 20 μs (8μs version also available).

(ii) A full scale unipolar input range of 0 to 10 V is handled.

(iii) Output coding is complementary binary.

(iv) Resolution is 12-bit (1 part in 4096).

(v) A 12-bit parallel output and a serial output together with clock are available.

In the present applicat. a 100 conversions for both port and starboard channels are performed per second. Channel selection and initiation of conversions are controlled by outputs CH SEL and COMMAND-TO-CONVERT from the microcomputer (Section 5.5).

Alignment of the signal conditioning amplifiers is carefully performed[16] to provide an overall sensitivity of $0{\cdot}6\%$ rated torque per bit as read by the microcomputer and to set amplifier zero to correspond to $2{\cdot}6\%$ rated torque. Since the four lowest order bits are not read by the microcomputer the effective sensitivity relative to the 12-bit ADC output is 0·6/16 (equal to 0·0375) per cent rated torque per bit. These four bits of lowest significance, which are displayed via the Flight-Line Function Tester (Section 6), allow the system to be accurately aligned and shifts in calibration to be detected. The indicated torque is given by:

$$T = 0{\cdot}0375\,Y + 2{\cdot}6\% \tag{57}$$

where Y is the ADC reading.

The converter also generates a serial output. To reduce the demand for external cable conductors the serial output has been used in conjunction with the Tester (Section 6).

Some performance figures for the actual signal conditioning circuit were obtained. Measured overall linearity (transducer output to ADC output) was found to be within $\pm 0{\cdot}15\%$ rated torque over a torque range of 150%. Crosstalk was very low being less than $0{\cdot}04\%$ rated torque for a full scale torque (150%) change on the opposite channel.

Amplifier zero stability is the most important consideration for the signal conditioner. Tests of amplifier drift with temperature over the range 0–50°C demonstrated that zero shift in the pre-amplifier is the only variation worthy of consideration. Negligible shift in transducer excitation voltage and in amplifier sensitivity occurs over this range and any contribution to drift from the output amplifier is imperceptible. A series of ten pre-amplifiers (type AD522AD—Fig. 19) were tested and yielded the following shifts over the 0 to 50°C temperature range.

Pre-amplifier No.	1	2	3	4	5
Drift referred to pre-amplifier output	−5·6 mV	−17·3 mV	−2·7 mV	−20·9 mV	−20·5 mV
Equivalent rated torque approximately	−0·17%	−0·52%	−0·08%	−0·63%	−0·62%
Pre-amplifier No.	6	7	8	9	10
Drift referred to pre-amplifier output	+5·9 mV	+3·7 mV	+2·9 mV	+8·2 mV	−19·0 mV
Equivalent rated torque approximately	+0·18%	+0·11%	+0·09%	+0·25%	−0·57%

Considerable spread in draft figures is apparent and greatly improved performance results if the pre-amplifiers are selected for minimum drift.

5.5 Microcomputer

The microcomputer system (Fig. 21) chosen for in-flight estimation of gear fatigue life usage is based on the Motorola MC6800 microprocessing unit (MPU) and associated components. This eight-bit processor is eminently suited to the present application which conveniently requires eight-bit input and eight-bit output digital data.

Crystal controlled clock signals at 1 MHz frequency are provided by U2. An alternative 2 MHz clock signal generator is also available and may be used in lieu of the lower frequency clock if a high speed version of the MPU is used. However since adequate response to dynamic components of torque is achievable with the lower frequency clock, it has been used in the present application.

Results of fatigue life usage computations performed during flight and other data required for post flight printout are stored in the 256 word (where 1 word ≡ 8 bits) static random access memory (RAM) formed by U7 and U8.

Read-only-memory (ROM) devices U5 and U6, which are of the ultra-violet light eraseable type, allow for program storage of up to 4K (4096) words. In the present application total program storage requirement is 2045 words, and hence only one ROM storage device U6 is required.

None of the microcomputer bus signals except RESET are used remotely. A single peripheral interface adaptor (PIA) U9 provides all input/output communication for the system. All input/output lines are utilized according to the specification of the following table.

PIA I/O Line Designation	Whether used as Input or Output	Signal Description		Comment
PA0	Input	ADC Bit 0		All outputs from the Analogue to Digital Converter are complemented
PA1	Input	ADC Bit 1		
PA2	Input	ADC Bit 2		
PA3	Input	ADC Bit 3		
PA4	Input	ADC Bit 4		
PA5	Input	ADC Bit 5		
PA6	Input	ADC Bit 6		
PA7	Input	ADC Bit 7 (MSB)		
CA1	Input	Print Request Manual		Positive transition active
CA2	Input	Print Request Auto		Positive transition active
PB0	Output	CH SEL (Port/Stbd)	Print D0	$\overline{\text{CH SEL}}$ =0 for Port transducer
PB1	Output	CTC (ADC Command to convert)	Print D1 Print D1	
PB2	Output	Gear 1 Count (1=true)	Print D2	Status Bit PB7 selects either Normal (as indicated in left-hand column) or Print mode. Print outputs D0 to D6 are in 7-bit ASCII code
PB3	Output	Gear 2 Count (1=true)	Print D3	
PB4	Output	Gear 3 Count (1=true)	Print D4	
PB5	Output	Gear 4 Count (1=true)	Print D5	
PB6	Output	Total Flying Time (1=true)	Print D6	
PB7	Output	Status 0= FLU Indicator	1=Printer Character Enable	
CB1	Input	Printer Ready for Data	(1=Ready)	Positive transition active
CB2	Output	Printer Data Valid	(0=Valid)	Write strobe with MPU clock restore

Lines PA0 to PA7 are set under program control as inputs and are used to read the eight bits of highest significance from the 12-bit ADC (Section 5.4). Lines PB0 to PB7 are set under program control as outputs which control analogue conversions, electromechanical counter advances and data printout.

When status bit PB7 is 0 PB0 controls transducer channel selection (port or starboard) and PB1 initiates conversions in the ADC. PB2 to PB6 control the electromechanical counters which can be actuated asynchronously under program control. The duration of the readout pulse is program controlled. Gear 1 to Gear 4 counters are advanced by one for each micro-life unit expended and the Total Flying Time Counter is advanced by one for each second of flying time elapsed.

When status bit PB7 is 1 data may be transferred to the printer. At the end of a flight this bit is set and the printout is initiated automatically. Alternatively a printout can be requested at any time by depressing a manual pushbutton external to the FLU Indicator.

These aspects of hardware performance relating to data input and output are controlled by the software which is described in more detail in Section 8.

Decoder U3 provides simple selection of ROM1, ROM2, RAM or I/O (PIA) according to the logic levels applied to the 16-bit address bus A0 to A15 from the MPU. Under normal operation, gate input G2 to the decoder is grounded so that the decoder outputs can be expressed by the logical AND expressions below.

$$\text{ROM1} = \text{VMA} \cdot \text{A15} \cdot \text{A14} \cdot \text{A11} \tag{58}$$

$$\text{ROM2} = \text{VMA} \cdot \text{A15} \cdot \text{A14} \cdot \text{A11} \tag{59}$$

$$\text{I/O} = \text{VMA} \cdot \text{A15} \cdot \text{A14} \cdot \text{A11} \tag{60}$$

$$\text{RAM} = \text{VMA} \cdot \text{A15} \cdot \text{A14} \cdot \overline{\text{A11}} \tag{61}$$

With the selection logic specified above the memory map below results.

Device	Address																Address Range (Hex) for Programming*
	A15	A14	A13	A12	A11	A10	A9	A8	A7	A6	A5	A4	A3	A2	A1	A0	
RAM1 (U7)	0	0	×	×	0	×	×	×	0	—	—	—	—	—	—	—	0000–007F
RAM2 (U8)	0	0	×	×	0	×	×	×	1	—	—	—	—	—	—	—	0080–00FF
PIA (U9)	0	0	×	×	1	×	×	×	×	×	×	×	×	1	—	—	1804–1807†
ROM1 (U5)	1	1	×	×	0	—	—	—	—	—	—	—	—	—	—	—	C000–C7FF
ROM2 (U6)	1	1	×	×	1	—	—	—	—	—	—	—	—	—	—	—	C800–CFFF

'×' means 'not decoded'.

'—' means 'program variable'.

* These address ranges are the most convenient of those which are valid for all memory options.
† If alternative 4K ROM is used in lieu of the 2K ROM the logic levels applicable to A11 in the above table will be transferred to A12. The designated PIA address for programming purposes will be valid for either ROM.

Because some of the address lines are not decoded the memory will respond to a number of bus addresses throughout the address space. For example ROM2 (according to the above table) will respond to any of the following ranges:

C800—CFFF

D800—DFFF

E800—EFFF

F800—FFFF

Using the alternative link connection (Fig. 21) address line A13 may also be decoded so that the logical AND of factor A13 needs to be introduced into equations 58 to 61. In particular equation 59 becomes:

$$\text{ROM2} = \text{VMA} \cdot \text{A15} \cdot \text{A14} \cdot \text{A13} \cdot \text{A11} \tag{62}$$

By decoding A13 in this manner the memory range is restricted to the lower 32K and hence ROM2 will then respond only to the following ranges:

C800—CFFF

D800—DFFF

In the above instance the microcomputer will not respond to the RESET vector address FFFE placed on the address bus at power-up or during alternative initialization. Such an arrangement is convenient for initial program debugging using external test programs.

To provide for future expansion and improved versatility of the microcomputer printed circuit board when used in alternative applications, links have been included to allow type 2732 4K ROMS (in lieu of the 2K ROMS) to be accommodated using the same circuit with alternative link to decode A12 instead of A11 (refer to previous table). Furthermore a 2K RAM (e.g. Texas Instruments type TMS4016 or Hitachi type HM6116) can be used in place of either ROM with alternative link to enable the WE (WRITE ENABLE$\overline{\text{E}}$) line to be decoded.

A reset signal RESET which is automatically generated at power-up (Section 5.6) and which can be manually introduced from a pushbutton located on the Flight-Line Function Tester (Section 6) is taken to the MPU and PIA for appropriate program initialization.

One of the design goals for the microcomputer was to produce a circuit for which all the processing functions were confined to a single printed circuit board which would plug into the 44-pin edge connector (Section 5.1). In this way the need to buffer and transfer address bus and data bus signals to external circuits would be obviated. The goal was indeed achieved with considerable ROM expansion capability in reserve (only 2K of available 8K required for the present application).

Because the address and data buses are local to the microcomputer board, an alternative means of access had to be established for initial program debugging. By removing the MPU from its socket and inserting a flat extension cable to an external development unit (Section 8.3), complete with its own microcomputer and monitor program, the programs were initially conveniently checked and corrected using external RAM in place of the circuit ROM.

5.6 Reset Signal Generator And Output Driver

A functional schema for the Reset Signal Generator and Output Driver is drawn in Fig. 22. This circuit performs two major functions:

(i) Automatic generation of a reset signal at power-up to initialize the microcomputer program sequence at the correct starting address.

(ii) Provision of circuits to interface with external equipment and with front panel mounted counters on the FLU Indicator.

All circuits with the exception of those which drive the electromechanical counters derive power from the aircraft 115 VAC 400 Hz supply. When power is first applied during the start-up sequence the Vcc (+5 V) regulator will take a small time to stabilize. During the stabilization period the behaviour of the microcomputer is unpredictable. It is essential that the $\overline{\text{RESET}}$ signal be held low until stabilization is achieved. Transfer to the program starting address will occur at the instant $\overline{\text{RESET}}$ switches to the high state.

Voltage comparator U1 and associated components generate an appropriate reset signal when system power is first applied. At the instant of switch-on C1 will be discharged and hence the voltage level on the '−' input to the comparator will be initially higher than that on the '+' input. After a delay period equal to 0·7(C1)(R1) (0·33 s for the values shown in Fig. 22) approximately the comparator will switch to its normal state and RESET will remain high thereafter. At the same time relay K1 will be energized and will transfer 28 VDC from the aircraft supply to the electromechanical counters and associated circuits. Diode CR1 allows capacitor C1 to rapidly discharge through the circuits loading the +5 V regulator when 115 VAC power is switched off.

During normal in-flight operation the INTERNAL FLU ENB line will be high and the PB7 (STATUS) line low. Under such circumstances readout pulses appearing on the PB2 to PB6 lines (from the microcomputer) will be transferred via the optical isolators and Darlington transistor drivers to the FLU Indicator counters. If the PB7 line goes high (as when printing is in progress) the transfer of the pulses to the FLU Indicator counters will be inhibited. If the Flight-Line Function Tester is connected to the FLU Indicator the INTERNAL FLU ENB line will switch low thus inhibiting the transfer of pulses to the FLU Indicator counters. Operation as in this latter mode is required to prevent additional gear usage counts being registered on the FLU Indicator counters during system checkout.

To meet the stringent demands of a high performance measuring system, a single point connection of system common to FLU Indicator chassis (which is attached directly to aircraft frame) is incorporated near the analogue signal conditioning circuit. To prevent ground loop current flowing through the system, the optical isolators (Fig. 22) have been used. The 28 VDC return line is remotely grounded to aircraft frame. Manual and automatic print request lines (Fig. 22) have similar isolation.

Flip-flop U5 accepts the pulse strobe input CB2 used to initialize the transfer of any given character to the printer. When the printer returns a negative going DAC pulse to indicate that the print data have been accepted the flip-flop switches thus terminating the Data Valid (DAV) input to the printer. The duration of the DAV pulse is fairly critical and is set by the printer to 375 μs approximately.

6. FLIGHT-LINE FUNCTION TESTER FOR TRANSMISSION FATIGUE LIFE USAGE INDICATOR

6.1 General

The Flight-Line Function Tester (Fig. 16) provides a simple method of testing the fatigue life usage indicating system. It is intended primarily for use at squadron level for testing an installation in an aircraft. Such tests are required periodically on a routine basis and always when the system is removed and re-installed in the aircraft. In addition the Tester can be used for system calibration checks.

To perform a system functional test the Tester is simply plugged via an integral cable into a 32-pin connector accessible at the front of the Transmission Fatigue Life Usage Indicator (Fig. 13). System performance is completely checked by observing outputs on the front panel of the Tester. All power for the Tester is taken from the Indicator via the mating 32-line cable.

Provision is made in the Tester to perform the following:

(i) Simulate specific torque values for each engine by applying resistive shunts from an internal circuit board to port and starboard strain gauge pressure transducers.

(ii) Display the full 12-bit output from the analogue to digital converter (Section 5.4) in three-digit hexadecimal code using a light emitting diode display.

(iii) Allow switch selection of external shunts, in lieu of the internal ones, for use in system alignment (normally not performed in the aircraft).

(iv) Allow switch selection of Gear 1 to Gear 4 fatigue life usage tests which provide electromechanical counter readout consistent with simulated torque values.

(v) Provide switch selection of Total Flying Time test which is used to check that counter advances at 1 Hz rate under computer program control.

(vi) Provide a manual Reset button which allows the program to be returned to the start address whenever required.

(vii) Provide a manual Print button which allows the printer to be simply checked.

(viii) Provide test points which allow amplifier alignment and more extensive functional checks to be performed.

Two plug-in printed circuit boards are used in the tester:

(i) Transducer shunt resistance board.

(ii) Digital test board.

The functions of these circuits will be considered in more detail in the following sections.

6.2 Simulation of Applied Torque Using Resistance Shunts

Any level of torque may be simulated using a shunt resistance across one arm of the strain gauge bridge in the pressure transducer. Such a method is used to simulate values of torque for test purposes. Switch selectable values of shunt resistance (Fig. 23) simulate values of torque sufficient to incur fatigue life usage for Gear 1 to Gear 4 (Section 4.3).

Values of shunt resistance may be accurately trimmed using potentiometers not shown in Fig. 23. Analogue-to-digital converter readings corresponding to simulated torque values form the basis for system calibration checks. However checking is limited to the signal path after the transducer strain gauge. To check the pressure to voltage relationship for the bridge a dead weight calibrator may be used.

When the Flight-Line Function Tester is plugged into the Transmission Fatigue Life Usage Indicator the TESTER ENB line (Fig. 23) is normally switched high thus setting the selected output line high. This property enables the various functions to be checked using a single electromechanical counter in the Tester. Normally the electromechanical counters in the Transmission Fatigue Life Usage Indicator are automatically 'frozen' when the Tester is connected.

Initially the settings indicated in the following table have been used. The resulting life usage rate is a function of the endurance relationship (Section 2.1) used for the life usage computations. To compute these rates gear rotational speed has been taken as 103·0% rated value (mean for RAN conditions) as indicated in the table of Section 4.3.

Parameter Parameter	Gear 1		Gear 2		Gear 3		Gear 4	
	Port	Stbd	Port	Stbd	Port	Stbd	Port	Stbd
Test Torque Setting	124·1%	10·1%	10·1%	124·1%	122·9%	122·9%	117·5%	117·5%
FLU Rate μ Life/s	19·0		19·0		5·7+5·7 11·4		10·6	
Counter Rate	16·7 Hz* (max. readout rate)		16·7 Hz* (max. readout rate)		11·4 Hz		10·6 Hz	

* Counting will continue when simulated load is removed until all life usage increments have been registered.

If Transmission Fatigue Life Usage Indicators are installed in a number of aircraft a separate shunt resistance board, trimmed to match the particular transducers used, will be required for each installation.

6.3 Digital Signal Handling

A functional schema of the digital board is drawn in Fig. 24.

To reduce the number of data lines connected to the Flight-Line Function Tester the serial output from the analogue to digital converter is used rather than the 12-bit parallel output. Using a series of delay circuits the serial output is appropriately clocked into the shift register. A timing diagram for the signals of interest is presented in Fig. 25. The numbers within circles in Figs 24 and 25 relate signal timing to circuit locations.

By using the retriggering capability of the monostable multivibrator devices, a gate signal CONV GATE is generated. This signal remains low while the serial data are transferred and switches high a short time after the last data bit is transferred.

Transfer of the shift register contents to a light-emitting diode display (three-digit) is accomplished by the display strobe which transfers port or starboard channel readings according to the setting of a front panel mounted selector switch.

A front panel mounted potentiometer allows the reading update repetition period to be adjusted within the range 70 to 520 ms. Such a feature makes reading of the analogue-to-digital converter output simpler under noisy conditions.

Any one of Gear 1 FLU, Gear 2 FLU, Gear 3 FLU, Gear 4 FLU or Total Flying Time may be selected for test via the multi-pole switch of Fig. 23. A high state on the appropriate enable (ENB) line connects that channel via the optical isolator and output driving circuit to the resettable electromechanical counter mounted on the front panel of the tester. Transfer of pulses to the counter occurs under normal program control. The pulse rate varies according to the levels of torque simulated on the port and starboard input channels.

7. POST-FLIGHT PRINTOUT

The printer (Fig. 14) which as indicated in Section 5.2 is a Datel Type APP-20 slightly modified for airborne use, incorporates a thermal type printhead. Standard 58 mm wide thermal sensitive paper, which can be readily written on with pen or pencil, is used. The latter feature is necessary as ground staff are required to enter additional information in writing. Up to 20 characters may be printed per line. The maximum printing rate is approximately 1·5 lines per second.

The printer is capable of printing any of the ASCII (American Standard Code for Information Interchange) set of characters either line-by-line or character-by-character. However the printer is operated only in the line-by-line mode in the present application.

The relative timing of the printer control signals is presented in Fig. 26. When the printer is waiting for data it sends out negative going pulses (Fig. 26) at regular intervals on the READY FOR DATA (RFD) line. This latter signal is inverted in the Reset Signal Generator and Output Driver circuit (Section 5.6) and coupled to the Microcomputer circuit (Section 5.5) via the CB1 line. Before transferring a new line of data to the printer the program interrogates the CB1 input to ascertain whether the printer is ready to receive data.

To print a line of data the following operations are performed:

(i) The requisite seven-bit ASCII characters are sequentially transferred in parallel form to the print buffer under the action of the DATA VALID (DAV) signal.

(ii) When the printer has accepted a character it signals the fact by setting DATA ACCEPTED (DAC) low for a short interval (Fig. 26).

(iii) The DAV signal is set low under the action of the CB2 strobe (Fig. 22) used in the pulse mode. When a low transition is detected on the DAC line the DAV signal is terminated (i.e. returned to the high state).

(iv) Prior to the transfer of each character the CONTROL CHARACTER ENABLE line (referred to as PRINTER ENB in Fig. 22) is set high under program control. Under these conditions printing of a new line (Fig. 26) will be initiated on receipt of a carriage return character.

Depressing the manual PRINT button included in the modified printer hardware or that on the Flight-Line Function Tester will cause a Manual Print Request to be unconditionally transferred to the microcomputing system. To transfer an Automatic Print Request (which should occur automatically after each flight) the following conditions, which are established using a reed relay circuit in the Terminator, must be satisfied:

(i) Aircraft must be on the ground as sensed by a switch associated with the nose-wheel of the aircraft undercarriage system.

(ii) Fuel to either No. 2 (starboard) or No. 1 (port) engine must be switched off via the appropriate high pressure cock.

The aircrew can over-ride condition (ii) by depressing a 'Print' button mounted in the cockpit. Such capability is sometimes advantageous when the aircraft has to take off again quickly and also when a printout is required between sorties for which neither engine is stopped.

It is normal for fuel to be switched off No. 2 engine just after landing and for the aircraft to taxi using No. 1 engine. Under true emergency conditions, when an in-flight engine shut-down is necessary, condition (ii) will obviously be satisfied before landing and printout will occur automatically on landing when condition (i) is satisfied.

A sample printout is shown in Fig. 27. Readings from the counters on the Transmission Fatigue Life Usage Indicator and flight identification data are entered by ground staff after each flight in the appropriate spaces provided in the printout.

8. SOFTWARE FOR TRANSMISSION FATIGUE LIFE USAGE INDICATOR

The airborne system requires a computer program stored in ROM (Section 5.5). Functions of the program are:

(i) Real-time estimation and indication of fatigue life usage for the requisite four gears.

(ii) Real-time indication of total flying time.

(iii) Real-time storage of basic torque data for post-flight printout.

(iv) Post-flight printout of basic torque band data together with gear fatigue life usage and flying time data for the current flight.

The basic computation philosophy is in accordance with that outlined in Section 2.2.2. To take account of the finite measurement resolution the analytical techniques discussed in Section 3.4 and further developed in Appendix 2 have been employed, System hardware decisions (Section 5.5) form the basis for much of the system software development.

8.1 Fatigue Life Usage Computation Program

For reasons expounded in Section 3.4 high torque measurement accuracy is essential but high measurement resolution is not. By utilizing the eight more significant bits of the 12-bit ADC output (Section 5.4) a resolution of 0·6% rated torque per bit results. Such resolution for torque measurement is quite adequate for life usage estimation purposes provided allowance is made for the mean under-estimate applicable to such measurements. To accommodate worst case conditions (Section 4.2) it must be possible to handle twin-engine total torque values at least to 123% and single-engine torque values at least to 150%. For the four gears of interest (Section 4.3) the factored endurance limits (according to Fatigue Curve 1 relationships of Section 2.1) vary from about 105% for G4 subject to total torque to about 118% for G1 or G2 subject to individual engine torque. It follows that, based on 0·6% torque input resolution, the number of input values which need to be handled for fatigue life usage computation purposes will only be of the order of 50 for each of the test gears for Sea King.

According to the analysis of Section 3.3 the demands on sampling rate are not very stringent although the system must respond to blade passing frequency (17 Hz). For each 'sample' both torque inputs must be read and the usage for each of the four gears computed. It has been demonstrated that a sampling rate of 100 Hz can be readily achieved, so that value of sampling rate has been adopted. The '100 Hz' rate is chosen specifically because the counting of time periods is greatly simplified using such a figure.

Analytical computations according to the relationships defined in Section 3.4 cannot, in general, be performed in real time at the 100 Hz rate if software computation techniques alone are used. Hardware elements now available for high speed computations could be used but considerably more complex hardware than that discussed in Section 5.5 would then be required. On the other hand, analytical computations for the fatigue life usage per sample for values of torque within the range of interest discussed above can be pre-computed and entered as values

in look-up tables (Appendix 2). Because all microcomputing systems are capable of very fast acquisition of values stored in tables such a method has been adopted. Use of look-up tables and of integer arithmetic allowed the 100 Hz sampling rate to be realized.

One practical disadvantage of the use of tables is that there may be a need for the tedious repetition of the computation of table entries and their subsequent transfer to an assembly language program. Even a slight change in the value of any of the basic parameters (e.g. the endurance limit) can necessitate a repeat of the laborious computational process. To avoid the disadvantages of the above approach a Fortran program[16,17] LIFCAL·FOR which runs on a DEC system 10 computer has been written. This program accepts basic data (factored endurance limit, gear rotational speed etc.) entered at the terminal, generates an output file which is written directly in Motorola MC6800 assembly language and provides all the relevant look-up values.

Initially the Fatigue Curve 2 relationship (Section 2.1 and Fig. 2) has been used for computing the table entries. Only a slight modification to the program is required to provide a table conforming to the Fatigue Curve 1 relationship. Outputs from the LIFCAL program for Gear 1 to Gear 4 are reproduced in Figs 28 and 29. The endurance limit *TB* in these tables corresponds to the factored base endurance limit T_{BS} indicated in Section 4.3.

Each table entry is allocated two bytes (16 bits) of program storage. The fatigue life usage per reading (i.e. for each 0·01 s for the current application) is represented by an integer between 256 and 65535 (i.e. between 2^8 and $2^{16}-1$). An arbitrary representation 500 is allocated for the second table entry. The first entry is special in that integration is normally over only part of a 0·6% bit width since the endurance limit does not normally reside on a bit boundary. Hence the first entry may have an integer value below 256.

If the usage per reading overflows the 65535 value the number is shifted eight bits to the right and the fact is indicated by the entry at the earlier part of the table corresponding to the '2-BYTE BREAKPOINT'. A micro-life fatigue life usage unit is represented by a six-byte integer computed by LIFCAL and entered at the early part of the table. For the Fatigue Curve 2 relationship for Sea King this usage unit has four leading zeros.

For the Fatigue Curve 1 relationship for Sea King and for other applications the ratio of maximum to minimum life usage per reading may be much greater than for the present case. In such instances a wider range of table entry values would result. The LIFCAL program has been written with such broader applications in mind.

Table entries for Gear 1 and Gear 2 are the same, hence three tables are required for the airborne system.

The system software will provide a resolution of better than 0·2% (i.e. one part in 500 where '500' is the second fatigue life usage entry in the tables) in the specification of the current value of fatigue life usage for values of torque just above the endurance limit. As the value of torque is increased the resolution will improve, except that it could drop to a value not less than one part in 256 in the vicinity of a breakpoint, if the torque range were high enough to include such a breakpoint.

An example of the use of the tables in the airborne system program is included in Section 8.2.

8.2 Airborne System Program

The airborne system source program[16,18] TRMLIF . M68 is written in Motorola MC6800 assembly language and includes the fatigue life usage tables discussed in the previous section. Total program storage requirement is 2045 words (8-bit). As indicated in Section 5.5 there is one peripheral interface adaptor (PIA) allocated for input/output according to the specification given in that section. The source program has been written with generous use of subroutines to facilitate initial program debugging (Section 8.3).

The program may be divided into two broad areas:

(i) Regular handling of torque inputs and real time indication of fatigue life usage.

(ii) Post-flight printout of information relating to the current flight.

To accurately compute the number of stress cycles which occur per unit time (Section 3.1) and hence to estimate the rate of fatigue life usage, it is essential that sampling for (i) be regular. On the other hand the post-flight printout for (ii) can be performed without any restrictions on timing.

Regular sampling and handling of torque data can be achieved in two basic ways:

(i) By operating the system in a non-interrupt mode and incorporating time delay loops to guarantee that all program paths are suitably equalized to provide regular sampling (once every 10 000 machine cycles for 100 Hz sample rate and a 1·00 MHz clock).

(ii) By dividing the clock frequency by 10^4 using external hardware and causing program interrupts to occur at 100 Hz rate.

The former approach has been adopted for the Transmission Fatigue Life Usage Indicator as it results in the simplest hardware. Although additional program instructions are required for time equalization of all program paths there is no hardware penalty as the complete program may be stored in a single 2K ROM. Initially there was some apprehension relating to this approach as it was thought that the effort required to write and debug a program which would have all paths time equalized may be considerable. However it was found that the uneasiness was totally unfounded as both the initial program development and the later debugging proceeded smoothly with very little additional effort being attributable to the need for time equalization. To achieve this result some special programming techniques were used and debugging was greatly enhanced with the aid of a logic analyser.

Use of the more conventional interrupt approach still involves careful timing considerations. Normally an interrupt program would require all possible paths to be executed before the next interrupt occurs. However since execution times for the most common paths are significantly lower than that for the longest path, it is possible that a higher sampling rate could be achieved by stacking consecutive readings (with the need for more RAM storage possibly) and thus enabling completion of program execution relative to a particular reading to be delayed to a time later than the end of the sampling period associated with that reading.

A broad appreciation of the program operation may be obtained with reference to the flow charts of Figs 30 to 41.

The major program paths are illustrated in Fig. 30. START is the address of the instruction executed when the RESET line (Sections 5.5 and 5.6) switches from low to high. It is automatically entered at power-up and whenever the Reset button on the Flight-Line Function Tester (Section 6.1) is depressed. During normal operation the subroutine FRAME is executed repetitively at exactly 100 times per second. When an automatic print request is received at the end of a flight, or when the manual print request pushbutton (on the printer assembly or on the Tester) is depressed, exit from FRAME to the subroutine PRINT will occur.

There are six major passes (Figs 31–33) which occur within the subroutine FRAME prior to exit. The value stored at RAM location CURADR (current address) is used by the program to keep track of pass number. Actions which occur for each pass are summarizeed in the following table.

In those sections of the TRMLIF program for which execution times are important the values (in machine cycles) have been indicated on the flow charts (Figs. 30–38). For simplicity time equalization paths have been omitted from these charts.

The main time delay of the frame which is entered unconditionally at SETRAT (Fig. 32) takes 3191 machine cycles or 31·91% of the total frame execution time. It follows that the present program is capable of operating at 146·9 Hz frame repetition rate. There is therefore considerable reserve capacity for any future program extensions.

Analogue channel advance, issue of command-to-convert signal to the ADC and reading of the torque data are accomplished via the ADCONV subroutine (Fig. 34) which is called when CURADR has zero value. The resultant timing relationship for these signals is indicated in Fig. 42.

CURADR	ACTION
0	Reads both channels of torque data, computes torqueband duration data, handles print requests, totalizes flying time, handles flying time counter readout and introduces the main time delay of the frame to set the rate to exactly 100 frames per second
1	Handles Gear 1 fatigue life usage computation and counter readout
2	Handles Gear 2 fatigue life usage computation and counter readout
3	Handles Gear 3 fatigue life usage computation for port engine torque loading only and omits counter readout
4	Handles Gear 3 fatigue life usage computation for starboard engine torque loading and handles counter readout for both port and starboard loading
5	Handles Gear 4 fatigue life usage computation and counter readout

Subroutine FLUCH (Fig. 33) is used for fatigue life usage conputatiom and for advancing the readouts for each gear. If torque exceeds the endurance limit for the particular gear, subroutine LIFRCT is entered. The current values of usage for all gears are stored as six-byte (48-bit) numbers in RAM. If the usage value for a particular gear exceeds that which corresponds to a micro-life unit of expenditure, the corresponding readout is advanced one count and a micro-life usage unit is subtracted from the progressive sum via subroutine SUBTST (Figs 33 and 38).

An appreciation of the way in which the look-up tables (Section 8.2) are to be interpreted by the airborne system program can readily be obtained with the aid of a simple example. If the eight more significant bits of the analogue-to-digital converter output for Gear 4 (Spiral Bevel Pinion—Fig. 29), say, represent a value of 187 (decimal) the following procedure is followed to compute the fatigue life usage for the current 0·01 s sample.

(i) The second entry in the MGBTBL table indicates that the current reading of 187 is not less than the endurance limit reading of 177 and hence some fatigue life usage will occur.

(ii) The third and fourth entries indicate that the torque range for this table does not include a two-byte or a three-byte breakpoint and hence the multiplication factor for all table values will be unity (not 256 or 65536 as would be required if two-byte or three-byte breakpoints respectively were indicated for certain readings).

(iii) From the table the entry corresponding to a reading of 187 is the integer 1185 (decimal).

(iv) Entries 5, 6 and 7 in the table (i.e. values 0, 0 and 16295) indicate that a micro-life usage unit is equivalent to an integer value of 16295.

(v) The integer value to be added into a summing store each time a new conversion yields a reading of 187, is 1185.

(vi) Integer addition of the look-up table values is performed each time the converter reading falls within the range of the table.

(vii) The value of the progressive sum held in the summing store is tested to see whether the micro-life unit value of 16295 is exceeded.

(viii) If the value is exceeded the appropriate electromechanical counter reading is advanced by one and the integer value 16295 is subtracted from the progressive sum.

A separate summing store is required to minotor the fatigue life usage of each of the four selected gears.

Torque band limits (Section 4.2) are also stored as look-up tables in ROM. For each sample period (0·01 s in this case) the bands within which the current torque values lie are ascertained for each of the three requisite torque spectra (port engine, starboard engine and total torque spectra). To accommodate the requisite 10 bands (Section 4.2) per spectrum three 10-element storage arrays are used. The appropriate array element is incremented (an addition of one to the element contents represents the addition of 0·1 s to the totalized time) at the sampling rate. The totalized times that the torque falls within the various bands during the current flight are computed at the end of the flight from the array element contents and form part of the post-flight printout.

Each time the readouts are advanced the corresponding coils are energized for the duration of three frames (0·03 s). Subroutine OPTEST (Fig. 33) ensures that at least another 0·03 s elapses before another readout pulse can occur. Thus the readout pulse repetition period is constrained to be greater than or equal to 0·06 s. Hence the maximum instantaneous rate of expenditure which can be handled by the readouts is $16\frac{2}{3}$ micro-life units per second. Under high torque load conditions it is quite possible for the computed rate of fatigue life usage to exceed the maximum readout rate. Buffer storage inherent in the six-byte value representing current value of usage allows the excess usage to be stored for readout as soon as the torque level drops. In the case of the Sea King gear tables (Section 8.1) the buffer storage exceeds the total safe gear life value so there would be no chance of overflow from the progressive sum even if very high torque loads were maintained for a considerable time.

It is essential that the readouts absorb any gear usage indicated in the progressive sums before post-flight printout occurs. In practice such usage can always be handled since very high torque loading never occurs just prior to the termination of the flight.

Separate flags IRQA1 and IRQA2 are set in the PIA whenever an external 'manual' or 'auto' print request respectively is received. These flags are examined via subroutine PRTENB (Figs 34 and 37) and *if* other conditions indicated subsequently are satisfied printing as indicated in Fig. 27 will be initiated. When printing is in progress normal torque measurement and life usage computation always cease until the printing has been completed.

When IRQA1 is set by a manual print request (either by pressing the pushbutton on the Flight-Line Function Tester or that mounted at the rear of the modified printer) transfer to the PRINT subroutine will occur as soon as it is detected that all the electromechanical counters have been simultaneously inactive (coils de-energized) for the duration of one frame (0·01 s).

When IRQA2 is set under the action of an automatic print request meeting the hardware conditions specified in Section 7, subroutine PRTENB checks whether the following conditions monitored by software are satisfied.

(i) A certain level of torque (50% total torque for the initial program) has been exceeded since power-up (or previous print-out).

(ii) A certain time (five minutes for the initial program) has elapsed since power-up (or previous print-out).

(iii) Any life usage in excess of one micro-life unit which is still pending, or which is being regularly generated due to a high value of current torque, has been transferred to the appropriate electromechanical counter.

(iv) All counters, including that which indicates Total Flying Time, have been simultaneously inactive (coils de-energized) for the duration of one frame (as for the manual print request).

If all of the above conditions are satisfied transfer to the PRINT subroutine will occur. The requirement for these conditions to be satisfied serves to eliminate extraneous printing during the start-up period.

If the printer is not connected or is out of paper, the program will return after a nominal one second delay (Fig. 41) to normal operation without clearing the data stored in RAM. In practice this means that a portable printer may be plugged into the Transmission Fatigue Life Usage Indicator after a flight and the data extracted using the manual print button to initiate

the printout. Alternatively, if the printer runs out of paper during a printout it is possible to insert a new roll and still obtain a complete printout using the manual print button to initiate the printout. However as the data are stored in volatile memory not supported with battery back-up power, it is essential that all the requisite data be extracted before power-down.

Fixed alphanumeric data for printout are stored as a print table in ROM. Numerical data which require computation and suitable conversion for printout are accessed via subroutine GETSUB (Fig. 40). A null entry in the print table causes the program to transfer to GETSUB. There are nine separate computational/conversion routines required for the post-flight printout. The routines are selected in sequence for each successive call to GETSUB.

During the normal flight, transfer of indeterminate data to the print buffer can occur as the printer lines always follow the PIA outputs PB0 to PB7 (Sections 5.5 and 5.6). Thus it is desirable that the print buffer in the Datel printer be cleared at the time the PRINT subroutine is called. A special feature of the printer is that the ASCII delete character (7F in hex code) will cause the contents of the buffer to be cleared if the CONTROL CHARACTER ENABLE bit is set (i.e. if PB7 is set in the present instance). Clearance in this manner is performed prior to the transfer of any print characters.

8.3 Arrangement for Validating System Program

Any microcomputing system requires an efficient arrangement for initially testing and editing programs. Altering of programs stored in erasable ROM is slow and cumbersome; hence it is preferable to store programs in RAM when editing will be required. Since much of the system program relates to the specific hardware arrangement of the Fatigue Life Usage Indicator (FLUI), it is essential that the test configuration be capable of transferring data to or from the PIA in the FLUI.

A block schema of the arrangement used for system program checking is drawn in Fig. 43. Special hardware referred to as an In-Circuit Emulator (ICE) has been designed and manufactured at these laboratories for testing airborne systems of the type used in the FLUI. To implement the system of checking using the ICE a flat cable is connected between the ICE bus system and the bus system of the FLUI. In practice the connection is made by removing the MPU (Fig. 21) from its socket and plugging the cable termination directly into that socket. The erasable ROM device is normally removed from the FLUI for system program checking. Care has to be exercised in the allocation of addresses so that each element in the overall system has a unique address.

Generation and editing of source programs written in Motorola 6800 assembly language is performed using the teleprinter or visual display unit terminal connection (Fig. 43) to the main computer (in this instance a DECsystem 10 manufactured by Digital Equipment Corporation). Program assembly into a loadable file is performed using a Motorola M68SAM cross-assembler available from the main computer.

All processing is controlled by the MC6800 microcomputer in the ICE. The MICROBUG 8A monitor[19] ROM is plugged into the ICE and provides convenient operator interface. It enables

(i) Load files to be transferred directly from the main computer to RAM via the RS-232 serial duplex interface to the ICE which includes an Asynchronous Communications Interface Adaptor (ACIA).

(ii) Reading and modifying the contents of memory using simple commands entered via the terminal device.

(iii) Execution of test programs via the simple command sequence * G XXXX where 'XXXX' is the requisite starting address.

For test purposes the airborne system program is stored in the ICE RAM which has considerable storage reserve. Additional program sequences required for testing are readily accommodated.

At power-up or when the RESET button on either the Flight-Line Function Tester or the ICE is actuated, the program will return to the MICROBUG starting address and indicate its readiness to accept operator commands by typing the prompt '*' character at the terminal.

Adjustable solder links in the ICE allow different RAM address ranges to be selected. As indicated in Section 5.5, a link connection may be arranged so that the Reset vector address in the airborne system ROM is not accessed at power-up or when the system is manually reset, Under these conditions it is impossible to operate the system program (stored in ROM in the FLUI) under the control of the monitor program which is automatically engaged at power-up.

To facilitate program testing it has been found advantageous to make liberal use of subroutines in the system program. Simple test programs may be written to call individual subroutines for checking.

A logic analyser is regarded as an essential item of test equipment for efficient debugging of programs. The analyser is connected to the address and date buses in such a way that the operation of both the FLUI and the ICE can be monitored in real time. In particular, in those sections of the program where timing is critical, it greatly simplifies the equalization of the execution times of the various program paths.

9. SYSTEM OVERVIEW

9.1 Current Status of Transmission Fatigue Life Monitoring Program

Two Sea King aircraft operated by the RAN are currently fitted with prototype transmission fatigue life usage indicating systems. Some large zero shifts were initially encountered in the measurement of torquemeter pressure for the first system, due mainly to ingestion of corrosive contaminants into the vented section of the Bell and Howell transducers and into the mating connector assembly (Section 4.1). Following modification of these transducers by the manufacturers the first system was re-installed in Sea King in July 1982 and has been operating satisfactorily since then. The second system employing the alternative but similar type Druck transducers (Section 4.1) was originally installed in Sea King in March 1983 and has operated satisfactorily since installation.

In-service torque load and fatigue life usage data which are automatically printed out after each flight are regularly sent to these laboratories. It is envisaged that the load data will be used to estimate the safe fatigue lives in operating hours for critical gears in Sea King helicopters operating in the Australian environment. It is estimated that at least 500 hours of load data must be accumulated before prediction work[3] with the aid of a ground-based digital computer can proceed. At the present rate of data collection 500 hours should have been accumulated by late-1984. A data base management program has been developed to facilitate storage and selective retrieval of the transmission data.

Trends in the data gathered so far tend to indicate that fatigue damage occurs for less than 20% of flights. It may be difficult to associate life usage with sortie type as was done for Wessex[3] and hence fleetwide prediction may be very difficult. However this type of expenditure could be readily accommodated in a program of individual transmission fatigue life monitoring.

Currently the RAN replace fatigue-critical gears on expiry of the 'blanket' life promulgated by the manufacturer to cover sortie patterns for all operators. Furthermore RAN sometimes replace gears after known overtorquing incidents as currently there is no accepted way of assessing damage under such circumstances. Gear box overhauls may of course be undertaken because of factors not related to fatigue life considerations.

RAN has indicated an interest[20] in promoting a scheme of individual transmission fatigue monitoring for the whole Sea King fleet. Of particular interest to the RAN is the anticipated reduction in the number of very expensive transmission overhauls, including those which are undertaken following isolated overtorquing incidents.

To implement a gear replacement policy based on estimated life expenditure of individual transmission components it would be appropriate for the operator to seek formal or tacit approval from the Aircraft Design Authority. It is possible that the operator could persuade his national airworthiness authority to agree to the setting of fatigue lives which differ from those set by the manufacturer. Currently there is no aircraft operator in the world who employs a maintenance policy for which replacement of fatigue-critical gears is based on individual gear indicated life expenditure.

Before an individual transmission fatigue replacement program could be implemented it would be necessary to establish values of indicated life expenditure at which fatigue-critical gears should be replaced. The values will be very much dependent (Section 3.1) on the accuracy applicable to the torque load measurement. Currently the prototype systems are realigned if the pressure-to-voltage relationship has shifted by more than about 0·5% since the previous alignment. The systems have not been installed long enough to establish the period over which the calibration is likely to be maintained within such limits. The accuracy of the aircraft system of torque-to-pressure conversion is still being investigated (Section 4.1). However it is anticipated that the overall torque measurement accuracy is likely to fall within the range 2·5 to 5·0%.

The value of indicated fatigue life expenditure at which gear replacement should be undertaken cannot be simply deduced from the attainable torque load measurement accuracy. An analysis along the lines discussed in Section 3.1 would provide an appropriate derating factor if the torque spectra applicable for all fatigue-critical gears were known.

An alternative simpler approach would be to derate the factored endurance limits for each critical gear according to the attainable accuracy and replace gears when indicated fatigue life is expended. However, if the gear fatigue relationships were re-estimated and modified for any reason the value of indicated life for replacement purposes would need to be modified for all gear boxes with partially expired fatigue lives at the time of the re-estimation. Hence measurement of torque load spectra, at least on a sample of helicopters, is probably a wise precaution in any event as it would provide the basis for a realistic upgrade of the replacement fatigue life figure in such circumstances.

9.2 Applicability of Airborne System to Alternative Measurements

The system of transmission fatigue life usage estimation and indication as described herein is directly applicable to any twin-engine helicopter with hydraulic torque sensing. Different gear fatigue data relationships and different values of gear endurance limit will yield different life usage tables but the LIFCAL . FOR program (Section 8.1) can readily accommodate such changes. No changes to the system program except for the life usage tables would be necessary.

Fatigue life usage of single-engine helicopter transmission systems can, of course, be readily monitored with the present system. However part only on the system capability would be utilized.

Helicopters which do not have a hydraulic system of torque sensing may require a different analogue signal conditioner. Alternative methods of torque sensing may inherently produce a non-linear relationship between torque input and ADC output. In such instances the non-linearity would have to be taken into consideration when fatigue life usage table values are computed. In other respects the present system program should be directly applicable.

If insufficient gear fatigue data are available to implement a fatigue life usage indicating system the instrumentation described herein can be utilized solely to gather basic torqueband data which are printed out after each flight. If desired more torquebands can be handled without any change in the hardware.

Measurements other than gear-fatigue life usage or total time spent within the various torquebands, can be made with the present airborne system hardware. For instance level excursions, or more specifically the number of times a certain band of torque or other parameter is traversed, can be readily counted. Total count values can be printed out after flight. Modified software would, of course, be necessary.

Generally the airborne system can be used in any application which has definable computations to be made and for which the required amount of output data is not very extensive.

While the basic fatigue life usage indicating system described in this report has been applied only to airborne applications it can, of course, be equally applied to other less stringent applications.

9.3 Changes and Additional Capabilities Worth Considering for Any Future Developments

The basic system of gear fatigue life usage estimation and indication which has been described in this report is applicable to any transmission system for which gear rotational speed is constant. Helicopter transmission systems are well suited because gear rotational speed is essentially constant.

The present instrumentation is not suited to the estimation of gear fatigue life usage in mechanical systems for which significant variations in gear rotational speed occur. However as indicated in Section 3.1 a 1% inaccuracy in torque measurement could readily be equivalent to a 25% inaccuracy in speed measurement so it might be argued that speed fluctuations of $\pm 20\%$, say, could with little effect on the indicated rate of fatigue life usage, be approximated by a mean speed. In applications where the speed variations are very large it would be necessary to measure gear speed and transfer the measured value as an additional input to the microcomputing system. Although gear usage look-up tables could still be used, a multiplication by the current speed value would be essential for each torque reading. From considerations discussed in Section 3.3 it is probable that the sampling rate could be reduced to allow software multiplication routines to be implemented with the present hardware for this purpose. If the resulting response speed were inadequate to allow transients to be followed in a particular application, a hardware multiplication capability might be necessary to allow the sampling rate to be increased and the required speed of operation to be attained. Such a computing capability would considerably extend the range of applications in which the system could be used. An extension of the input data reading capability would be essential to enable gear rotational speed to be read.

While the prototype fatigue life indicating hardware installed in Sea King has performed well there are a number of changes which may be worth including in an advanced airborne model.

The prototype system requires a signal conditioning card which plugs into the main Transmission Fatigue Life Usage Indicator, to be adjusted according to the specific characteristics of the associated transducers used to measure torquemeter pressure. Since transducer in-service characteristic changes and unserviceability have generated most of the maintenance demands thus far, it would seem appropriate to arrange for transducer zero and sensitivity adjustments external to the Indicator. In that way all Indicators would be interchangeable and transducer/matching card combinations would also be interchangeable.

Although faultless operation of the electromechanical counters, used for cumulative fatigue damage and total flying time indication, has been demonstrated in the airborne environment the Indicator size could be substantially reduced by the use of liquid crystal displays with long-life battery back-up. The battery would allow data retention and display when system power is switched off.

While the printer is a suitable unit for use in the early development stage it does require post-flight printout paper removal at least daily and periodic paper roll replacement. Furthermore great care has to be exercised to keep the printer mechanism clean and free of contaminants. A more robust system with data storing capability, such as could be provided by semiconductor, magnetic bubble or magnetic tape cartridge systems would be recommended. The stored information could be read periodically and transferred simply to a ground based computer.

Inclusion of some Built-in-Test (BITE) functions in the on-board Indicator rather than in the Flight-Line Function Tester would be advantageous for maintaining the system functional.

Further refinement such as the inclusion of a real-time clock with battery back-up and the capability to simply enter identification data would be advantageous. The clock could be used to automatically log date-of-flight and take-off time. Identification data would include gearbox and aircraft numbers requiring initial entry only, and sortie type requiring an entry for each flight.

The degree of conservatism applied in the specification of a safe fatigue relationship and the inability to precisely measure transmission loads are factors which limit the period over which fatigue-critical gears can be operated with confidence. Improvements in the estimation of the safe fatigue relationship or in the accuracy of transmission load measurement would allow the lives of fatigue-critical gears to be confidently extended.

10. CONCLUSIONS

(*a*) Fatigue life expenditure of helicopter transmission components can be estimated if sufficient gear fatigue data are available and if the load histories for the components are known.

(*b*) The requisite gear fatigue data may be obtained from tests to failure on samples of gears and from in-service experience.

(*c*) Special torque data logging instrumentation must be fitted to one or preferably more helicopters in the fleet to provide details on the load history.

(*d*) In-service load spectra may vary significantly for different operational roles and hence it is usually necessary for each operator to measure his own spectra.

(*e*) Absolute torque load measurement accuracy should be optimized and high attenuation of alternating noise components which do not reflect true torque should be provided.

(*f*) The torque load measuring instrumentation should have adequate bandwidth to pass dynamic torque components, at least up to blade passing frequency (17 Hz for Sea King).

(*g*) The resolution of the torque measurement need not be particularly high.

(*h*) High precision in the estimation or measurement of gear rotational speed is not a requirement.

(*i*) For twin-engine helicopters, three torque spectra, those for individual engine torques and that for total torque, are necessary for estimating the safe lives of all gears.

(*j*) Safe fatigue lives in operating hours may be predicted for critical gears using a ground based computer analysis, provided in-service load data are available from sufficiently large samples of sorties of the various types.

(*k*) Fatigue life usage for critical helicopter transmission components may be estimated and indicated during flight with the aid of an on-board microcomputer provided adequate gear fatigue data are available.

(*l*) Fatigue life usage indicators of the type described could be used for monitoring individual transmissions and would enable an 'on-condition' maintenance policy to be implemented.

(*m*) The estimated safe-life of critical gears increases dramatically as the factored endurance limit is increased (either because of an inherently high unfactored limit or because a low scatter factor is used).

(*n*) To take account of measurement inaccuracies the summation of life fractions expended to a value less than unity is recommended when real-time indication of gear fatigue life usage is employed. The value may be set closer to unity for gears having relatively short fatigue lives.

(*o*) Gear life usage increments may be conveniently pre-computed and stored in tabular form in the airborne system program used for fatigue life usage indication.

(*p*) Basic torque spectrum information may be printed out after each flight and used for re-estimation of safe-lives of critical components, as would be required if the gear fatigue relationships were updated for any reason.

(*q*) Airborne instrumentation developed primarily to provide real-time indication of helicopter transmission fatigue life usage can be used in a variety of alternative applications with little alteration.

ACKNOWLEDGEMENTS

The author wishes to acknowledge the considerable contributions by other members of the scientific staff at these laboratories. In particular the following are worthy of special note:

(i) Expert guidance in all matters relating to gear fatigue relationships and safe life predictions by Mr. C. N. King.

(ii) Assistance with hardware design concepts and overall management of detailed specifications, manufacture, testing and commissioning of the system by Mr U. R. Krieser.

(iii) Advice on and selection of suitable transducers by Mr D. H. Edwards.

(iv) Assistance with the engineering development of the Transmission Fatigue Life Usage Indicator and the associated Tester by Mr K. W. Vaughan.

(v) Assistance with system checkout, especially in the program debugging area, and with the generation of program firmware by Mr O. H. Holland.

(vi) Detailed drafting and manufacturing of much of the system hardware by members of the Engineering Facilities Division.

REFERENCES

1. Fraser, K. F., and King, C. N. Helicopter Transmission Fatigue Life. Proceedings of Fifth International Symposium on Air Breathing Engines. Bangalore. Paper 09, February 1981.

2. Fraser, K. F. In-Flight Computation of Helicopter Transmission Fatigue Life Expenditure. AIAA Paper 81-2434. AIAA First Flight Testing Conference. Nevada. November 1981. Republished in revised form AIAA Journal of Aircraft. Vol. 20, No. 7, pp. 663-640. July 1983.

3. King, C. N. RAN Wessex Mk 31B Helicopter. Fatigue Life of Main Rotor Gear Box. ARL report to be published.

4. Fraser, K. F., and Krieser, U. R. Load Spectrum Measuring Equipment. Part 1. Details of Mk 1 System Presently Used to Acquire Data in Wessex Mk 31B Helicopters. ARL M/E Note 371. August 1978.

5. Fraser, K. F., and Krieser, U. R. Load Spectrum Measuring Equipment. Part 2. Details of Mk 2 System Used to Acquire Torque Load Data in Sea King Helicopters. ARL M/E Note 372. September 1978.

6. Wessex HAS Mark 1 Main Gearbox Fatigue Test. Westland Aircraft Ltd. Report G663 Part A. November 1961.

7. Wessex Structural Integrity Study Marks 1, 2, 3 and 5—Fatigue Life Substantiation of the Main Drive Gears in the Main Gear Box. Westland Helicopters Ltd. Report S.D. 895. July 1970.

8. Fatigue Tests Carried Out on the Sea King Main Gearbox—Sea King Mk 1, 2 and 3. Westland Helicopters Ltd. Report G4. 7256/1. January 1978.

9. Analysis of the Fatigue Test Results of a Large Sample of Ground Speed Bevel Gears. Westland Helicopters Ltd. Report S.D. 867. May 1967.

10. Miner, M. A. Cumulative Damage in Fatigue. Journal of Applied Mechanics. ASME, Vol. 12. 1945.

11. Design and Life Substantiation of Parts Subject to Fatigue Loading. Westland Helicopters Ltd. Report S.D. 886. June 1968.

12. Pavia, R. V. Measurement of the Input Torque to the Main Rotor Gearbox of a Wessex Mk 31B Helicopter. ARL M/E Note 361. March 1976.

13. Everleigh, V. W. Introduction to Control Systems Design. McGraw-Hill. Copyright 1972.

14. Bossler, R. B. Rotorshaft Torquemeter. Journal of the American Helicopter Society. April 1983.

15. Engine and Transmission Limitations. Westland Helicopters Ltd. Sea King Document A.P. (RAN) 300-8-1.

16. Krieser, U. R. Helicopter Transmission Fatigue Life Usage Indicating System Detail. ARL Mechanical Engineering Technical Memorandum 406. November 1980.

17. Fraser, K. F. Fortran F10 Program LIFCAL . FOR—for computing entries in gear usage tables. ARL Software. December 1978.

18. Fraser, K. F. Assembly Language Program TRMLIF . M68—airborne system operating program. ARL Software. March 1980.

19. MICRObug Source Listing—M68MM08A Micromodule 8A. Motorola Publication. Copyright 1978.

20. Gillard, L. F. The Way Ahead for Torque Spectra and Fatigue Life Usage Measurements in the Sea King. Report of the Fourth Meeting of Air Standardization Coordinating Committee—Working Party 18—Annex AAA. Ottawa. 21 September-8 October 1982.

APPENDIX 1

Evaluation of Integrals for Estimating the Effect of Absolute Measurement Inaccuracies

Using the relationships derived in Section 3.1, expressions for the measurement error α resulting from absolute torque measurement inaccuracy can be determined for the two torque versus life cycles curves defined by equations 14 and 15 and for the two torque spectra defined by equations 16 and 17.

(*a*) *Expression for* α *for Curve 1 and Torque Spectrum 1*

Equations 14, 16, 18 and 20 (Section 3.1) yield the following expression for α.

$$\alpha = \frac{\int_0^{\sigma+\varepsilon} X^{B_1}\, dX}{\int_0^{\sigma} X^{B_1}\, dX} - 1$$

$$= \left(1+\frac{\varepsilon}{\sigma}\right)^{B_1+1} - 1 \qquad \text{(A1)}$$

(*b*) *Expression for* α *for Curve 1 and Torque Spectrum 2*

To take account of the apparent shift of the upper torque limit from σT_{ES} to $(\sigma+\varepsilon)T_{ES}$ the relationship of equation 17 (Section 3.1) for Torque Spectrum 2 needs to be modified slightly as shown below.

$$-\frac{dq}{dX} = \frac{K_2}{\sigma}\left(\sigma+\varepsilon-X\right) \qquad \text{(A2)}$$

Equations 14, 17, 18 and 20 (Section 3.1) with the above modification then yield the following expression for α.

$$\alpha = \frac{\int_0^{\sigma+\varepsilon} (\sigma+\varepsilon-X)\, X^{B_1}\, dX}{\int_0^{\sigma} (\sigma-X) X^{B_1}\, dX} - 1$$

$$= \left(1+\frac{\varepsilon}{\sigma}\right)^{B_1+2} - 1 \qquad \text{(A3)}$$

(c) *Expression for α for Curve 2 and Torque Spectrum 1*

As indicated in Section 3.1 (equation 15) the relationship

$$\frac{1}{N} = C_2 \, e^{X/B_2} \tag{A4}$$

applies in the range $0{\cdot}1542 \geqslant X \geqslant 0{\cdot}0393$.

For generality the lower limit for X of $0{\cdot}0393$ has been defined by the symbol X_L in Section 3.1. For convenience the upper limit in the value of X for which the above relationship applies will be defined as X_M (i.e. $X_M = 0{\cdot}1542$). Thus the above relationship applies for $X_M \geqslant X \geqslant X_L$ and the Curve 1 relationship (Section 3.1)

$$\frac{1}{N} = \left(\frac{X}{A_1}\right)^{B_1} \tag{A5}$$

applies for $X \geqslant X_M$.

To estimate the measurement error α resulting from absolute torque measurement inaccuracy it is necessary to develop a different expression for the case $\sigma < X_M$ to that for $\sigma > X_M$.

Equations 16, 18 and 20 yield the following general expression for α:

$$\alpha = \frac{\displaystyle\int_{X_L}^{\sigma+\varepsilon} \left(-\frac{dq}{dX}\right)\frac{1}{N}dX}{\displaystyle\int_{X_L}^{\sigma} \left(-\frac{dq}{dX}\right)\frac{1}{N}dX} - 1 \tag{A6}$$

For Torque Spectrum 1

$$\frac{dq}{dX} = -K_1$$

and hence

$$\alpha = \frac{\displaystyle\int_{X_L}^{\sigma+\varepsilon} \frac{1}{N}dX}{\displaystyle\int_{X_L}^{\sigma} \frac{1}{N}dX} - 1 \tag{A7}$$

Each of the integrals in the above equation may be more generally defined as

$$I_1(\eta) = \int_{X_L}^{\eta} \frac{1}{N}\,dX \tag{A8}$$

where $\eta = \sigma$ or $\sigma+\varepsilon$ as appropriate.

Because the analytical expressions (equations A3 and A4) which apply for $1/N$ in the ranges $X \leqslant X_M$ and $X \geqslant X_M$ differ, the expressions representing the value of the integral $I_1(\eta)$ in the ranges $\eta \leqslant X_M$ and $\eta \geqslant X_M$ will likewise by different. To distinguish between these a second suffix will be added such that:

$$I_{1_1}(\eta) = I_1(\eta) \text{ in the range } X_L \leqslant \eta \leqslant X_M$$

and

$$I_{12}(\eta) = I_1(\eta) \text{ in the range } \eta \geqslant X_M$$

Thus for $X_L \leqslant \eta \leqslant X_M$

$$I_{11}(\eta) = \int_{X_L}^{\eta} C_2 \, e^{X/B_2} \, dX$$
$$= L_1(e^{(\eta - X_L)/B_2} - 1) \tag{A9}$$

where L_1 is a constant given by

$$L_1 = C_2 B_2 e^{X_L/B_2} \tag{A10}$$

For $\eta \geqslant X_M$

$$I_{12}(\eta) = \int_{X_L}^{X_M} C_2 e^{X/B_2} dX + \int_{X_M}^{\eta} \left(\frac{X}{A_1}\right)^{B_1} dX$$
$$= L_2(\eta^{B_1+1} + L_3) \tag{A11}$$

where L_2 and L_3 are constants given by

$$L_2 = \frac{1}{(B_1+1)A_1^{B_1}} \tag{A12}$$

and

$$L_3 = X_M^{B_1+1}\left\{\frac{B_2(B_1+1)}{X_M}\left[1 - e^{-(X_M - X_L)/B_2}\right] - 1\right\} \tag{A13}$$

since the curves represented by equations A4 and A5 coincide at

$$X = X_M$$

i.e.

$$C_2 e^{X_M/B_2} = \left(\frac{X_M}{A_1}\right)^{B_1}.$$

Using the relationships of equations A9 to A13 the following expressions for the measurement error α result.

For $X_L \leqslant \sigma \leqslant X_M$ and $X_L \leqslant (\sigma+\varepsilon) \leqslant X_M$ (ε can be considered to be either positive or negative)

$$\alpha = \frac{I_{11}(\sigma+\varepsilon)}{I_{11}(\sigma)} - 1$$
$$= \frac{e^{(\sigma+\varepsilon - X_L)/B_2} - 1}{e^{(\sigma - X_L)/B_2} - 1} - 1 \tag{A14}$$

For $\sigma \geqslant X_M$ and $(\sigma+\varepsilon) \geqslant X_M$

$$\alpha = \frac{I_{12}(\sigma+\varepsilon)}{I_{12}(\sigma)} - 1$$
$$= \frac{(\sigma+\varepsilon)^{B_1+1} + L_3}{\sigma^{B_1+1} + L_3} - 1 \tag{A15}$$

Neither equation A14 nor A15 applies in the immediate vicinity of $\sigma = X_M$ but the general expressions of A9 and A11 can be applied.

For $\sigma \leqslant X_M$ and $(\sigma+\varepsilon) \geqslant X_M$

$$\alpha = \frac{I_{12}(\sigma+\varepsilon)}{I_{11}(\sigma)} - 1$$

$$= \frac{L_2\{(\sigma+\varepsilon)^{B_1+1} + L_3\}}{L_1\{e^{(\sigma - X_L)/B_2} - 1\}} - 1 \tag{A16}$$

and for $\sigma \geqslant X_M$ and $(\sigma+\varepsilon) \leqslant X_M$

$$\alpha = \frac{I_{11}(\sigma+\varepsilon)}{I_{12}(\sigma)} - 1$$

$$= \frac{L_1\{e^{(\sigma+\varepsilon - X_L)/B_2} - 1\}}{L_2\{\sigma^{B_1+1} + L_3\}} - 1 \tag{A17}$$

(*d*) *Expression for* α *for Curve 2 and Torque Spectrum 2*

The general relationship of equation A6 applies for α. However, as indicated in (*b*), the apparent shift in the upper limit of integration from σ to $\sigma+\varepsilon$ for the upper integral means that the modified relationship of equation A2 applies for dq/dX.

Hence

$$\alpha = \frac{\int_{X_L}^{\sigma+\varepsilon} (\sigma+\varepsilon-X)\frac{1}{N}dX}{\int_{X_L}^{\sigma} (\sigma-X)\frac{1}{N}dX} - 1 \tag{A18}$$

Each of the integrals in the above equation may be more generally defined as

$$I_2(\eta) = \int_{X_L}^{\eta} (\eta - X)\frac{1}{N}dX \tag{A19}$$

where $\eta = \sigma$ or $\sigma+\varepsilon$ as appropriate.

In a similar manner to that used in (*c*) a second suffix will be used to distinguish between the integral which applies for η less than X_M and that which applies for η greater than X_M.

Thus

$$I_{21}(\eta) = I_2(\eta) \text{ in the range } X_L \leqslant \eta \leqslant X_M$$

and

$$I_{22}(\eta) = I_2(\eta) \text{ in the range } \eta \geqslant X_M.$$

Hence for $X_L \leqslant \eta \leqslant X_M$

$$I_{21}(\eta) = \int_{X_L}^{\eta} (\eta - X)C_2 e^{X/B_2}dX$$

$$= L_4\left\{e^{(\eta - X_L)/B_2} - \left(1 + \frac{\eta - X_L}{B_2}\right)\right\} \tag{A20}$$

where L_4 is a constant given by

$$L_4 = C_2 B_2^2 e^{X_L/B_2}$$

$$= B_2 L_1 \tag{A21}$$

For $\eta \geqslant X_M$

$$I_{22}(\eta) = \int_{X_L}^{X_M} (\eta - X) e^{X/B_2} dX + \int_{X_M}^{\eta} (\eta - X) \left(\frac{X}{A_1}\right)^{B_1} dX$$

$$= L_5 \left\{ \left(\frac{\eta}{X_M}\right)^{B_1+2} + L_6 \left(\frac{\eta}{X_M}\right) - L_7 \right\} \tag{A22}$$

where L_5, L_6 and L_7 are constants given by

$$L_5 = \frac{C_2 \, X_M^{\,2} \, e^{X_M/B_2}}{(B_1+1)(B_1+2)}$$

$$= \frac{X_M^{\,B_1+2}}{(B_1+1)(B_1+2) A_1^{\,B_1}}$$

$$= \frac{X_M^{\,B_1+2}}{B_1+2} L_2 \tag{A23}$$

$$L_6 = (B_1+2) \left\{ \frac{B_2(B_1+1)}{X_M} \left[1 - e^{-(X_M - X_L)/B_2} \right] - 1 \right\} \tag{A24}$$

and

$$L_7 = (B_1+1) \left\{ \frac{B_2^{\,2}(B_1+2)}{X_M^{\,2}} \left[\left(1 - \frac{X_L}{B_2}\right) e^{-(X_M - X_L)/B_2} + \frac{X_M}{B_2} - 1 \right] - 1 \right\} \tag{A25}$$

since the curves represented by equations A4 and A5 coincide at

$$X = X_M$$

i.e.

$$C_2 e^{X_M/B_2} = \left(\frac{X_M}{A_1}\right)^{B_1}.$$

Using the relationships of equations A20 to A25 the following expressions for the measurement error α result.

For $X_L \leqslant \sigma \leqslant X_M$ and $X_L \leqslant (\sigma+\varepsilon) \leqslant X_M$

$$\alpha = \frac{I_{21}(\sigma+\varepsilon)}{I_{21}(\sigma)} - 1$$

$$= \frac{e^{(\sigma+\varepsilon-X_L)/B_2} - \left(1 + \dfrac{\sigma+\varepsilon-X_L}{B_2}\right)}{e^{(\sigma-X_L)/B_2} - \left(1 + \dfrac{\sigma-X_L}{B_2}\right)} - 1 \tag{A26}$$

For $\sigma \geqslant X_M$ and $(\sigma+\varepsilon) \geqslant X_M$

$$\alpha = \frac{I_{22}(\sigma+\varepsilon)}{I_{22}(\sigma)} - 1$$

$$= \frac{\left(\dfrac{\sigma+\varepsilon}{X_M}\right)^{B_1+2} + L_6 \left(\dfrac{\sigma+\varepsilon}{X_M}\right) - L_7}{\left(\dfrac{\sigma}{X_M}\right)^{B_1+2} + L_6 \left(\dfrac{\sigma}{X_M}\right) - L_7} - 1 \tag{A27}$$

Neither equation A26 nor A27 applies in the immediate vicinity of $\sigma = X_M$ but the general expressions of A20 and A22 can be applied.

For $\sigma \leqslant X_M$ and $(\sigma+\varepsilon) \geqslant X_M$

$$\alpha = \frac{I_{22}(\sigma+\varepsilon)}{I_{21}(\sigma)} - 1$$

$$= \frac{L_5\left\{\left(\frac{\sigma+\varepsilon}{X_M}\right)^{B_1+2} + L_6\left(\frac{\sigma+\varepsilon}{X_M}\right) - L_7\right\}}{L_4\left\{e^{(\sigma-X_L)/B_2} - \left(1+\frac{\sigma-X_L}{B_2}\right)\right\}} - 1 \qquad \text{(A28)}$$

and for $\sigma \geqslant X_M$ and $(\sigma+\varepsilon) \leqslant X_M$

$$\alpha = \frac{I_{21}(\sigma+\varepsilon)}{I_{22}(\sigma)} - 1$$

$$= \frac{L_4\left\{e^{(\sigma+\varepsilon-X_L)/B_2} - \left(1+\frac{\sigma+\varepsilon-X_L}{B_2}\right)\right\}}{L_5\left\{\left(\frac{\sigma}{X_M}\right)^{B_1+2} + L_6\left(\frac{\sigma}{X_M}\right) - L_7\right\}} - 1 \qquad \text{(A29)}$$

APPENDIX 2

Estimation of Life Usage Taking into Account Finite Resolution of Measuring System

It was shown in Section 3.4 that for an analogue to digital converter (ADC) reading 'i', the best estimate of life usage can be obtained by integrating and averaging the usage over the specified torque band $T_i \rightarrow T_{i+1}$ where T_i is that value of torque which will produce an ADC output just on the switching point $i-1 \rightarrow i$. The following relationship for the life usage u_i over the sample period (i.e. the time between successive torque readings for the particular gear under consideration) was derived in Section 3.4 and given in equation 43.

$$u_i = \frac{s}{f(T_{i+1}-T_i)} \int_{T_i}^{T_{i+1}} \frac{1}{N} dT \tag{A30}$$

where

N is the 'safe' cycles at torque T,

s is gear rotational speed (revolutions per second),

and f is ADC sampling rate (samples per second).

For convenience equation A30 may be rewritten in terms of the variable X (defined elsewhere as the normalized amount by which the torque exceeds the endurance limit).

$$u_i = \frac{s}{f(X_{i+1}-X_i)} \int_{X_i}^{X_{i+1}} \frac{1}{N} dX \tag{A31}$$

where

$$X_i = \frac{T_i}{T_{FS}} - 1 \tag{A32}$$

and T_{ES} is the 'safe' endurance limit.

Curve 2 (Section 2.1) has been initially used for life studies on Sea King main rotor gear box components and will be used for the subsequent analysis. For this curve no life usage occurs for $X < X_L$ (Section 2.1) and coincidence with Curve 1 applies for $X \geqslant X_M$.

The function $N(X)$ included in equation A31 does not remain invariant over the full torque range of interest but follows the relationship defined in Section 2.1 and reproduced below.

$$N = \left(\frac{A_1}{X}\right)^{B_1}$$

for $X \geqslant X_M$

$$N = e^{(A_2 - X)/B_2}$$

for $X_L \leqslant X \leqslant X_M$.

In Fig. 44 the bit boundaries corresponding to the finite resolution ADC output, are illustrated graphically in the torque range of interest. In general the limit X_L below which no life

usage occurs and the value X_M at which a change in the function N occurs, do not normally reside on bit boundaries. It follows that there are four zones (ZONE 1 to ZONE 4—Fig. 44) each requiring slightly different treatment.

For $X_i > X_L$ and $X_{i+1} < X_M$ (ZONE 2—Fig. 44)

$$U_i = \frac{s}{(X_{i+1}-X_i)f e^{A_2/B_2}} \int_{X_i}^{X_{i+1}} e^{X/B_2} dX$$

$$= \frac{s\,B_2}{(X_{i+1}-X_i)f e^{A_2/B_2}} \left(e^{X_{i+1}/B_2} - e^{X_i/B_2} \right) \tag{A33}$$

For $X_i < X_L < X_{i+1}$ (ZONE 1—Fig. 44)

$$U_i = \frac{s}{(X_{i+1}-X_i)f e^{A_2/B_2}} \int_{X_L}^{X_{i+1}} e^{X/B_2} dX$$

$$= \frac{s\,B_2}{(X_{i+1}-X_i)f e^{A_2/B_2}} \left(e^{X_{i+1}/B_2} - e^{X_i/B_2} \right) \tag{A34}$$

For $X_{i+1} > X_M$ (ZONE 4—Fig. 44)

$$U_i = \frac{s}{(X_{i+1}-X_i)f A_1^{B_1}} \int_{X_i}^{X_{i+1}} X^{B_1} dX$$

$$= \frac{s}{(X_{i+1}-X_i)f(B_1+1)A_1^{B_1}} \left(X_{i+1}^{B_1+1} - X_i^{B_1+1} \right) \tag{A35}$$

For $X_i < X_M < X_{i+1}$ (ZONE 3—Fig. 44)

$$U_i = \frac{s}{(X_{i+1}-X_i)f} \left\{ \frac{1}{e^{A_2/B_2}} \int_{X_i}^{X_M} e^{X/B_2} dX + \frac{1}{A_1^{B_1}} \int_{X_M}^{X_{i+1}} X^{B_1} dX \right\}$$

$$= \frac{s}{(X_{i+1}-X_i)f} \left\{ \frac{B_2}{e^{A_2/B_2}} \left[e^{X_M/B_2} - e^{X_i/B_2} \right] + \frac{1}{(B_1+1)A_1^{B_1}} \left[X_{i+1}^{B_1+1} - X_M^{B_1+1} \right] \right\} \tag{A36}$$

For real time computational purposes it is more convenient to express the life usage u_i in terms of T_i and T_{i+1} rather than X_i and X_{i+1}. From equation A32:

$$X_i = \frac{T_i}{T_{ES}} - 1$$

$$T_{BS} = T_{ES}(1 + X_L) \tag{A37}$$

Where T_{BS} is the 'base' torque limit below which no life usage occurs for the Curve 2 relationship.

To conform with limits defined by Westlands[6] the parameter T_{BS} will be used rather than T_{ES} in the following analysis:

$$T_i = \frac{T_{BS}}{1 + X_L}(1 + X_i) \tag{A38}$$

$$X_i = \frac{1 + X_L}{T_{BS}} T_i - 1 \tag{A39}$$

$$X_{i+1} - X_i = \frac{1 + X_L}{T_{BS}}(T_{i+1} - T_i) \tag{A40}$$

For convenience the following functions will be defined:

$$H_2(T) = e^{X_i/B_2}$$
$$= e^{[(1+X_L)T/T_{BS}-1]/B_2} \tag{A41}$$

$$H_1(T) = (X_i)^{B_1+1}$$
$$= \left[\left(\frac{1 + X_L}{T_{BS}}\right)T - 1\right]^{B_1+1} \tag{A42}$$

Equations A33 to A36 may be redefined as follows:

For $T_i < T_{BS} < T_{i+1}$ (ZONE 1)

$$u_i = K_1 K_2 s T_{BS}\{H_2(T_{i+1}) - e^{X_L/B_2}\} \tag{A43}$$

For $T_i > T_{BS}(1 + X_M)/(1 + X_L)$ and $T_{i+1} < T_{BS}(1 + X_M)/(1 + X_L)$ (ZONE 2)

$$u_i = K_1 K_2 s T_{BS}\{H_2(T_{i+1}) - H_2(T_i)\} \tag{A44}$$

For $T_i < T_{BS}(1 + X_M)/(1 + X_L) < T_{i+1}$ (ZONE 3)

$$u_i = K_1 s T_{BS}\{K_2(e^{X_M/B_2} - H_2(T_i)) + K_3(H_1(T_1 + 1) - X_M{}^{B_1+1})\} \tag{A45}$$

For $T_i > T_{BS}$ (ZONE 4)

$$u_i = K_1 K_3 s T_{BS}\{H_1(T_{i+1}) - H_1(T_i)\} \tag{A46}$$

where

$$K_1 = \frac{1}{f(1 + X_L)(T_{i+1} - T_i)} \tag{A47}$$

$$K_2 = \frac{B_2}{e^{A_2/B_2}} \tag{A48}$$

$$K_3 = \frac{1}{(B_1 + 1)A_1{}^{B_1}} \tag{A49}$$

Using equations A43 to A49 the life usage over an ADC sample period may be computed provided the relationship between torque values T_i and ADC reading i is known. These equations are quite valid if the relationship between T_i and i is non-linear. However, if a linear relationship does apply (as for the system of torque measurement in Sea King—Section 4.1) some simplification in the computational procedure does result.

A linear torque measurement system may be defined analytically by the following relationship:

$$T_i = Gi + T_Z \tag{A50}$$

where G is the sensitivity expressed in units of rated torque per bit and T_Z is the value of torque which applies for an ADC reading of zero ($i = 0$).

It is normal to express torque as a fraction or percentage of rated value (i.e. rated torque = 1·00 or 100%). For convenience T_i, G and T_Z will be expressed in that manner. For the system of fatigue life usage computation for Sea King the values for G and T_Z are:

$$G = 0{\cdot}006 \text{ rated torque per bit}$$

$$T_2 = 0{\cdot}026 \text{ rated torque}$$

For a linear measuring system the term $T_{i+1}-T_i$ can be replaced with the constant G and equation A47 becomes:

$$K_1 = \frac{1}{f(1+X_L)G} \tag{A51}$$

In practice it is necessary to establish the ADC readings (values of integer variable i) which correspond to the four 'zones' (Fig. 44) each of which requires different analytical treatment. For convenience define a continuous variable y which replaces integer variable i in equation A50. Thus

$$y = \frac{T-T_Z}{G} \tag{A52}$$

where T is torque expressed as a continuous variable.

The values of y for $X = X_L$ (i.e. $T = T_{BS}$) and for $X = X_M$ (i.e. $T = T_{BS}(1+X_M/1+X_L)$) are required. These will be defined as y_1 and y_2 respectively.

Thus

$$y_1 = \frac{T_{BS}-T_Z}{G} \tag{A53}$$

and

$$y_2 = \frac{T_{BS}(1+X_M)/(1+X_L)-T_Z}{G} \tag{A54}$$

Normally y_1 and y_2 will have fractional components. To comply with the ADC integer values indicated in Fig. 44 the boundaries of the bits within which y_1 and y_2 reside may be expressed as

$$n < y_1 < (n+1)$$

$$(n+r) < y_2 < (n+r+1)$$

where n and r are integers.

The ranges of ADC readings (integer variable i) corresponding to the four zones are tabulated below.

Zone	Corresponding ADC Reading(s)
1	$i = n$
2	$(n+1) \leqslant i \leqslant (n+r+1)$
3	$i = (n+r)$
4	$i \geqslant (n+r+1)$

Values of constants which define the relationship between torque and 'safe' cycles are given in Section 2.1. A summary of these values together with the values of associated constants defined in this Appendix are tabulated below.

Constant	Value	Constant	Value
A_1	48·90	X_M	0·1542
B_1	2·5846	f*	100 Hz
A_2	1·04246	K_1*	1·6036
B_2	0·05967	K_2	$1{\cdot}5442\times10^{-9}$
X_L	0·0393	K_3	$1{\cdot}2003\times10^{-5}$

* All constants in this table except for f and K_1 are independent of the torque measuring system. K_1 includes a measuring system sensitivity factor as well as the ADC sampling rate term f.

The values of some of the constants referred to in this Appendix vary according to the particular gear under consideration. For the Sea King transmission life studies discussed in this report, the lives of four gears (G1 to G4—Section 4.3) are considered. Values of the relevant constants are tabulated below. To obtain the values of n and $n+r$, equations A53 and A54 are first used to compute y_1 and y_2 which are then truncated to the requisite integer values.

Constant	Transmission Component			
	G1	G2	G3	G4
T_{BS}	1·230	1·230	1·185	1·090
s	325·4 Hz	325·4 Hz	54·85 Hz	54·85 Hz
n	200	200	193	177
$n+r$	223	223	215	201
r	23	23	22	24

The fundamental equation A30 and those developed in this Appendix for computing the increment of life usage over an ADC sampling period, express the usage as a fraction of unity where 'unity' represents total safe life. For the Transmission Fatigue Life Usage Indicator (Section 5) full life is conveniently represented by a count of 10^6 on the electromechanical read-outs. Hence in that case one count represents one micro-life unit of usage. In general the total count corresponding to full life can be represented by any desired integer value L_T. By adding the suffix 'R' to the life fraction increment u_i the usage over a sample period can be expressed in terms of readout life units (or 'counts'):

$$u_{iR} = L_T u_i \tag{A55}$$

As outlined in Section 2.2.2 summation of life fractions to a value less than unity may be desirable. In practice this can be conveniently achieved by totalizing readout life units to a specified value less than L_T. As noted above L_T has value 10^6 for the Sea King application.

To simplify the airborne system program (Section 8.2) and to allow high computation speed it is desirable to express the readout life increments as the ratio of two integers.

$$u_{iR} = \frac{J_i}{L_U} \tag{A56}$$

where J_i is an integer which varies according to the ADC reading i and L_U is a constant integer.

By expressing u_{iR} in this manner, integer arithmetic can be readily implemented to compute life usage. In the airborne program (Section 8.1) developed for the computation and indication of the life usage for Sea King transmission components, the value of J_i corresponding to $i = n+1$ (Fig. 44) has been made equal to the integer 500 (i.e. $J_{n+1} = 500$). The value of L_U may in that case be computed as:

$$L_U = \frac{J_{n+1}}{L_T u_{n+1}} \tag{A57}$$

where u_{n+1} is calculated according to equation A44 putting $i = n+1$. The value of n is deduced from equation A53, and has been tabulated above.

In practice L_U computed in this manner would normally have a fractional component but negligible error results if the value is rounded off to the nearest integer.

The values of L_U and of associated parameters used to compute its value are tabulated below for the four gears G1 to G4 referred to earlier.

Parameter	Transmission Component			
	G1	G2	G3	G4
L_T	10^6	10^6	10^6	10^6
T_{n+1}	1·232	1·232	1·190	1·094
I_{n+2}	1·238	1·238	1·196	1·100
u_{n+1}	$1{\cdot}7470 \times 10^{-7}$	$1{\cdot}7470 \times 10^{-7}$	$3{\cdot}0857 \times 10^{-8}$	$3{\cdot}0683 \times 10^{-8}$
J_{n+1}	500	500	500	500
L_U	2861	2861	16203	16295

The value of L_U and the range of values for J_i (obtained by putting $J_i = L_U L_T u_i$ where values of u_i are derived from equations A43 to A46) are pre-computed (Section 8.1) and entered into look-up tables (Figs 28 and 29) which form part of the airborne system program. The L_U entry and the range of J_i entries are clearly identified in Fig. 29.

Table entries J_i corresponding to ADC readings i are summed using integer arithmetic. The sum is progressively updated for each ADC reading of torque for the particular gear under consideration, the value of the sum is compared with the integer value L_U, and if it exceeds L_U the appropriate readout is advanced by one count and L_U is subtracted from the progressive sum. Such operations can be performed simply and executed at high speed.

TABLE I

Effect of Torque Measurements Error on the Indicated Fatigue Life Usage for Curve 1 Relationship Between Gear Loading and Life Cycles

Curve	Torque Spectrum	Values of Constants	Relationships	Normalized torque limit σ	Change in indicated rate of Fatigue Life Usage α				Change due to square wave noise α_N	
					α_{11} $\varepsilon = +0{\cdot}01$	α_{12} $\varepsilon = -0{\cdot}01$	α_{21} $\varepsilon = +0{\cdot}02$	α_{22} $\varepsilon = -0{\cdot}02$	$\frac{\alpha_{11}+\alpha_{12}}{2}$	$\frac{\alpha_{21}+\alpha_{22}}{2}$
1	1	$B_1 = 2{\cdot}5846$	$\alpha = \left(1+\frac{\varepsilon}{\sigma}\right)^{B_1+1} - 1$	0·3000	0·1247	−0·1144	0·2603	−0·2191	0·0051	0·0206
				0·2500	0·1510	−0·1361	0·3177	−0·2584	0·0074	0·0297
				0·2000	0·1911	−0·1680	0·4073	−0·3146	0·0116	0·0464
				0·1500	0·2603	−0·2191	0·5662	−0·4013	0·0206	0·0825
				0·1250	0·3177	−0·2584	0·7024	−0·4647	0·0297	0·1188
				0·1000	0·4073	−0·3146	0·9224	−0·5506	0·0464	0·1859
				0·0750	0·5662	−0·4013	1·3335	−0·6710	0·0825	0·3312
				0·0500	0·9224	−0·5506	2·3405	−0·8398	0·1859	0·7504
				0·0250	2·3405	−0·8398	7·2236	−0·9969	0·7504	3·1134
				0·0200	3·2778	−0·9166	10·9974	−1·0000	1·1806	4·9987
				0·0100	10·9974	−1·0000	50·3229	−1·0000	4·9987	24·6614
				0·0000	∞		∞			
1	2	$B_1 = 2{\cdot}5846$	$\alpha = \left(1+\frac{\varepsilon}{\sigma}\right)^{B_1+2} - 1$	0·3000	0·1622	−0·1440	0·3443	−0·2712	0·0091	0·0366
				0·2500	0·1970	−0·1707	0·4231	−0·3177	0·0132	0·0527
				0·2000	0·2507	−0·2096	0·5480	−0·3831	0·0206	0·0825
				0·1500	0·3443	−0·2712	0·7751	−0·4811	0·0366	0·1470
				0·1250	0·4231	−0·3177	0·9748	−0·5504	0·0527	0·2122
				0·1000	0·5480	−0·3831	1·3068	−0·6405	0·0825	0·3332
				0·0750	0·7751	−0·4811	1·9558	−0·7588	0·1470	0·5985
				0·0500	1·3068	−0·6405	3·6768	−0·9039	0·3332	1·3865
				0·0250	3·6768	−0·9039	13·8025	−0·9994	1·3865	6·4016
				0·0200	5·4168	−0·9583	22·9948	−1·0000	2·2292	10·9974
				0·0100	22·9948	−1·0000	152·9688	−1·0000	10·9974	76·4844
				0·0000	∞		∞			

TABLE 2

Effect of Torque Measurement Errors on the Indicated Fatigue Life Usage for Curve 2 Relationship Between Gear Loading and Life Cycles

Curve	Torque Spectrum	Values of Constants	Relationships	Normalized torque limit σ	Change in indicated rate of Fatigue Life Usage α				Change due to square wave noise α_s	
					α_{11} $+0{\cdot}01\varepsilon$	α_{12} $-0{\cdot}01\varepsilon$	α_{21} $+0{\cdot}02\varepsilon$	α_{22} $-0{\cdot}02\varepsilon$	$\frac{\alpha_{11}+\alpha_{12}}{2}$	$\frac{\alpha_{21}+\alpha_{22}}{2}$
2	1	$A_1 = 48{\cdot}90$ $B_1 = 2{\cdot}5846$ $B_2 = 0{\cdot}05967$ $X_L = 0{\cdot}0393$ $X_M = 0{\cdot}1542$ $C_2 = 2{\cdot}5879\times10^{-8}$ $L_4 = 2{\cdot}9836\times10^{-9}$ $L_5 = 1{\cdot}2003\times10^{-5}$ $L_6 = 2{\cdot}2729\times10^{-4}$	(i) For $\sigma > X_M$ and $\sigma+\varepsilon > X_M$ $\alpha = \frac{(\sigma+\varepsilon)^{B_1+1}+L_3}{\sigma^{B_1+1}+L_3} - 1$ where $L_3 = X_M^{B_1+1}\left\{\frac{B_2(B_1+1)}{X_M}\left(1-e^{-(X_M-X_L)/B_2}\right)-1\right\}$ (ii) For $\sigma < X_M$ and $\sigma+\varepsilon < X_M$ $\alpha = \frac{e^{(\sigma+\varepsilon-X_L)/B_2}-1}{e^{(\sigma-X_L)/B_2}-1} - 1$ For σ in the vicinity of X_M refer to Appendix I	0·3000	0·1226	0·1125	0·2559	0·2154	0·0051	0·0203
				0·2500	0·1462	0·1318	0·3076	0·2502	0·0072	0·0287
				0·2000	0·1782	0·1566	0·3796	0·2932	0·0108	0·0432
				0·1750	0·1972	0·1702	0·4241	0·3157	0·0135	0·0542
				0·1500	0·2162	0·1829	0·4705	0·3376	0·0166	0·0663
				0·1250	0·2394	0·2024	0·5224	0·3736	0·0185	0·0744
				0·1000	0·2858	0·2417	0·6237	0·4461	0·0220	0·0888
				0·0750	0·4052	0·3427	0·8844	0·6325	0·0313	0·1259
				0·0593	0·6406	0·5418	1·3982	1·0000	0·0494	0·1991
				0·0500	1·1114	0·9399	2·4256	1·0000	0·0857	0·7128
				0·0493	1·1824	1·0000	2·5806	1·0000	0·0912	0·7903
				0·0393	∞		∞			
2	2	$A_1 = 48{\cdot}90$ $B_1 = 2{\cdot}5846$ $B_2 = 0{\cdot}05967$ $X_L = 0{\cdot}0393$ $X_M = 0{\cdot}1542$ $C_2 = 2{\cdot}5879\times10^{-8}$ $L_4 = 1{\cdot}7804\times10^{-10}$ $L_5 = 4{\cdot}9663\times10^{-10}$ $L_6 = 0{\cdot}8472$ $L_7 = 0{\cdot}4361$	(i) For $\sigma > X_M$ and $\sigma+\varepsilon > X_M$ $\alpha = \frac{\left(\frac{\sigma+\varepsilon}{X_M}\right)^{B_1+2}+L_6\left(\frac{\sigma+\varepsilon}{X_M}\right)-L_7}{\left(\frac{\sigma}{X_M}\right)^{B_1+2}+L_6\left(\frac{\sigma}{X_M}\right)-L_7} - 1$ where $L_6 = (B_1+2)\left\{\frac{B_2(B_1+1)}{X_M}\left[1-e^{-(X_M-X_L)/B_2}\right]-1\right\}$ $L_7 = (B_1+1)\left\{\frac{B_2^2(B_1+2)}{X_M^2}\left[\left(1-\frac{X_L}{B_2}\right)e^{-(X_M-X_L)/B_2}+\frac{X_M}{B_2}-1\right]-1\right\}$ (ii) For $\sigma < X_M$ and $\sigma+\varepsilon < X_M$ $\alpha = \frac{e^{(\sigma+\varepsilon-X_L)/B_2}-\left(1+\frac{\sigma+\varepsilon-X_L}{B_2}\right)}{e^{(\sigma-X_L)/B_2}-\left(1+\frac{\sigma-X_L}{B_2}\right)} - 1$ For σ in the vicinity of X_M refer to Appendix I	0·3000	0·1559	−0·1386	0·3306	−0·2614	0·0086	0·0346
				0·2500	0·1841	−0·1603	0·3947	−0·2991	0·0119	0·0478
				0·2000	0·2226	−0·1883	0·4840	−0·3467	0·0171	0·0686
				0·1750	0·2480	−0·2065	0·5438	−0·3773	0·0208	0·0833
				0·1500	0·2823	−0·2315	0·6246	−0·4199	0·0254	0·1024
				0·1250	0·3390	−0·2721	0·7572	−0·4876	0·0335	0·1348
				0·1000	0·4503	−0·3463	1·0236	−0·6046	0·0520	0·2095
				0·0750	0·7443	−0·5123	1·7630	−0·8285	0·1160	0·4673
				0·0593	1·3888	−0·7641	3·5163	−0·1000	0·3123	1·2581
				0·0500	2·9675	−0·9960	8·2662	−1·0000	0·9858	3·6331
				0·0493	3·2399	−1·0000	9·1283	−1·0000	1·1199	4·0642
				0·0393	∞		∞			

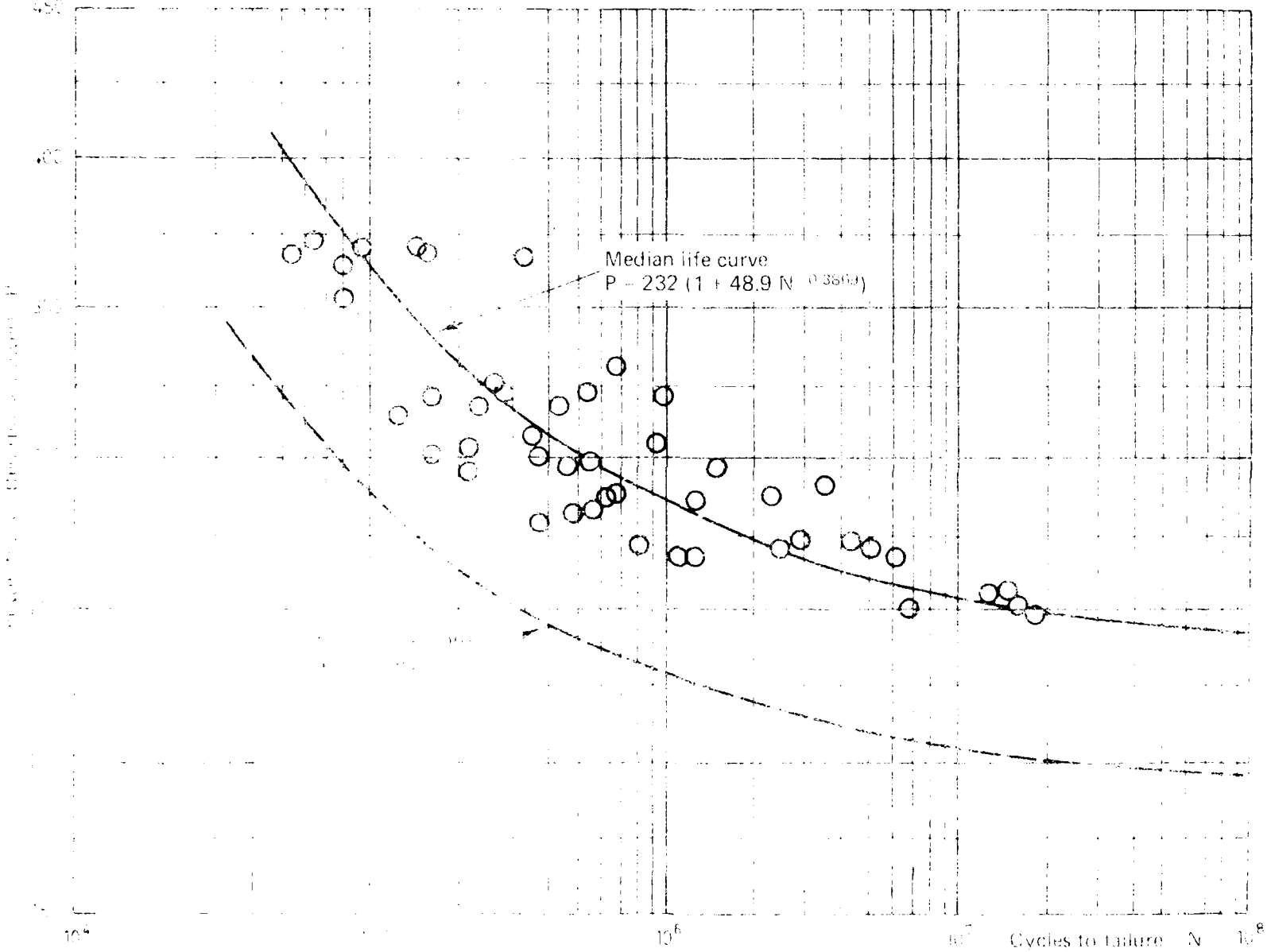

SEASEX TAIL ROTOR GEAR FATIGUE DATA

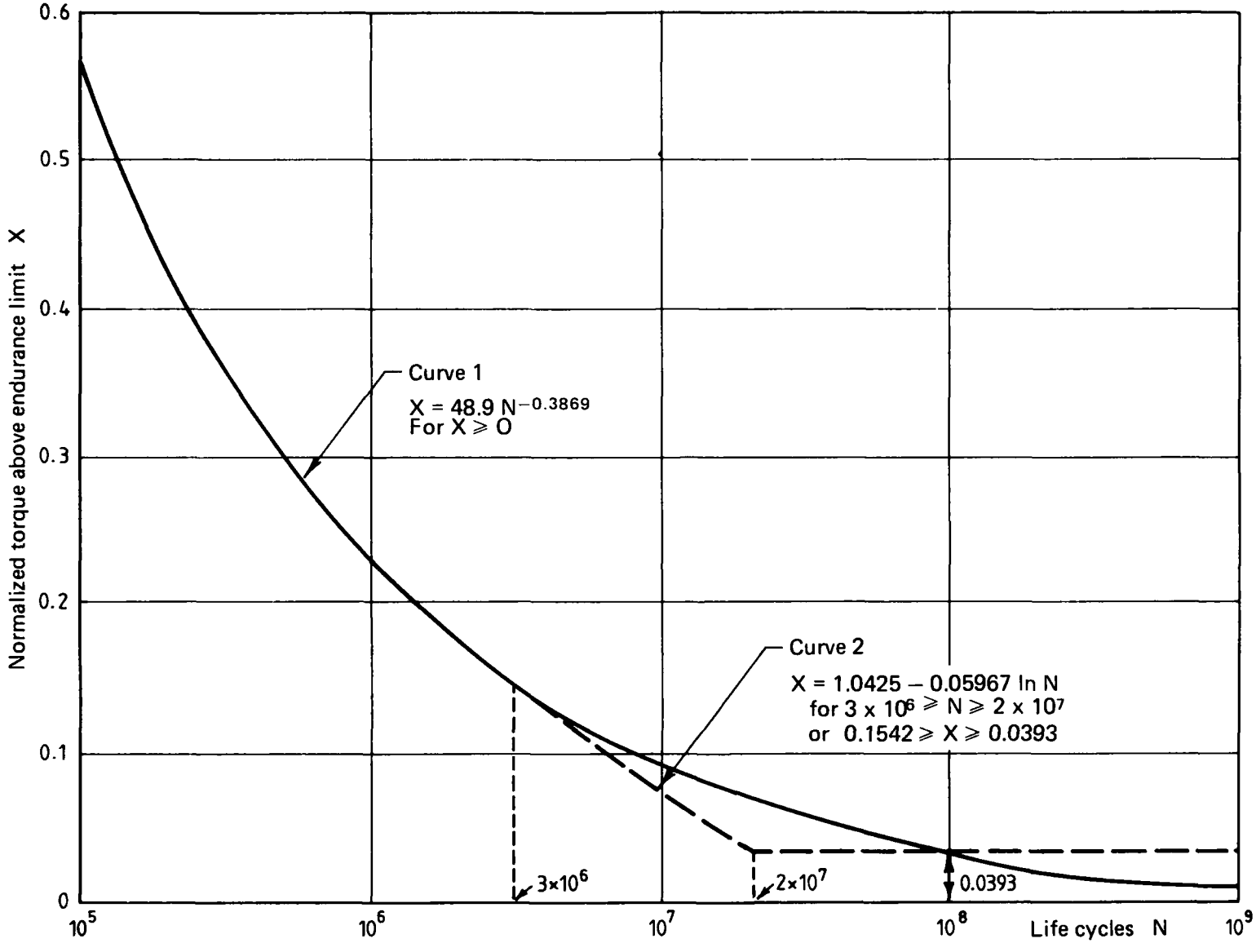

FIG. 2 NORMALISED TORQUE VS LIFE CYCLES CURVES

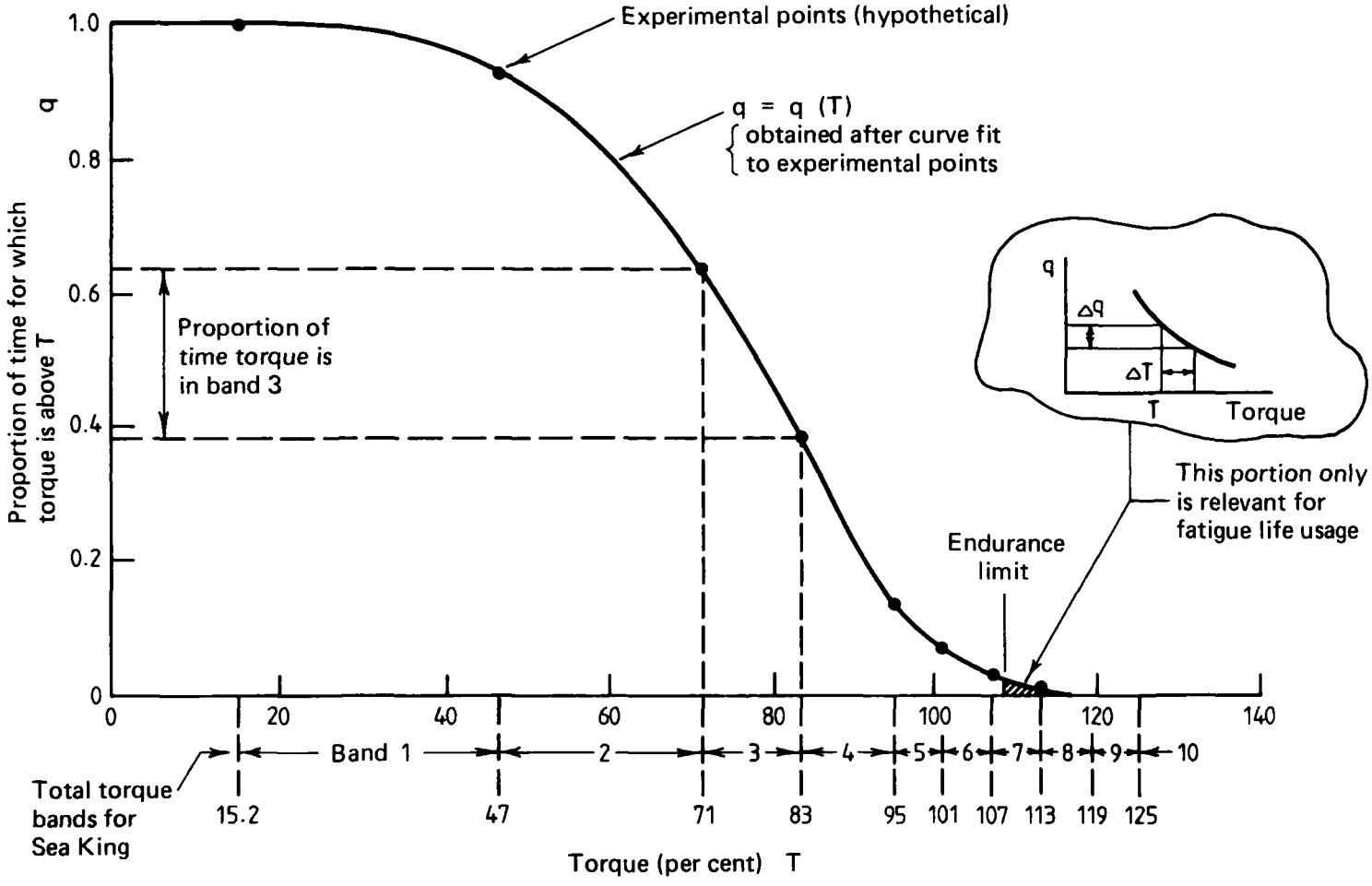

FIG. 3 TORQUE LOAD SPECTRUM

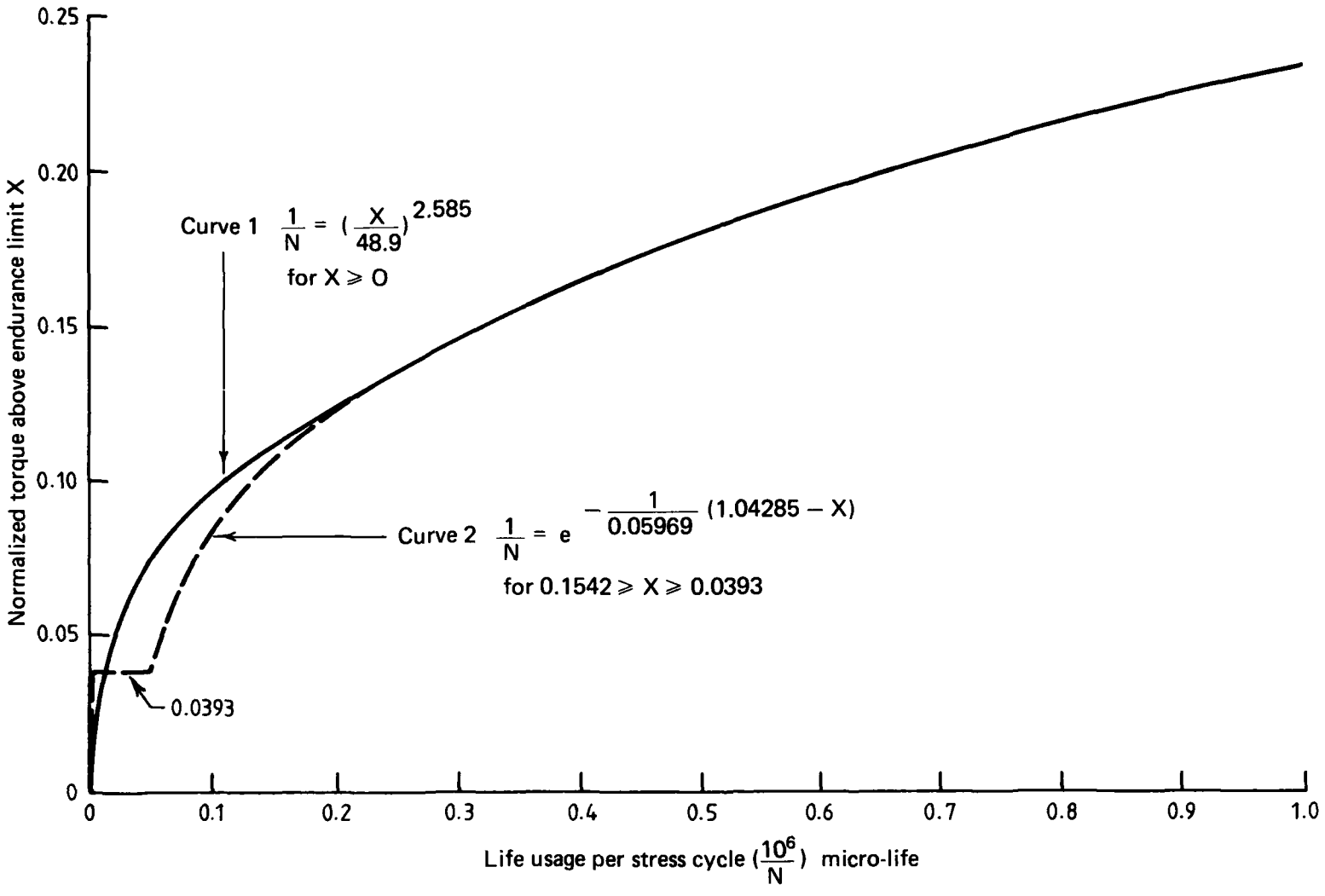

FIG. 4 RATE OF LIFE USAGE

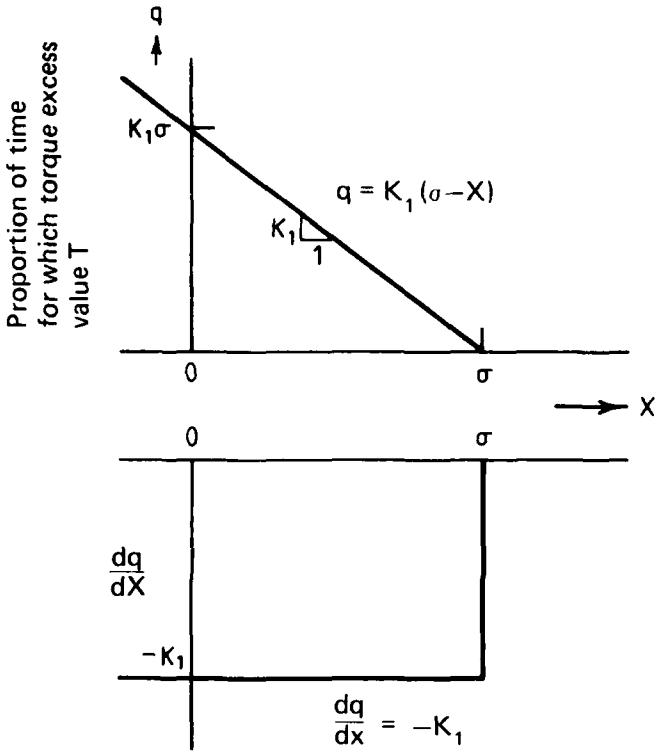

Test torque load spectrum 1

– Time spent in equal width torque bands above endurance limit is the same for all bands.

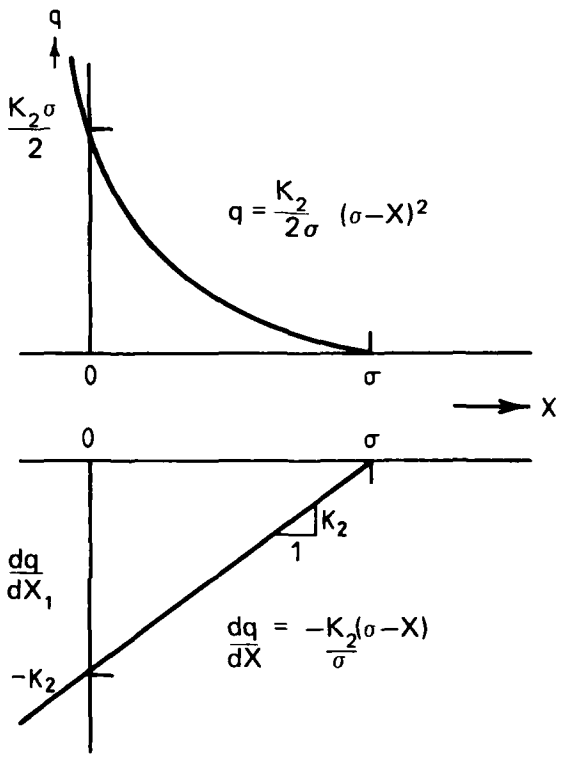

Test torque load spectrum 2

– Time spent in equal width torque bands above endurance limit decreases linearly with torque.

FIG. 5 TEST TORQUE LOAD SPECTRA

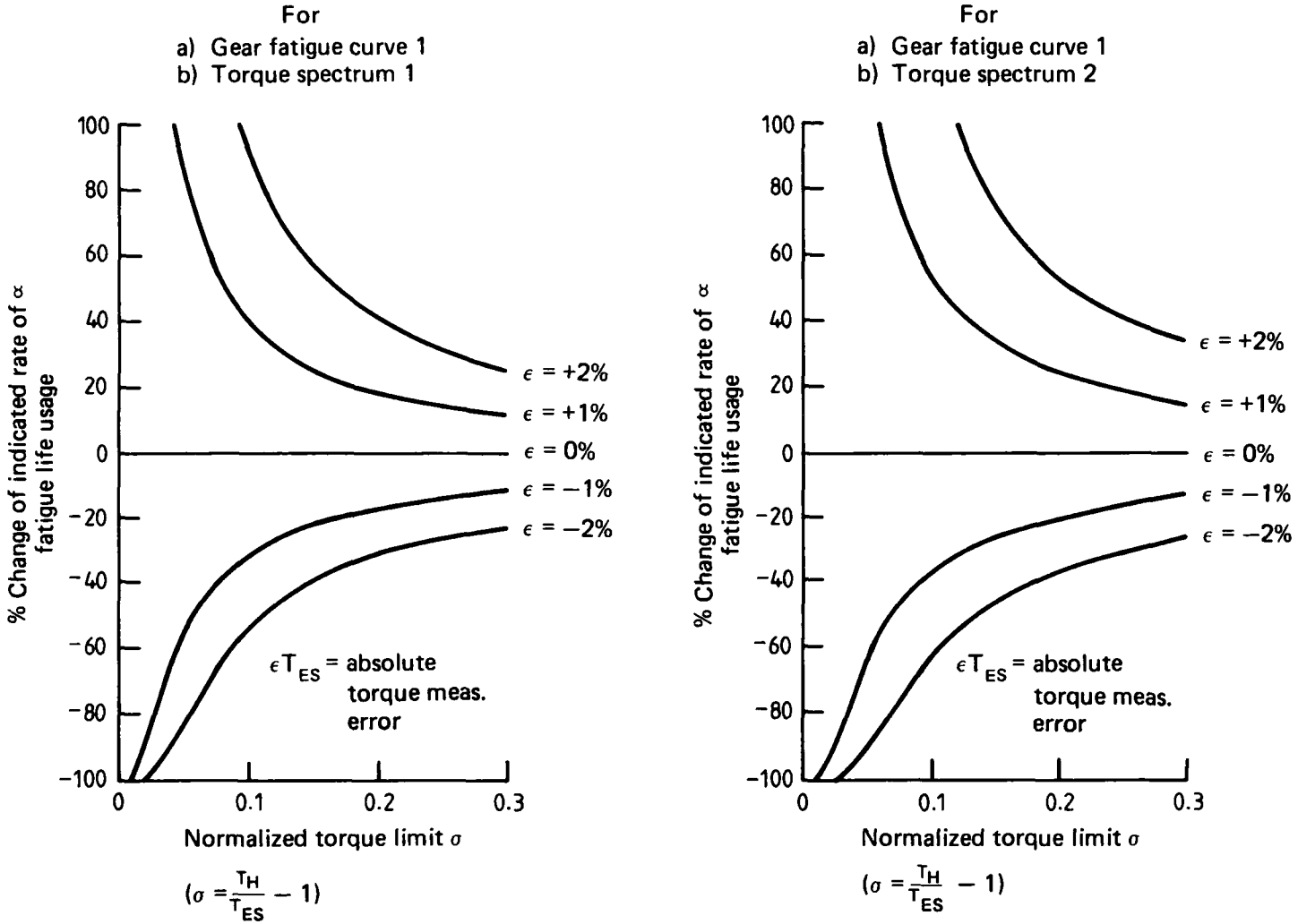

FIG. 6 EFFECT OF TORQUE MEASUREMENT INACCURACY FOR CURVE 1

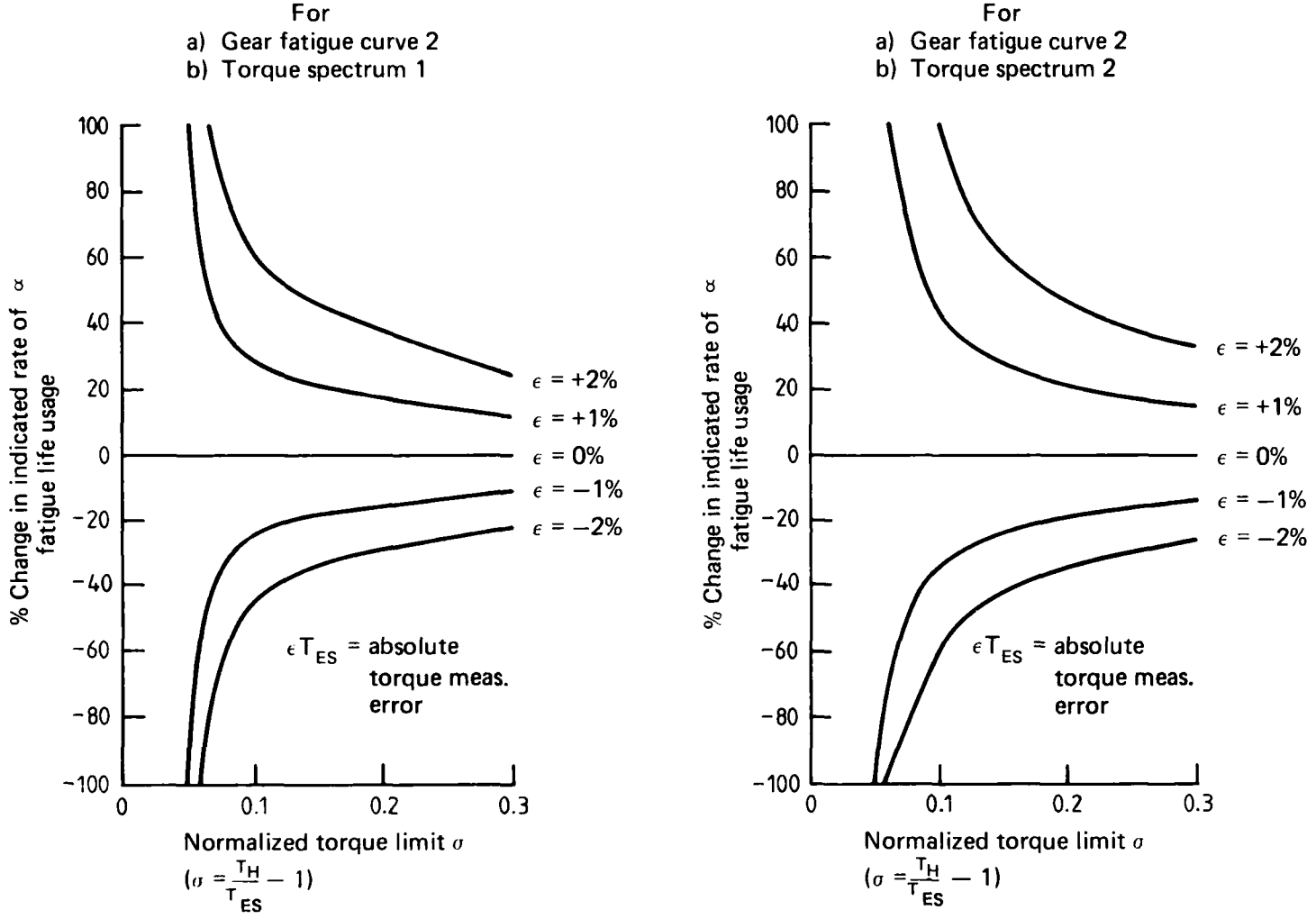

FIG. 7 EFFECT OF TORQUE MEASUREMENT INACCURACY FOR CURVE 2

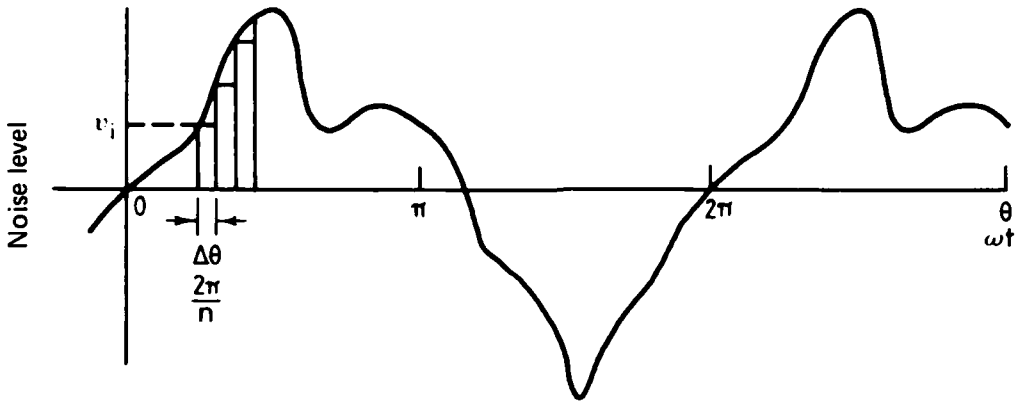

a) General noise signal

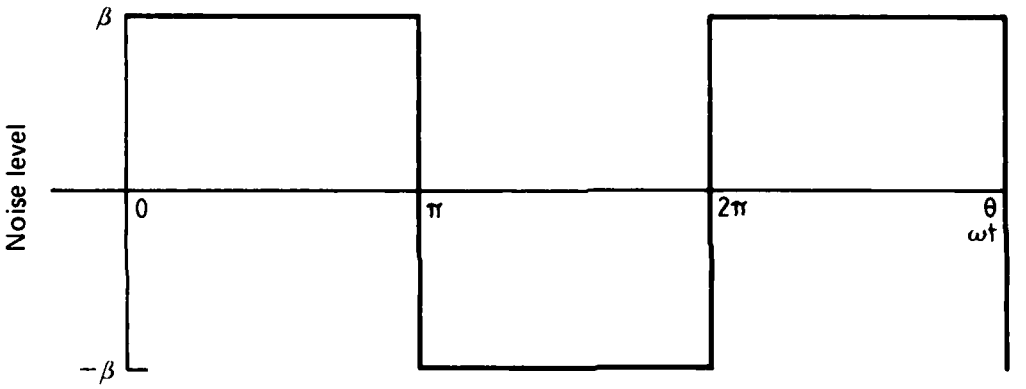

b) Square wave noise signal

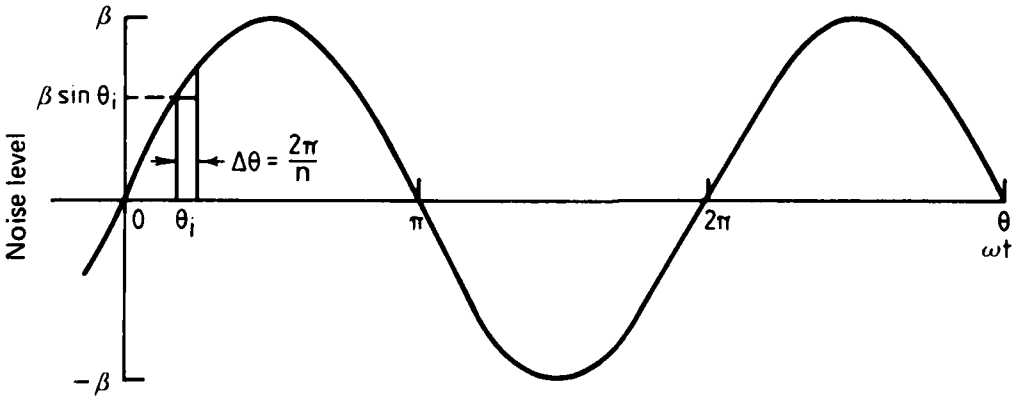

c) Sinusoidal noise signal

FIG. 8 NORMALIZED NOISE SIGNAL EXAMPLES

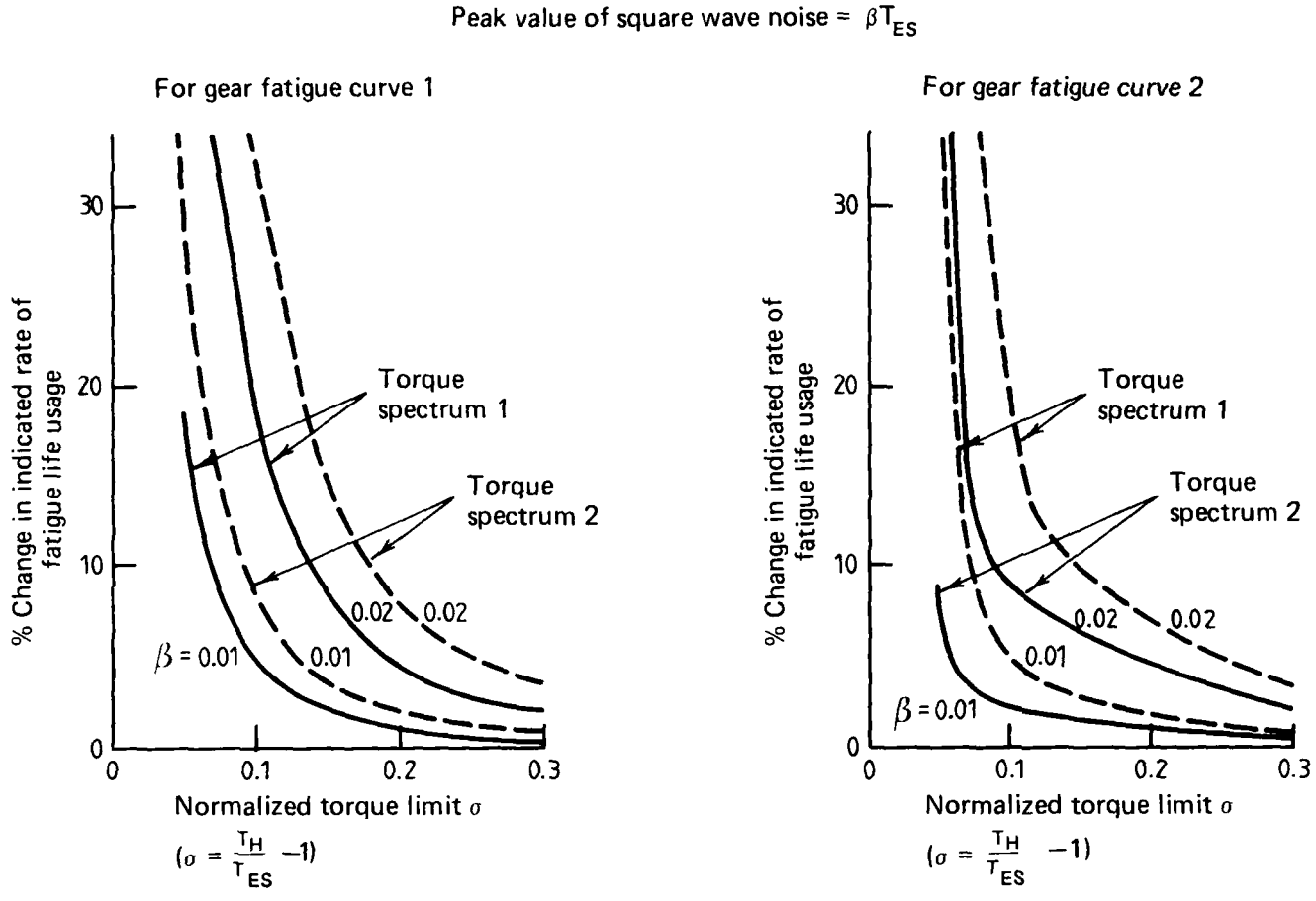

FIG. 9 EFFECT OF SQUARE WAVE NOISE ON INDICATED RATE OF FATIGUE LIFE USAGE

FIG. 10 STRAIN GAUGE PRESSURE TRANSDUCER

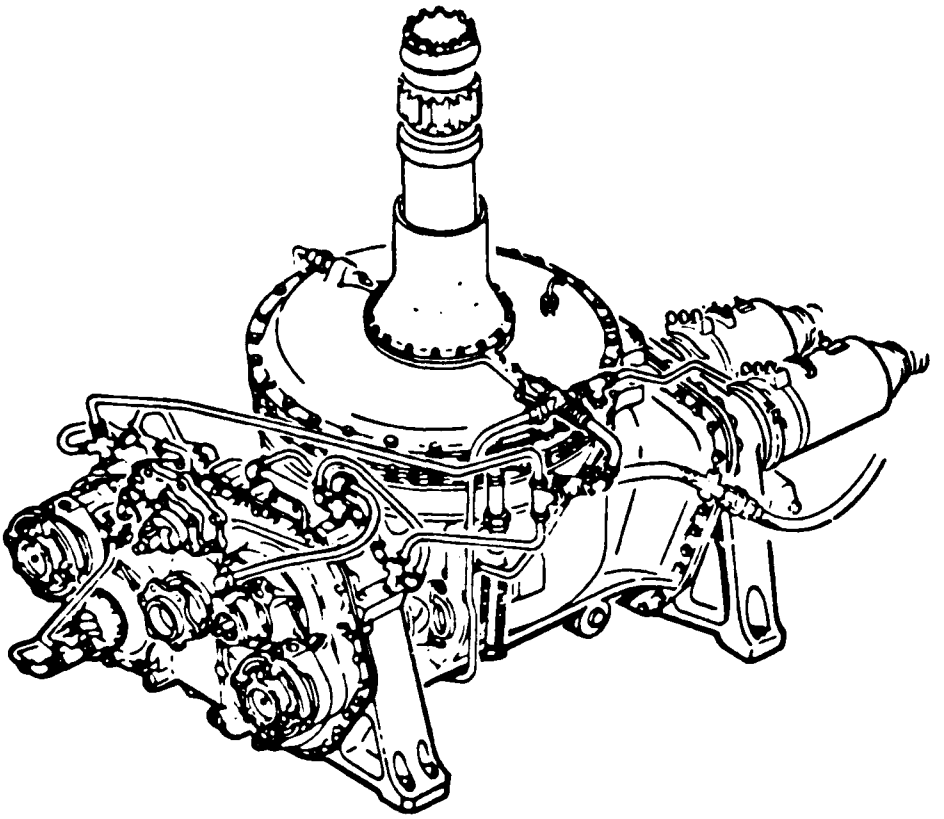

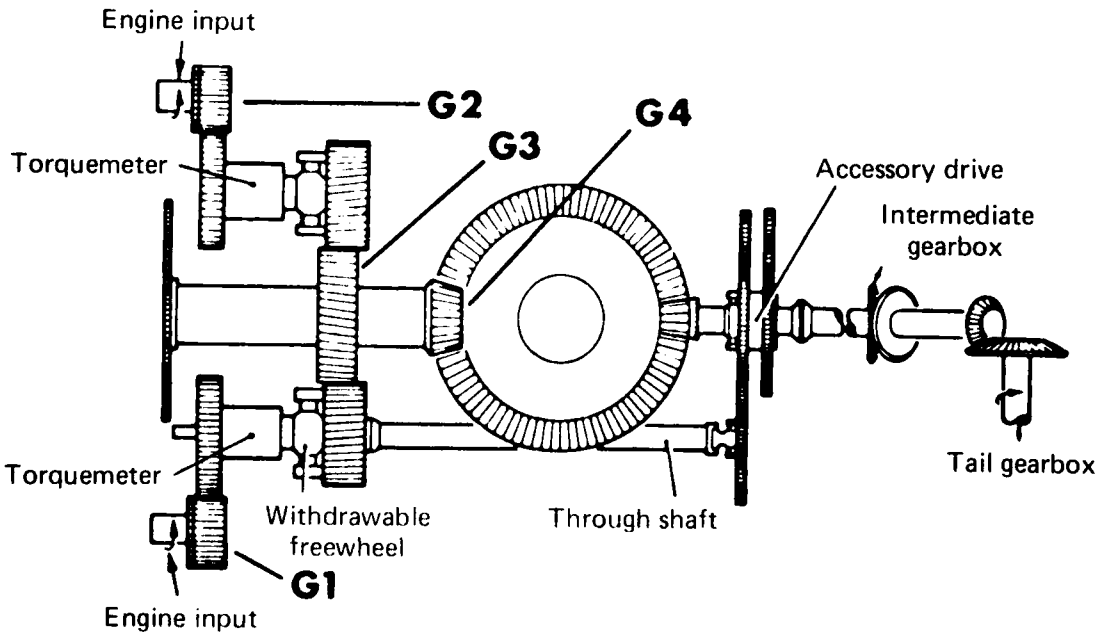

FIG. 11 SEA KING TRANSMISSION SYSTEM

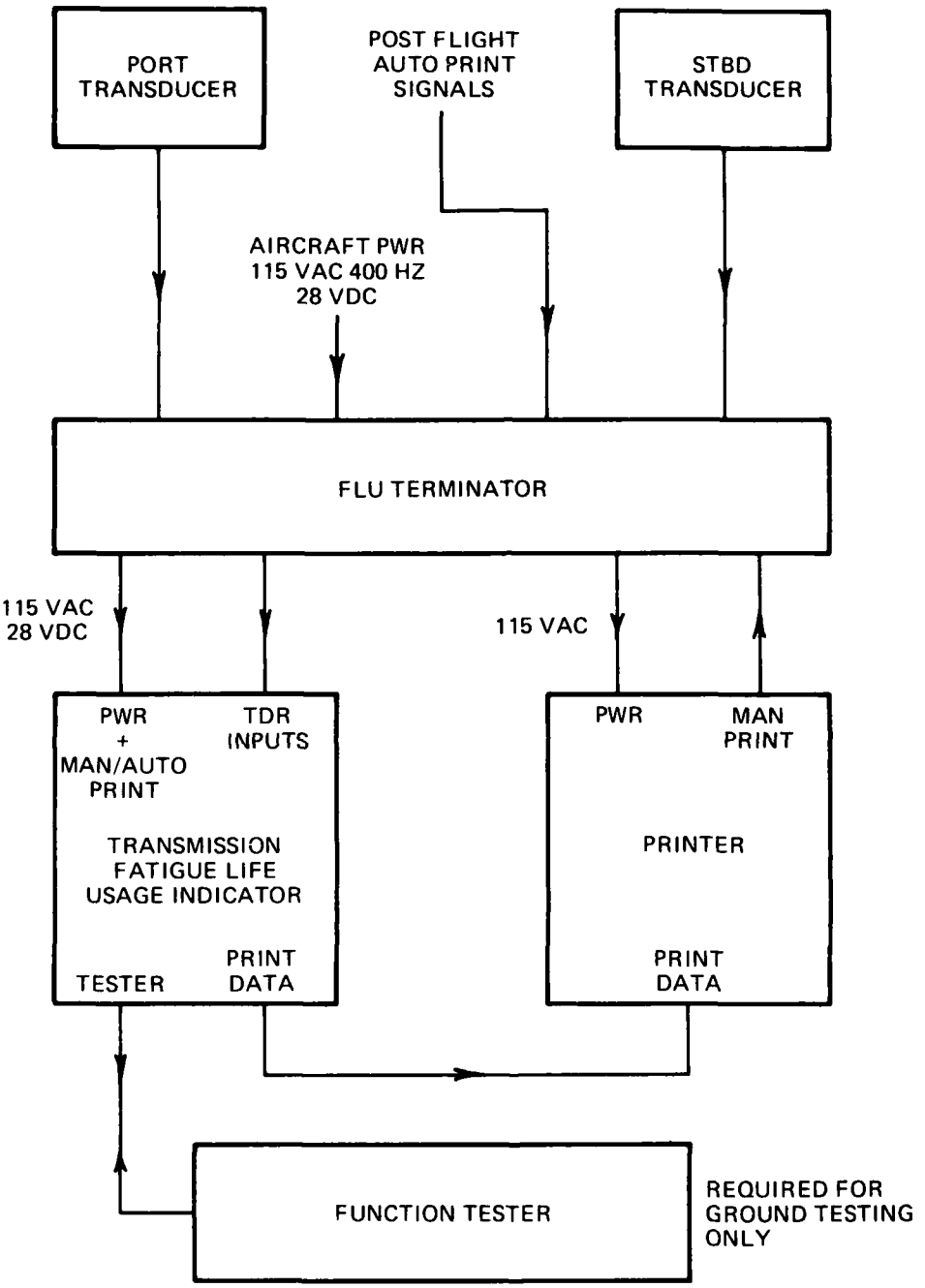

FIG. 12 FATIGUE LIFE USAGE INDICATING SYSTEM

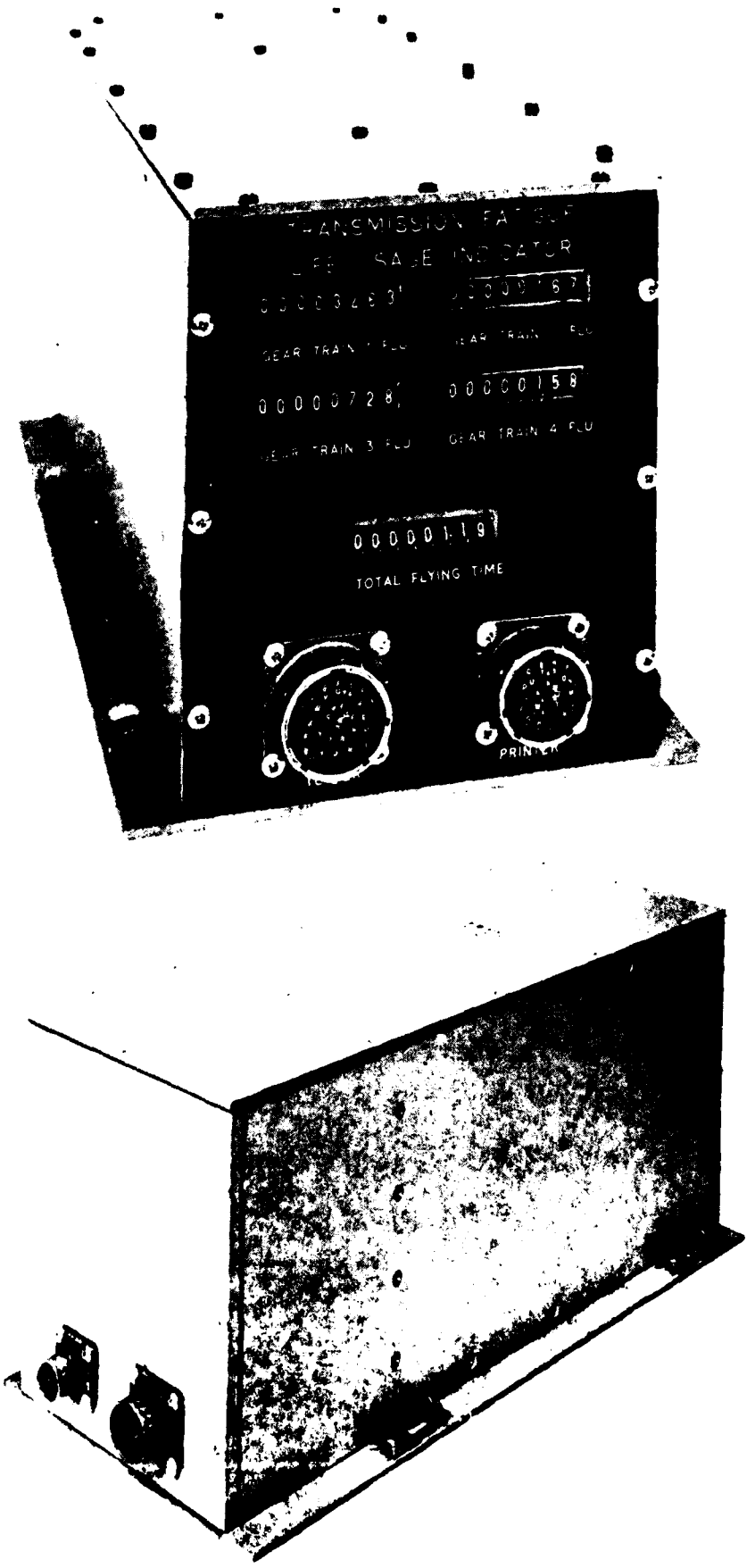

FIG. 13 TRANSMISSION FATIGUE LIFE USAGE INDICATOR

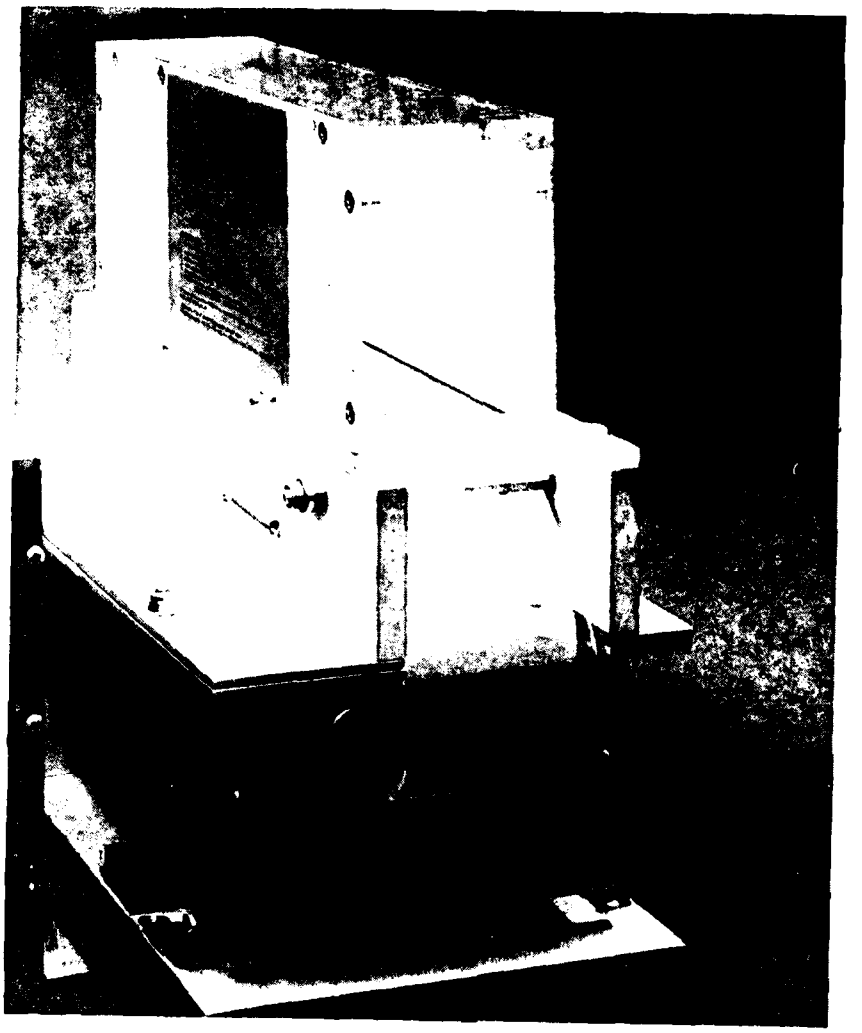

FIG. 14 PRINTER (MODIFIED FOR AIRCRAFT USE)

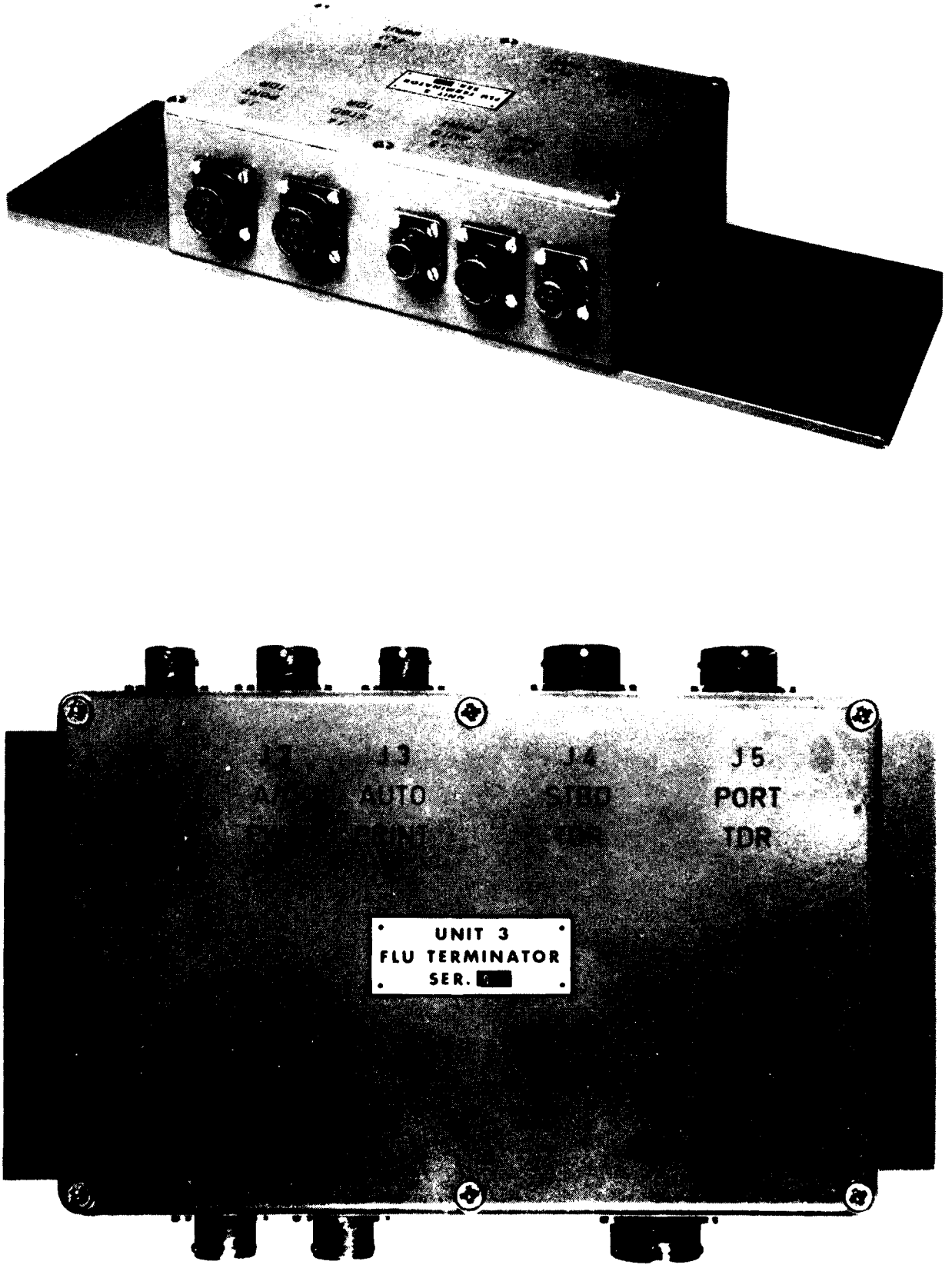

FIG. 15 TERMINATOR

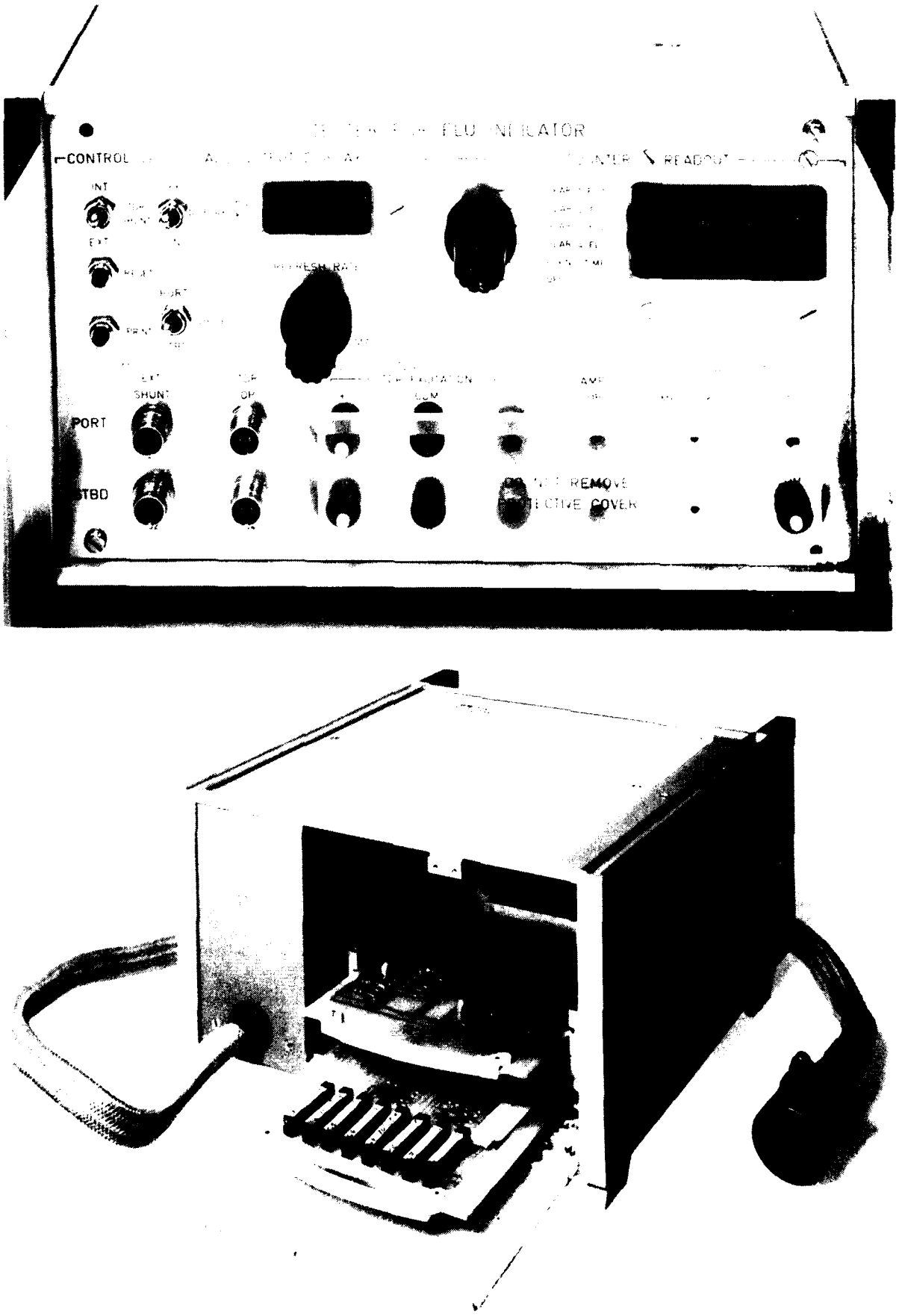

FIG. 16 FLIGHT LINE FUNCTION TESTER

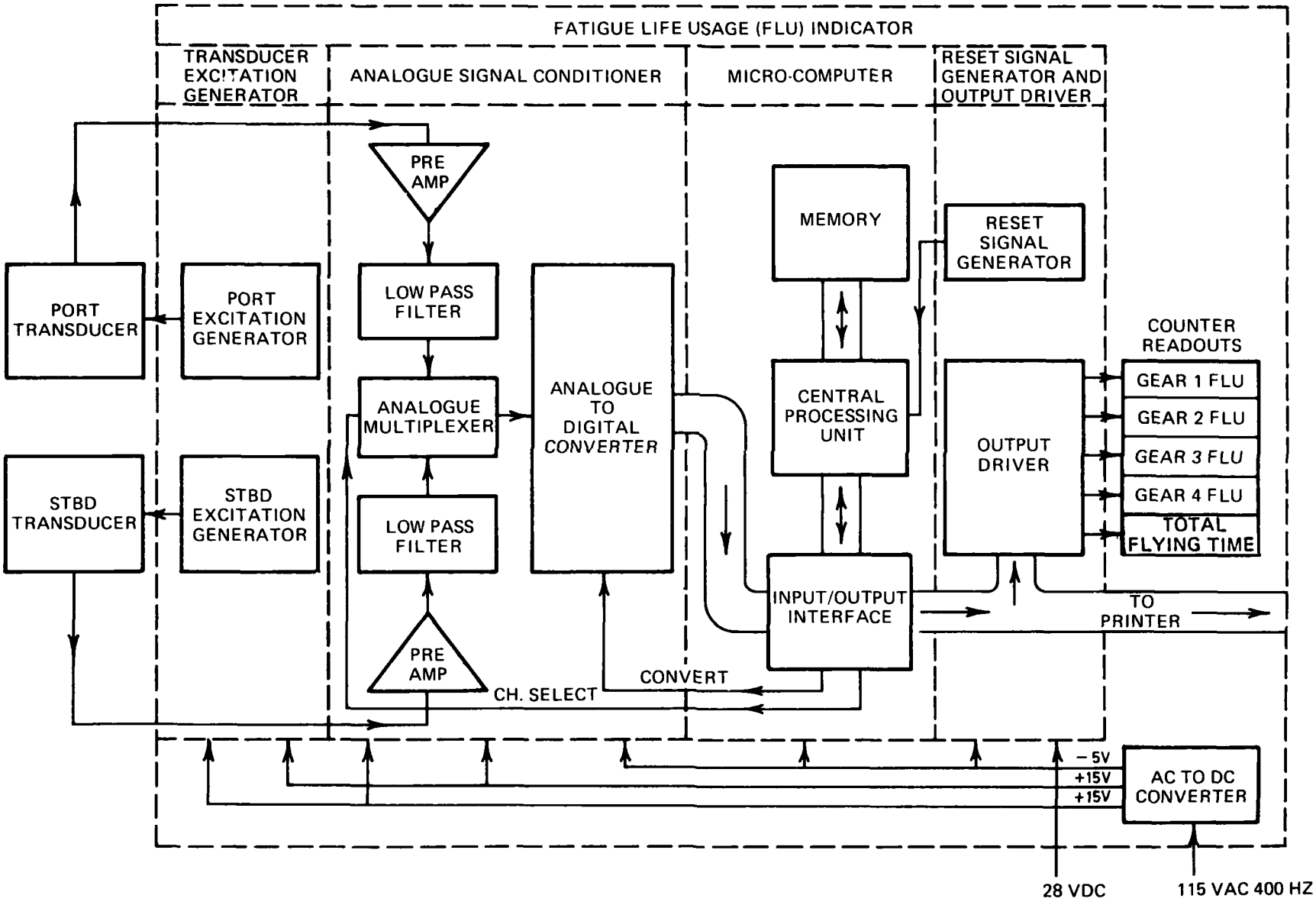

FIG. 17 BLOCK SCHEMA OF FATIGUE LIFE USAGE INDICATOR

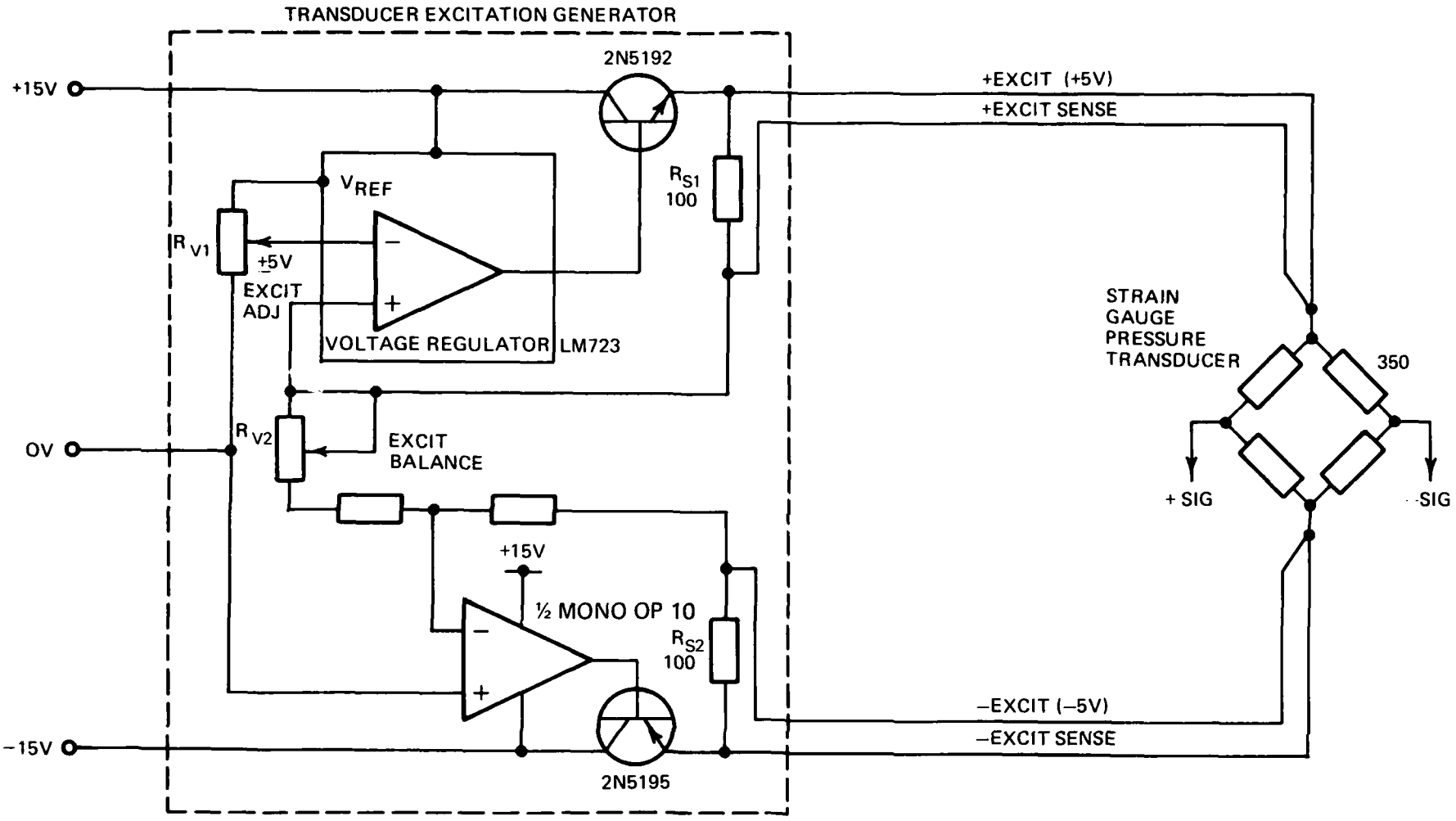

FIG. 18 TRANSDUCER EXCITATION GENERATOR FUNCTIONAL SCHEMA

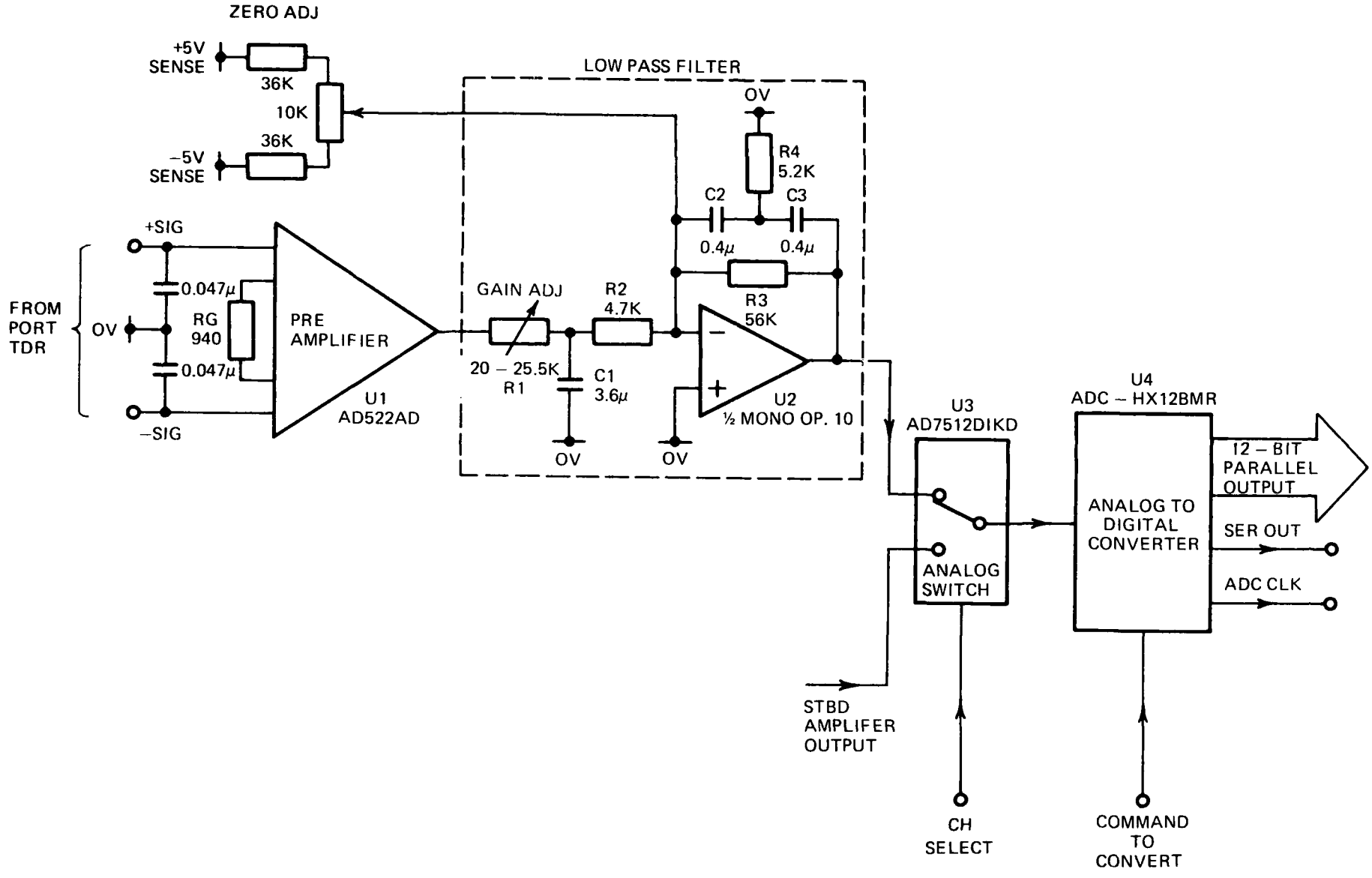

FIG. 19 ANALOGUE SIGNAL CONDITIONER FUNCTIONAL SCHEMA

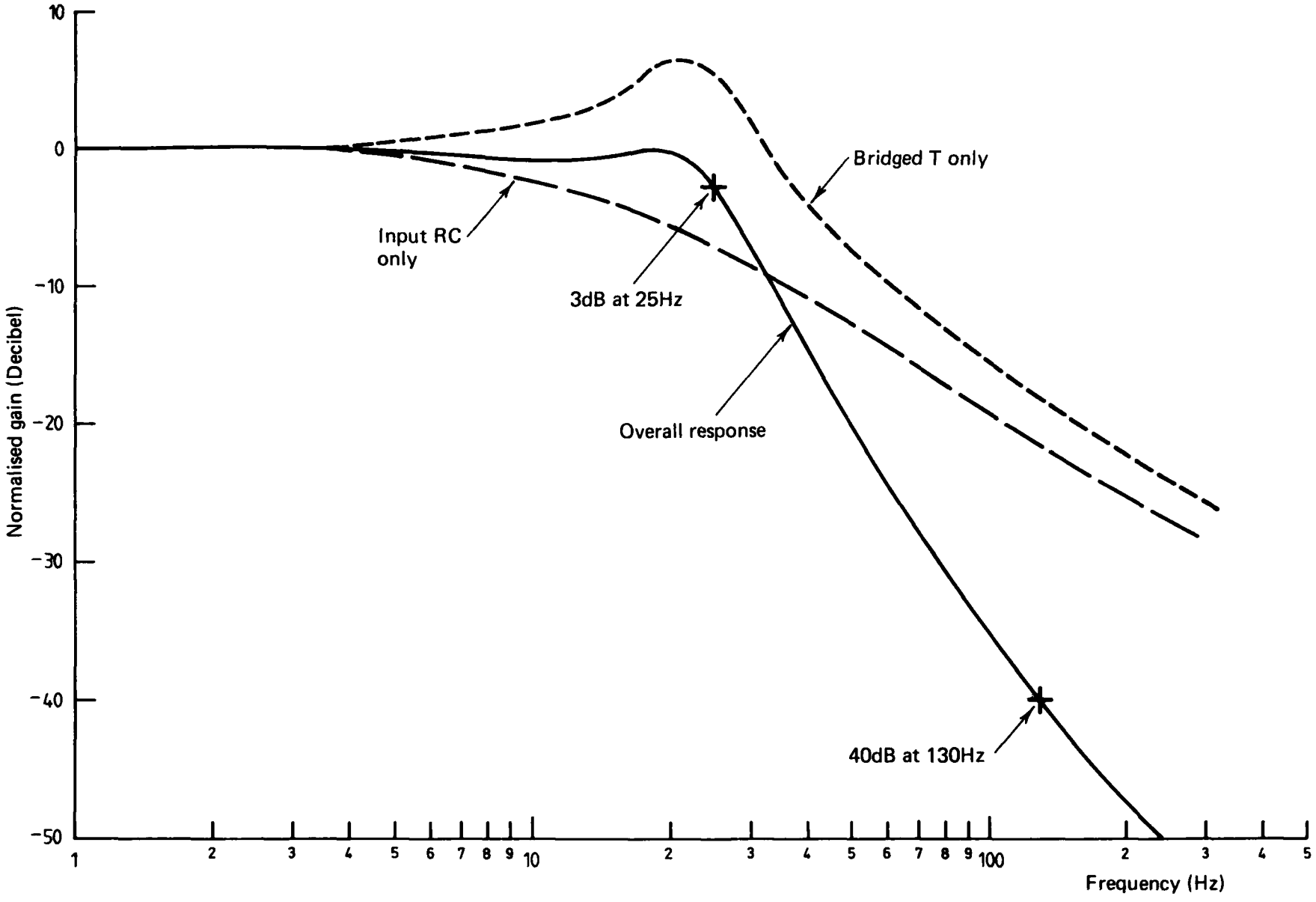

FIG. 20 FILTER RESPONSE CURVES

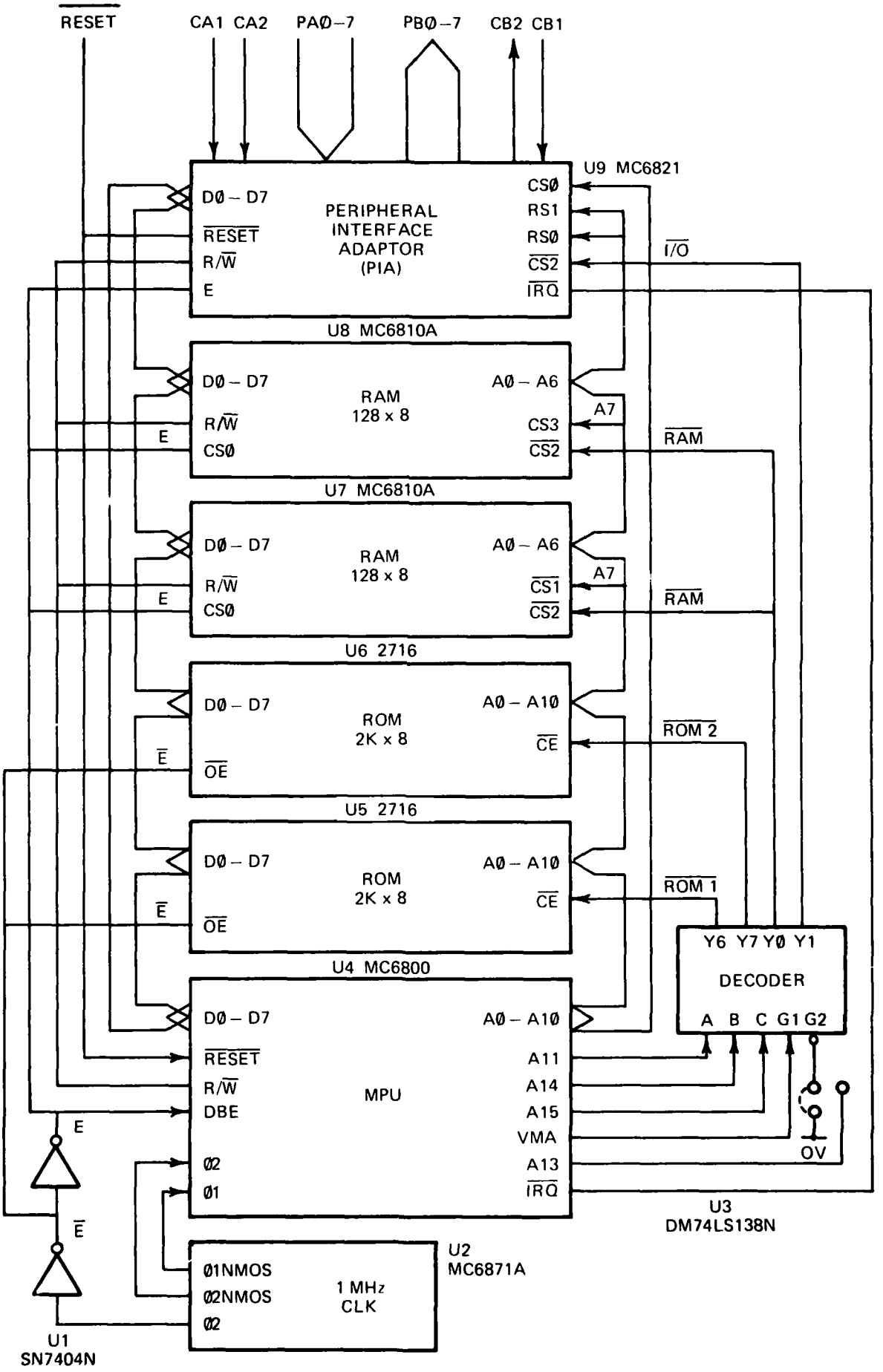

FIG. 21 MICROCOMPUTER FUNCTIONAL SCHEMA

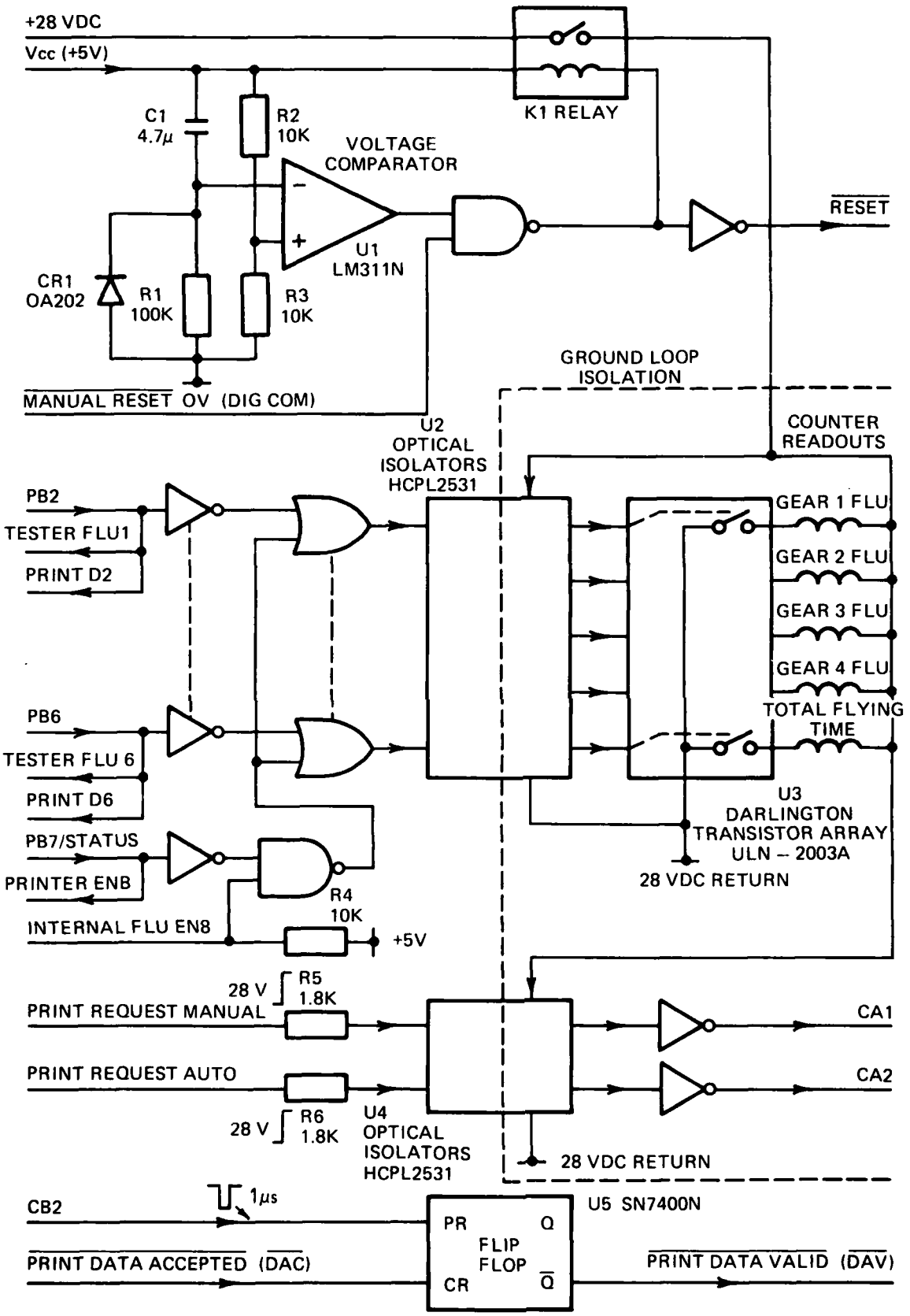

FIG. 22 RESET SIGNAL GENERATOR AND OUTPUT DRIVER
FUNCTIONAL SCHEMA

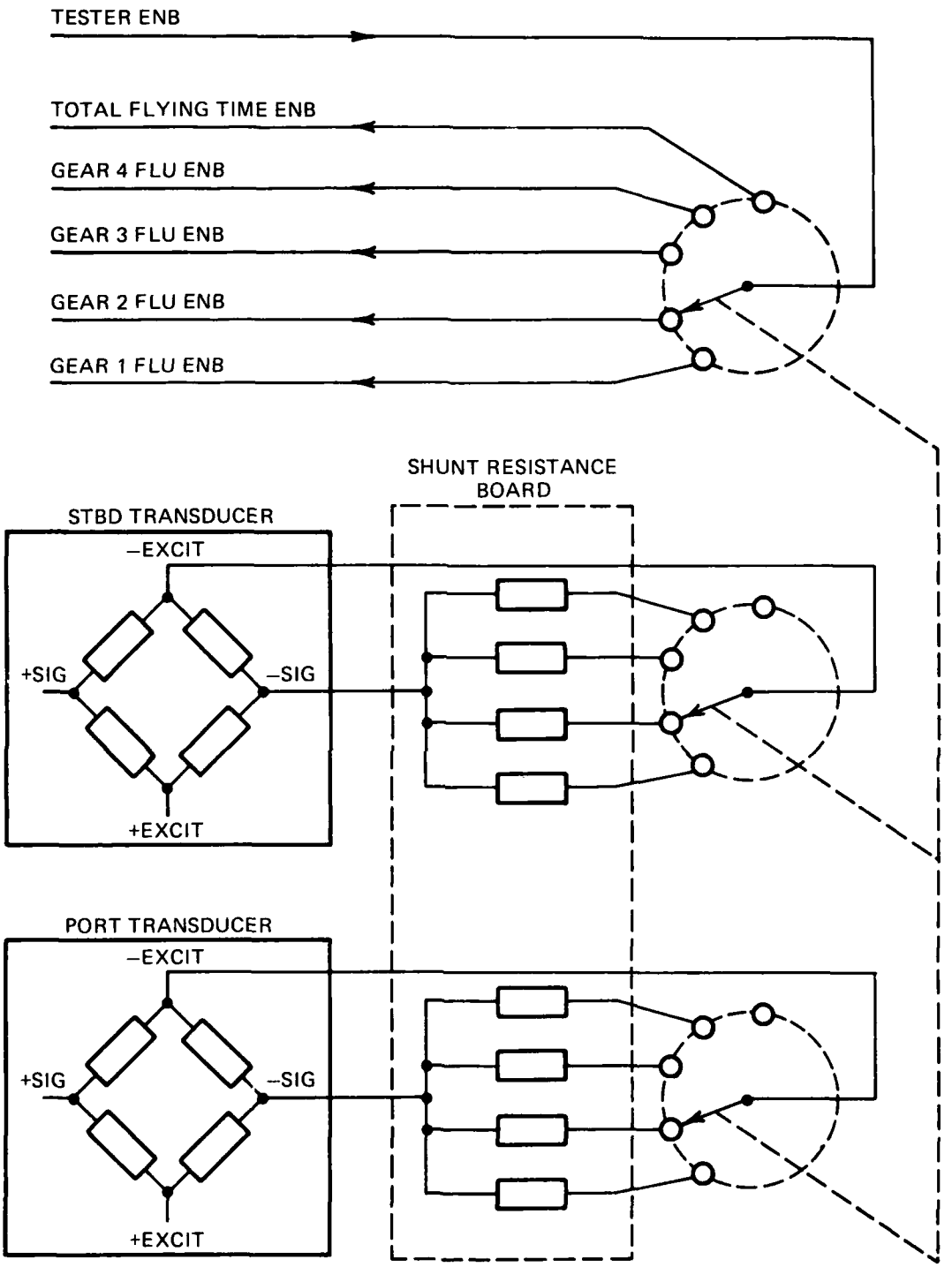

FIG. 23 SELECTION OF PARAMETER FOR READOUT TEST

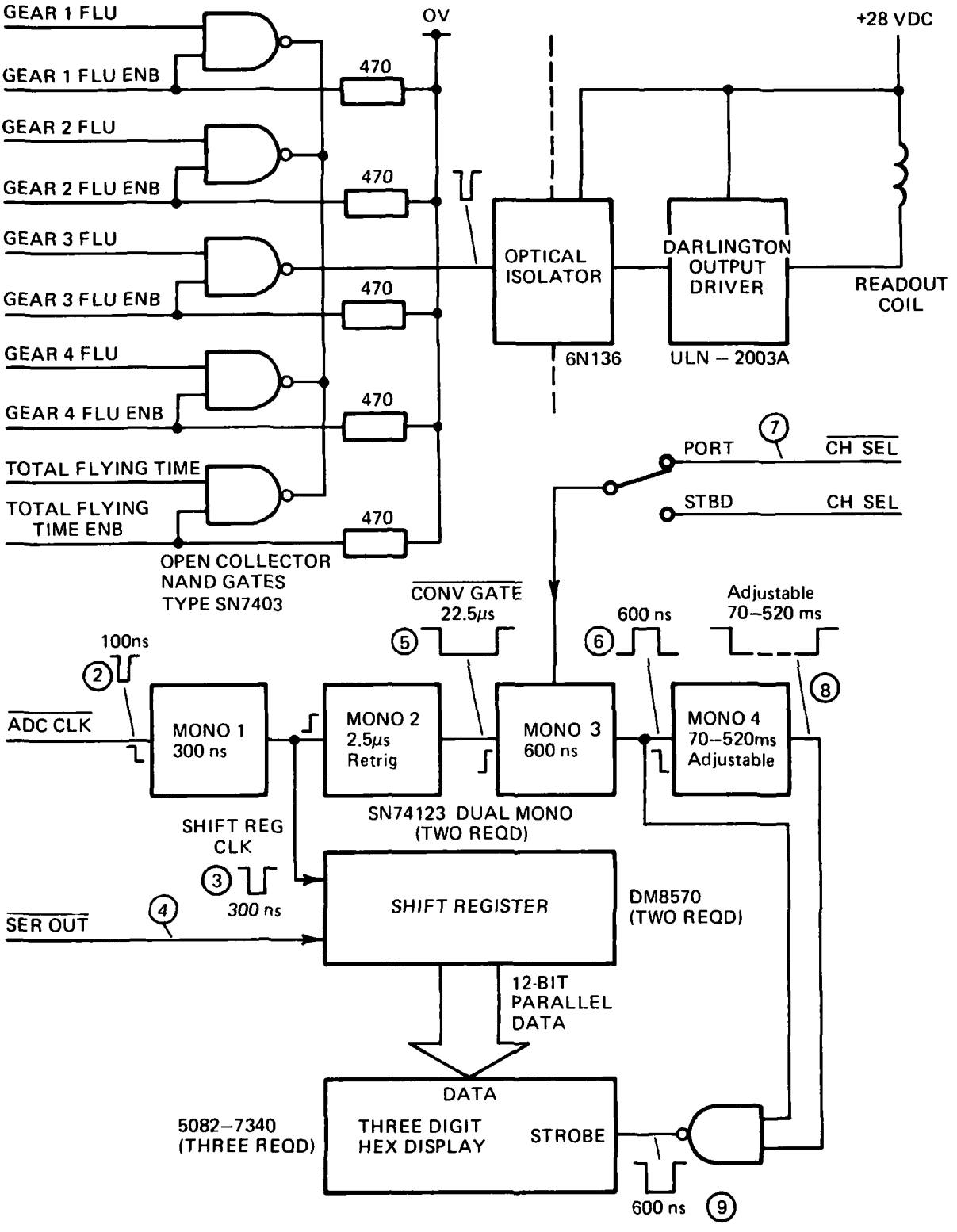

FIG. 24 FLIGHT-LINE FUNCTION TESTER FUNCTIONAL SCHEMA

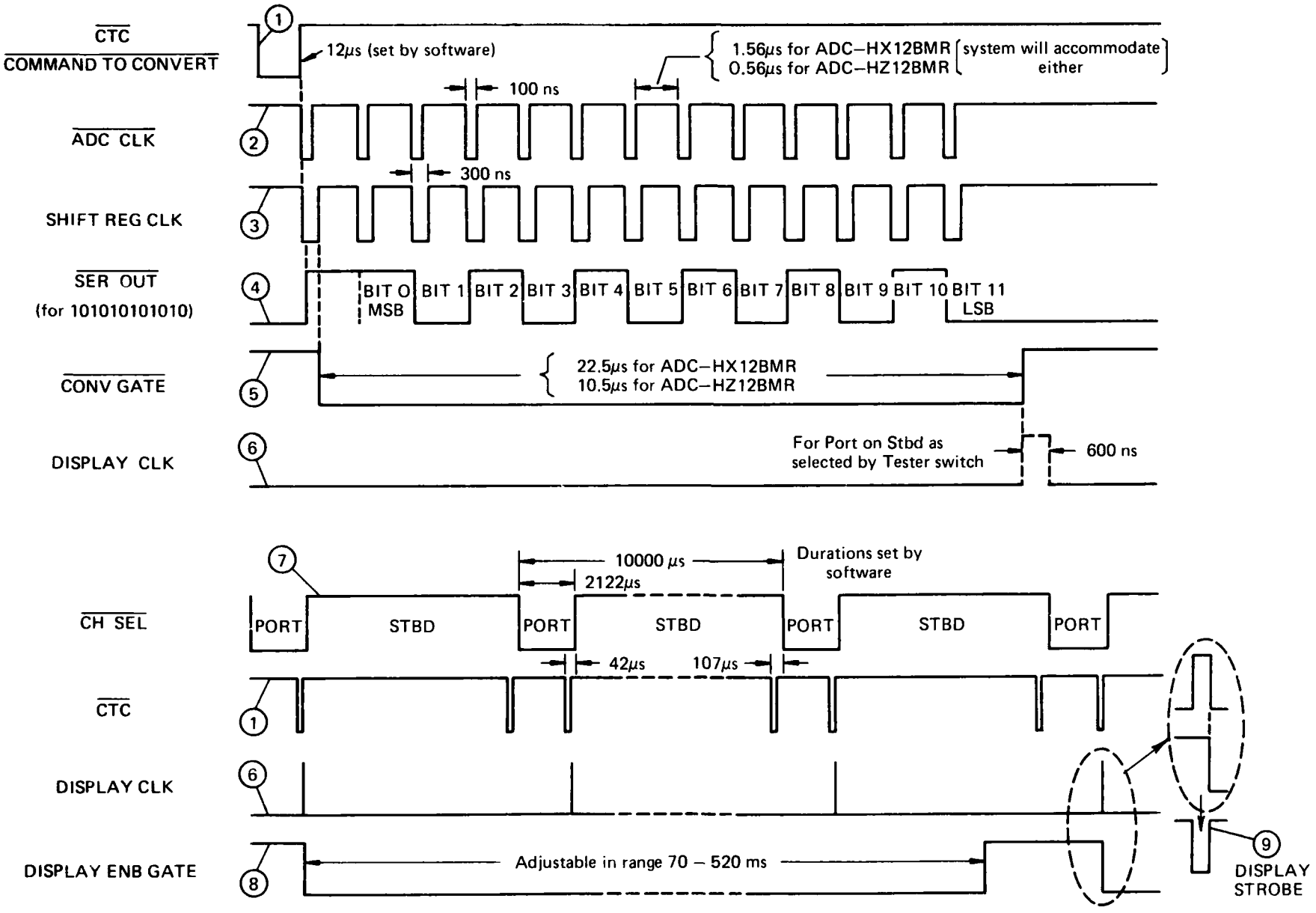

FIG. 25 FATIGUE LIFE USAGE TESTER TIMING DIAGRAM

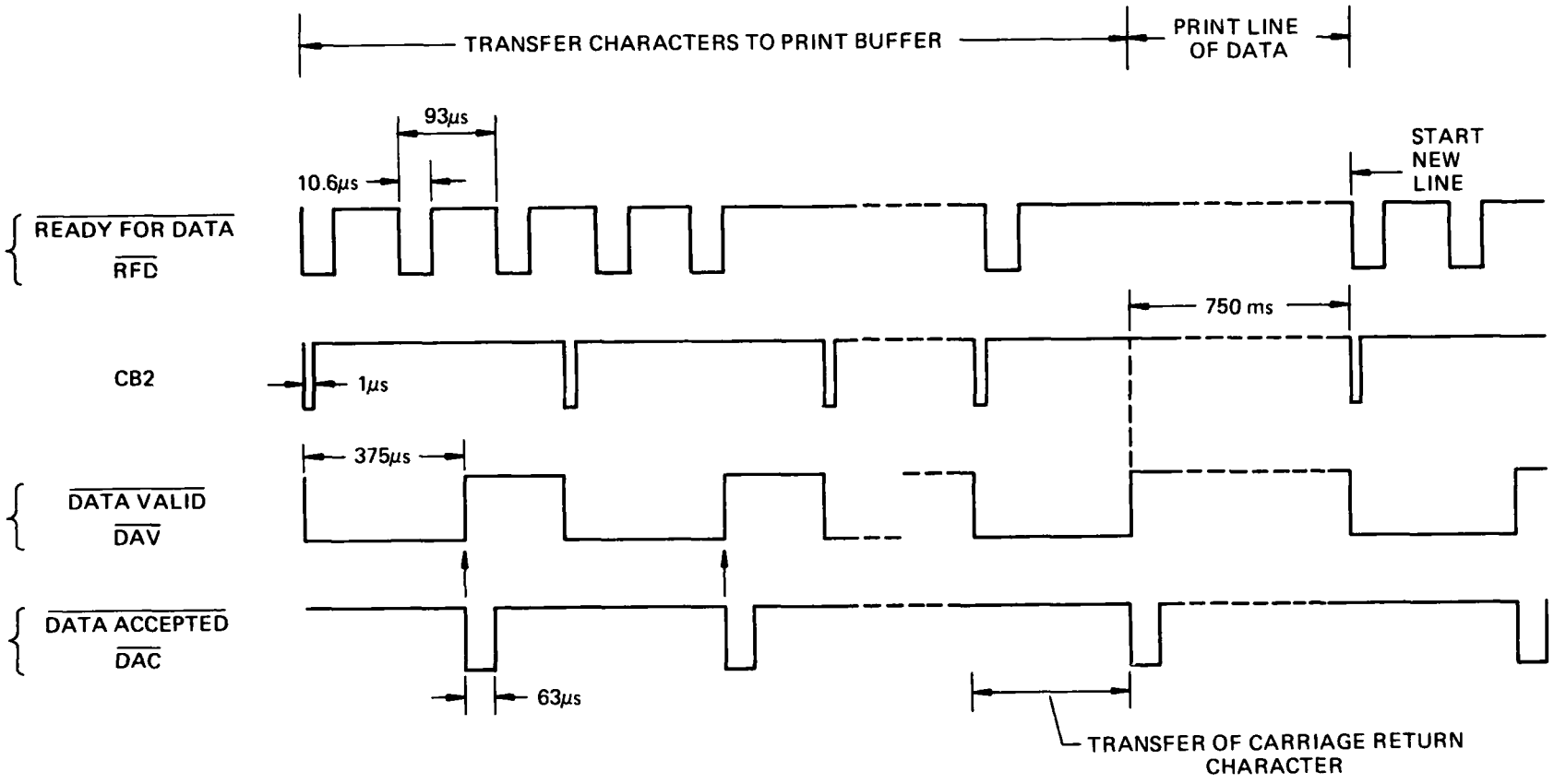

TIMES ARE APPROXIMATE ONLY

FIG. 26 PRINTER SIGNAL TIMING

SEA KING TRMLIF 01

BAND	DURN (SEC)
PORT-0	5694.09
PORT-1	3007.40
PORT-2	0396.61
PORT-3	0050.74
PORT-4	0009.33
PORT-5	0004.10
PORT-6	0000.00
PORT-7	0000.00
PORT-8	0000.00
PORT-9	0000.00
STBD-0	4956.44
STBD-1	3204.31
STBD-2	0310.77
STBD-3	0005.09
STBD-4	0000.00
STBD-5	0000.00
STBD-6	0000.00
STBD-7	0000.00
STBD-8	0000.00
STBD-9	0000.00
TOTL-0	5321.02
TOTL-1	4108.30
TOTL-2	1856.32
TOTL-3	0202.13
TOTL-4	0001.23
TOTL-5	0000.06
TOTL-6	0000.00
TOTL-7	0000.00
TOTL-8	0000.00
TOTL-9	0000.00

GEAR	FLU
G1	00012
G2	00000
G3	00017
G4	00000

TOTAL FLYING TIME

11490 SEC
3.1914 HR

AIRCRAFT NO. N16 -118

DATE: 9-7-80

TAKE-OFF TIME: 1115

SORTIE TYPE: G.F.P.

COUNTER READINGS

GEAR 1: 2876

GEAR 2: 2798

GEAR 3: 7014

GEAR 4: 1207

TFTIME: 19902

ABOVE SECTION IS
FILLED IN AFTER
THE FLIGHT

FIG. 27 SAMPLE OF PRINTER OUTPUT

```
*
* LIFE TABLE : INPUT SPUR PINION S6137.23051/2
*
*   THE FOLLOWING OUTPUT FROM F10 PROGRAM LIFCAL
* PROVIDES TABLE ENTRIES FOR THE FATIGUE LIFE USAGE
* INCREMENT PER SAMPLE FOR VARIOUS LEVELS OF TORQUE
* LOADING.
*
* X  = T/TE-1      WHERE "TE" IS CURVE 1 ENDUR LIM
* TB = (1+XL)*TE   WHERE "TB" IS CURVE 2 ENDUR LIM
* N  = (A1/X)**B1          FOR  X > XM
* N  = EXP**((A2-X)/B2)    FOR  X < XM
* U  = F/(60*S*N)
*
* A1 = 48.90  B1 = 2.5846  A2 = 1.0425  B2 = 0.05967
* XL = 0.0393  XM = 0.1542
*
* T  = NORMALIZED APPLIED TORQUE (100% TORQUE =1.00)
* N  = TOTAL SAFE FATIGUE CYCLES AT TORQUE T
* U  = FATIGUE LIFE USAGE PER ADC SAMPLE AT TORQUE T
*
* TB = NORMALIZED (FACTORED) ENDUR LIM      = 1.2300
* TH = NORMALIZED MAX TORQUE OF INTEREST    = 1.540
* S  = GEAR ROTATIONAL SPEED (R.P.M.)       = 19525.0
* F  = ADC SAMPLES PER SEC (FOR EACH TORQ)  = 100.000
* G  = ADC SENSITIV FACTOR (NORM TORQ/BIT)  =  .00600
* TZ = TORQUE FOR ZERO ADC OUTPUT           =  .02600
* K  = READOUT UNIT (LIFE=10**K COUNTS)     = 6
* R  = READOUT ADDRESS CODE (HEX)           =$04
*
PSETBL  FCB     $04     OUTPUT ADDRESS CODE
        FCB     200     LIMIT BELOW WHICH FLU=0
        FCB     255     NO 2-BYTE BRKPT,255=DUMMY
        FCB     255     NO 3-BYTE BRKPT,255=DUMMY
        FDB        0    UPPER 2 BYTES OF FLU UNIT
        FDB        0    MIDDL 2 BYTES OF FLU UNIT
        FDB     2862    LOWER 2 BYTES OF FLU UNIT
        FDB      157    ADC = 200 ($C8) TRQ = 122.6 %
        FDB      500    ADC = 201 ($C9) TRQ = 123.2 %
        FDB      544    ADC = 202 ($CA) TRQ = 123.8 %
        FDB      593    ADC = 203 ($CB) TRQ = 124.4 %
        FDB      645    ADC = 204 ($CC) TRQ = 125.0 %
        FDB      702    ADC = 205 ($CD) TRQ = 125.6 %
        FDB      765    ADC = 206 ($CE) TRQ = 126.2 %
        FDB      832    ADC = 207 ($CF) TRQ = 126.8 %
        FDB      906    ADC = 208 ($D0) TRQ = 127.4 %
        FDB      987    ADC = 209 ($D1) TRQ = 128.0 %
        FDB     1074    ADC = 210 ($D2) TRQ = 128.6 %
        FDB     1169    ADC = 211 ($D3) TRQ = 129.2 %
        FDB     1273    ADC = 212 ($D4) TRQ = 129.8 %
        FDB     1386    ADC = 213 ($D5) TRQ = 130.4 %
        FDB     1509    ADC = 214 ($D6) TRQ = 131.0 %
        FDB     1643    ADC = 215 ($D7) TRQ = 131.6 %
        FDB     1788    ADC = 216 ($D8) TRQ = 132.2 %
        FDB     1947    ADC = 217 ($D9) TRQ = 132.8 %
        FDB     2120    ADC = 218 ($DA) TRQ = 133.4 %
        FDB     2307    ADC = 219 ($DB) TRQ = 134.0 %
        FDB     2512    ADC = 220 ($DC) TRQ = 134.6 %
        FDB     2735    ADC = 221 ($DD) TRQ = 135.2 %
        FDB     2977    ADC = 222 ($DE) TRQ = 135.8 %
        FDB     3241    ADC = 223 ($DF) TRQ = 136.4 %
        FDB     3522    ADC = 224 ($E0) TRQ = 137.0 %
        FDB     3817    ADC = 225 ($E1) TRQ = 137.6 %
        FDB     4127    ADC = 226 ($E2) TRQ = 138.2 %
        FDB     4452    ADC = 227 ($E3) TRQ = 138.8 %
        FDB     4793    ADC = 228 ($E4) TRQ = 139.4 %
        FDB     5149    ADC = 229 ($E5) TRQ = 140.0 %
        FDB     5520    ADC = 230 ($E6) TRQ = 140.6 %
        FDB     5908    ADC = 231 ($E7) TRQ = 141.2 %
        FDB     6312    ADC = 232 ($E8) TRQ = 141.8 %
        FDB     6732    ADC = 233 ($E9) TRQ = 142.4 %
        FDB     7169    ADC = 234 ($EA) TRQ = 143.0 %
        FDB     7623    ADC = 235 ($EB) TRQ = 143.6 %
        FDB     8095    ADC = 236 ($EC) TRQ = 144.2 %
        FDB     8584    ADC = 237 ($ED) TRQ = 144.8 %
        FDB     9090    ADC = 238 ($EE) TRQ = 145.4 %
        FDB     9614    ADC = 239 ($EF) TRQ = 146.0 %
        FDB    10157    ADC = 240 ($F0) TRQ = 146.6 %
        FDB    10718    ADC = 241 ($F1) TRQ = 147.2 %
        FDB    11297    ADC = 242 ($F2) TRQ = 147.8 %
        FDB    11895    ADC = 243 ($F3) TRQ = 148.4 %
        FDB    12513    ADC = 244 ($F4) TRQ = 149.0 %
        FDB    13149    ADC = 245 ($F5) TRQ = 149.6 %
        FDB    13805    ADC = 246 ($F6) TRQ = 150.2 %
        FDB    14481    ADC = 247 ($F7) TRQ = 150.8 %
        FDB    15177    ADC = 248 ($F8) TRQ = 151.4 %
        FDB    15893    ADC = 249 ($F9) TRQ = 152.0 %
        FDB    16629    ADC = 250 ($FA) TRQ = 152.6 %
        FDB    17385    ADC = 251 ($FB) TRQ = 153.2 %
        FDB    18163    ADC = 252 ($FC) TRQ = 153.8 %
```

```
*
* LIFE TABLE : HELICAL GEAR (SUMMING) S6137.23050/1
*
*   THE FOLLOWING OUTPUT FROM F10 PROGRAM LIFCAL
* PROVIDES TABLE ENTRIES FOR THE FATIGUE LIFE USAGE
* INCREMENT PER SAMPLE FOR VARIOUS LEVELS OF TORQUE
* LOADING.
*
* X  = T/TE-1      WHERE "TE" IS CURVE 1 ENDUR LIM
* TB = (1+XL)*TE   WHERE "TB" IS CURVE 2 ENDUR LIM
* N  = (A1/X)**B1          FOR  X > XM
* N  = EXP**((A2-X)/B2)    FOR  X < XM
* U  = F/(60*S*N)
*
* A1 = 48.90  B1 = 2.5846  A2 = 1.0425  B2 = 0.05967
* XL = 0.0393  XM = 0.1542
*
* T  = NORMALIZED APPLIED TORQUE (100% TORQUE =1.00)
* N  = TOTAL SAFE FATIGUE CYCLES AT TORQUE T
* U  = FATIGUE LIFE USAGE PER ADC SAMPLE AT TORQUE T
*
* TB = NORMALIZED (FACTORED) ENDUR LIM      = 1.1850
* TH = NORMALIZED MAX TORQUE OF INTEREST    = 1.540
* S  = GEAR ROTATIONAL SPEED (R.P.M.)       =  3291.0
* F  = ADC SAMPLES PER SEC (FOR EACH TORQ)  = 100.000
* G  = ADC SENSITIV FACTOR (NORM TORQ/BIT)  =  .00600
* TZ = TORQUE FOR ZERO ADC OUTPUT           =  .02600
* K  = READOUT UNIT (LIFE=10**K COUNTS)     = 6
* R  = READOUT ADDRESS CODE (HEX)           =$10
*
SUMTBL  FCB     $10     OUTPUT ADDRESS CODE
        FCB     193     LIMIT BELOW WHICH FLU=0
        FCB     255     NO 2-BYTE BRKPT,255=DUMMY
        FCB     255     NO 3-BYTE BRKPT,255=DUMMY
        FDB        0    UPPER 2 BYTES OF FLU UNIT
        FDB        0    MIDDL 2 BYTES OF FLU UNIT
        FDB    16203    LOWER 2 BYTES OF FLU UNIT
        FDB      384    ADC = 193 ($C1) TRQ = 118.4 %
        FDB      500    ADC = 194 ($C2) TRQ = 119.0 %
        FDB      546    ADC = 195 ($C3) TRQ = 119.6 %
        FDB      596    ADC = 196 ($C4) TRQ = 120.2 %
        FDB      651    ADC = 197 ($C5) TRQ = 120.8 %
        FDB      711    ADC = 198 ($C6) TRQ = 121.4 %
        FDB      777    ADC = 199 ($C7) TRQ = 122.0 %
        FDB      849    ADC = 200 ($C8) TRQ = 122.6 %
        FDB      927    ADC = 201 ($C9) TRQ = 123.2 %
        FDB     1012    ADC = 202 ($CA) TRQ = 123.8 %
        FDB     1106    ADC = 203 ($CB) TRQ = 124.4 %
        FDB     1208    ADC = 204 ($CC) TRQ = 125.0 %
        FDB     1319    ADC = 205 ($CD) TRQ = 125.6 %
        FDB     1441    ADC = 206 ($CE) TRQ = 126.2 %
        FDB     1573    ADC = 207 ($CF) TRQ = 126.8 %
        FDB     1719    ADC = 208 ($D0) TRQ = 127.4 %
        FDB     1877    ADC = 209 ($D1) TRQ = 128.0 %
        FDB     2050    ADC = 210 ($D2) TRQ = 128.6 %
        FDB     2239    ADC = 211 ($D3) TRQ = 129.2 %
        FDB     2445    ADC = 212 ($D4) TRQ = 129.8 %
        FDB     2671    ADC = 213 ($D5) TRQ = 130.4 %
        FDB     2917    ADC = 214 ($D6) TRQ = 131.0 %
        FDB     3184    ADC = 215 ($D7) TRQ = 131.6 %
        FDB     3468    ADC = 216 ($D8) TRQ = 132.2 %
        FDB     3766    ADC = 217 ($D9) TRQ = 132.8 %
        FDB     4080    ADC = 218 ($DA) TRQ = 133.4 %
        FDB     4410    ADC = 219 ($DB) TRQ = 134.0 %
        FDB     4755    ADC = 220 ($DC) TRQ = 134.6 %
        FDB     5116    ADC = 221 ($DD) TRQ = 135.2 %
        FDB     5493    ADC = 222 ($DE) TRQ = 135.8 %
        FDB     5887    ADC = 223 ($DF) TRQ = 136.4 %
        FDB     6298    ADC = 224 ($E0) TRQ = 137.0 %
        FDB     6726    ADC = 225 ($E1) TRQ = 137.6 %
        FDB     7172    ADC = 226 ($E2) TRQ = 138.2 %
        FDB     7635    ADC = 227 ($E3) TRQ = 138.8 %
        FDB     8116    ADC = 228 ($E4) TRQ = 139.4 %
        FDB     8615    ADC = 229 ($E5) TRQ = 140.0 %
        FDB     9133    ADC = 230 ($E6) TRQ = 140.6 %
        FDB     9669    ADC = 231 ($E7) TRQ = 141.2 %
        FDB    10224    ADC = 232 ($E8) TRQ = 141.8 %
        FDB    10798    ADC = 233 ($E9) TRQ = 142.4 %
        FDB    11392    ADC = 234 ($EA) TRQ = 143.0 %
        FDB    12005    ADC = 235 ($EB) TRQ = 143.6 %
        FDB    12638    ADC = 236 ($EC) TRQ = 144.2 %
        FDB    13291    ADC = 237 ($ED) TRQ = 144.8 %
        FDB    13964    ADC = 238 ($EE) TRQ = 145.4 %
        FDB    14658    ADC = 239 ($EF) TRQ = 146.0 %
        FDB    15373    ADC = 240 ($F0) TRQ = 146.6 %
        FDB    16108    ADC = 241 ($F1) TRQ = 147.2 %
        FDB    16865    ADC = 242 ($F2) TRQ = 147.8 %
        FDB    17643    ADC = 243 ($F3) TRQ = 148.4 %
        FDB    18443    ADC = 244 ($F4) TRQ = 149.0 %
        FDB    19265    ADC = 245 ($F5) TRQ = 149.6 %
        FDB    20108    ADC = 246 ($F6) TRQ = 150.2 %
        FDB    20974    ADC = 247 ($F7) TRQ = 150.8 %
        FDB    21863    ADC = 248 ($F8) TRQ = 151.4 %
        FDB    22774    ADC = 249 ($F9) TRQ = 152.0 %
        FDB    23708    ADC = 250 ($FA) TRQ = 152.6 %
        FDB    24665    ADC = 251 ($FB) TRQ = 153.2 %
        FDB    25645    ADC = 252 ($FC) TRQ = 153.8 %
```

FIG. 28 FATIGUE LIFE USAGE LOOK-UP TABLES FOR GEARS 1-3

```
*
*
* LIFE TABLE : SPIRAL BEVEL PINION S6137.23053/1
*
*   THE FOLLOWING OUTPUT FROM F10 PROGRAM LIFCAL
* PROVIDES TABLE ENTRIES FOR THE FATIGUE LIFE USAGE
* INCREMENT PER SAMPLE FOR VARIOUS LEVELS OF TORQUE
* LOADING.
*
* X  = T/TE-1      WHERE "TE" IS CURVE 1 ENDUR LIM
* TB = (1+XL)*TE   WHERE "TB" IS CURVE 2 ENDUR LIM
* N  = (A1/X)**B1          FOR  X > XM
* N  = EXP**((A2-X)/B2)    FOR  X < XM
* U  = F/(60*S*N)
*
* A1 = 48.90  B1 = 2.5846  A2 = 1.0425  B2 = 0.05967
* XL = 0.0393  XM = 0.1542
*
* T  = NORMALIZED APPLIED TORQUE (100% TORQUE =1.00)
* N  = TOTAL SAFE FATIGUE CYCLES AT TORQUE T
* U  = FATIGUE LIFE USAGE PER ADC SAMPLE AT TORQUE T
*
* TB = NORMALIZED (FACTORED) ENDUR LIM      = 1.0900
* TH = NORMALIZED MAX TORQUE OF INTEREST    = 1.300
* S  = GEAR ROTATIONAL SPEED (R.P.M.)       =  3291.0
* F  = ADC SAMPLES PER SEC (FOR EACH TORQ)  = 100.000
* G  = ADC SENSITIV FACTOR (NORM TORQ/BIT)  =  .00600
* TZ = TORQUE FOR ZERO ADC OUTPUT           =  .02600
* K  = READOUT UNIT (LIFE=10**K COUNTS)     = 6
* R  = READOUT ADDRESS CODE (HEX)           =$20
*
MGRTBL  FCB     $20     OUTPUT ADDRESS CODE
        FCB     177     LIMIT BELOW WHICH FLU=0
        FCB     255     NO 2-BYTE BRKPT,255=DUMMY
        FCB     255     NO 3-BYTE BRKPT,255=DUMMY
        FDB       0     UPPER 2 BYTES OF FLU UNIT
        FDB       0     MIDDL 2 BYTES OF FLU UNIT
        FDB   16295     LOWER 2 BYTES OF FLU UNIT
        FDB     308     ADC = 177 ($B1) TRQ = 108.8 %
        FDB     500     ADC = 178 ($B2) TRQ = 109.4 %
        FDB     550     ADC = 179 ($B3) TRQ = 110.0 %
        FDB     606     ADC = 180 ($B4) TRQ = 110.6 %
        FDB     667     ADC = 181 ($B5) TRQ = 111.2 %
        FDB     734     ADC = 182 ($B6) TRQ = 111.8 %
        FDB     808     ADC = 183 ($B7) TRQ = 112.4 %
        FDB     889     ADC = 184 ($B8) TRQ = 113.0 %
        FDB     978     ADC = 185 ($B9) TRQ = 113.6 %
        FDB    1077     ADC = 186 ($BA) TRQ = 114.2 %
        FDB    1185     ADC = 187 ($BB) TRQ = 114.8 %
        FDB    1304     ADC = 188 ($BC) TRQ = 115.4 %
        FDB    1435     ADC = 189 ($BD) TRQ = 116.0 %
        FDB    1580     ADC = 190 ($BE) TRQ = 116.6 %
        FDB    1739     ADC = 191 ($BF) TRQ = 117.2 %
        FDB    1914     ADC = 192 ($C0) TRQ = 117.8 %
        FDB    2106     ADC = 193 ($C1) TRQ = 118.4 %
        FDB    2318     ADC = 194 ($C2) TRQ = 119.0 %
        FDB    2552     ADC = 195 ($C3) TRQ = 119.6 %
        FDB    2808     ADC = 196 ($C4) TRQ = 120.2 %
        FDB    3090     ADC = 197 ($C5) TRQ = 120.8 %
        FDB    3394     ADC = 198 ($C6) TRQ = 121.4 %
        FDB    3716     ADC = 199 ($C7) TRQ = 122.0 %
        FDB    4056     ADC = 200 ($C8) TRQ = 122.6 %
        FDB    4414     ADC = 201 ($C9) TRQ = 123.2 %
        FDB    4791     ADC = 202 ($CA) TRQ = 123.8 %
        FDB    5187     ADC = 203 ($CB) TRQ = 124.4 %
        FDB    5603     ADC = 204 ($CC) TRQ = 125.0 %
        FDB    6038     ADC = 205 ($CD) TRQ = 125.6 %
        FDB    6494     ADC = 206 ($CE) TRQ = 126.2 %
        FDB    6970     ADC = 207 ($CF) TRQ = 126.8 %
        FDB    7467     ADC = 208 ($D0) TRQ = 127.4 %
        FDB    7985     ADC = 209 ($D1) TRQ = 128.0 %
        FDB    8524     ADC = 210 ($D2) TRQ = 128.6 %
        FDB    9085     ADC = 211 ($D3) TRQ = 129.2 %
        FDB    9669     ADC = 212 ($D4) TRQ = 129.8 %
```

L_U

J_i
$(177 \leq i \leq 212)$

FIG. 29 FATIGUE LIFE USAGE LOOK-UP TABLE FOR GEAR 4

AD-A151 580 THE IN-FLIGHT ESTIMATION AND INDICATION OF CUMULATIVE FATIGUE DAMAGE TO HELICOPTER GEARS(U) AERONAUTICAL RESEARCH LABS MELBOURNE (AUSTRALIA) K F FRASER MAR 84 2/2

UNCLASSIFIED ARL/AERO-PROP-164 F/G 13/9 NL

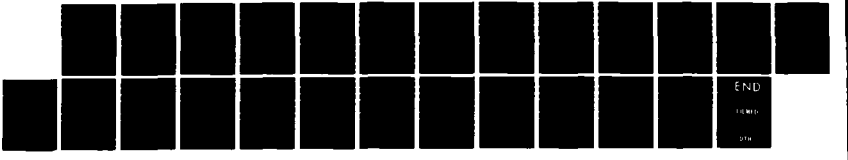

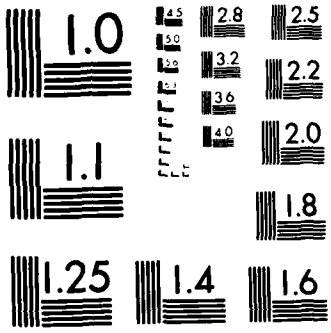

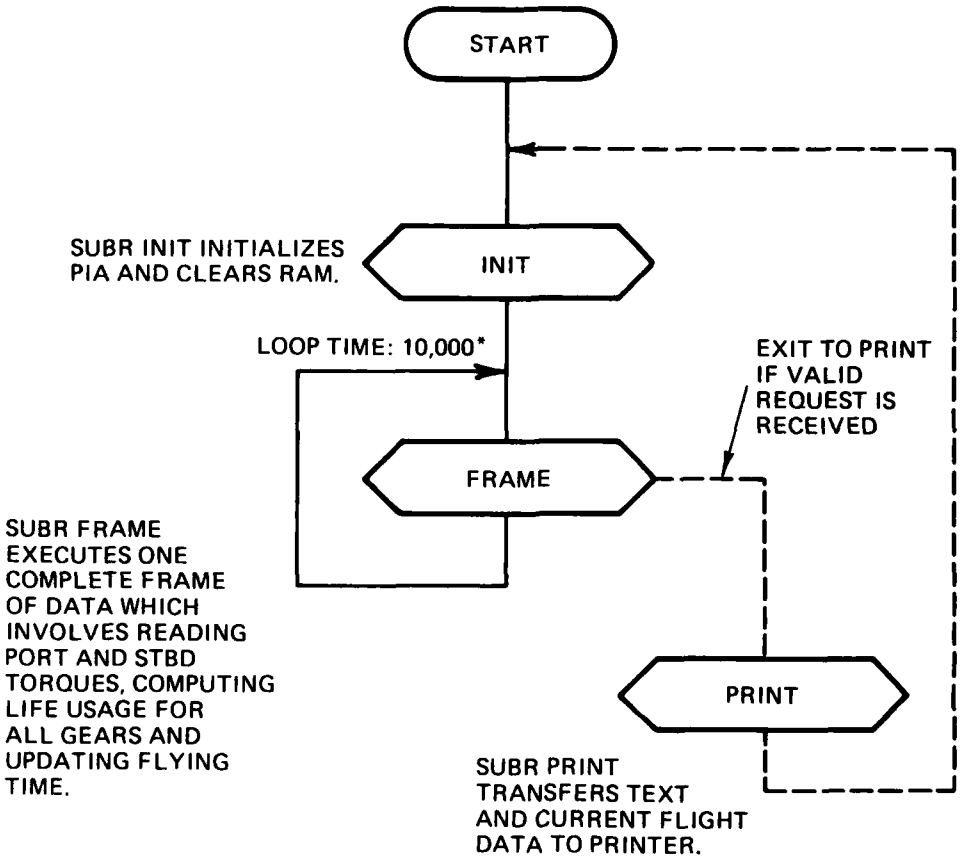

*LOOP TIMES ARE GIVEN AS THE NUMBER OF MACHINE CYCLE PERIODS. FOR THE PRESENT HARDWARE THE MACHINE CYCLE PERIOD IS 1.00 MICROSECOND.

FIG. 30 MAIN PROGRAM FLOW CHART

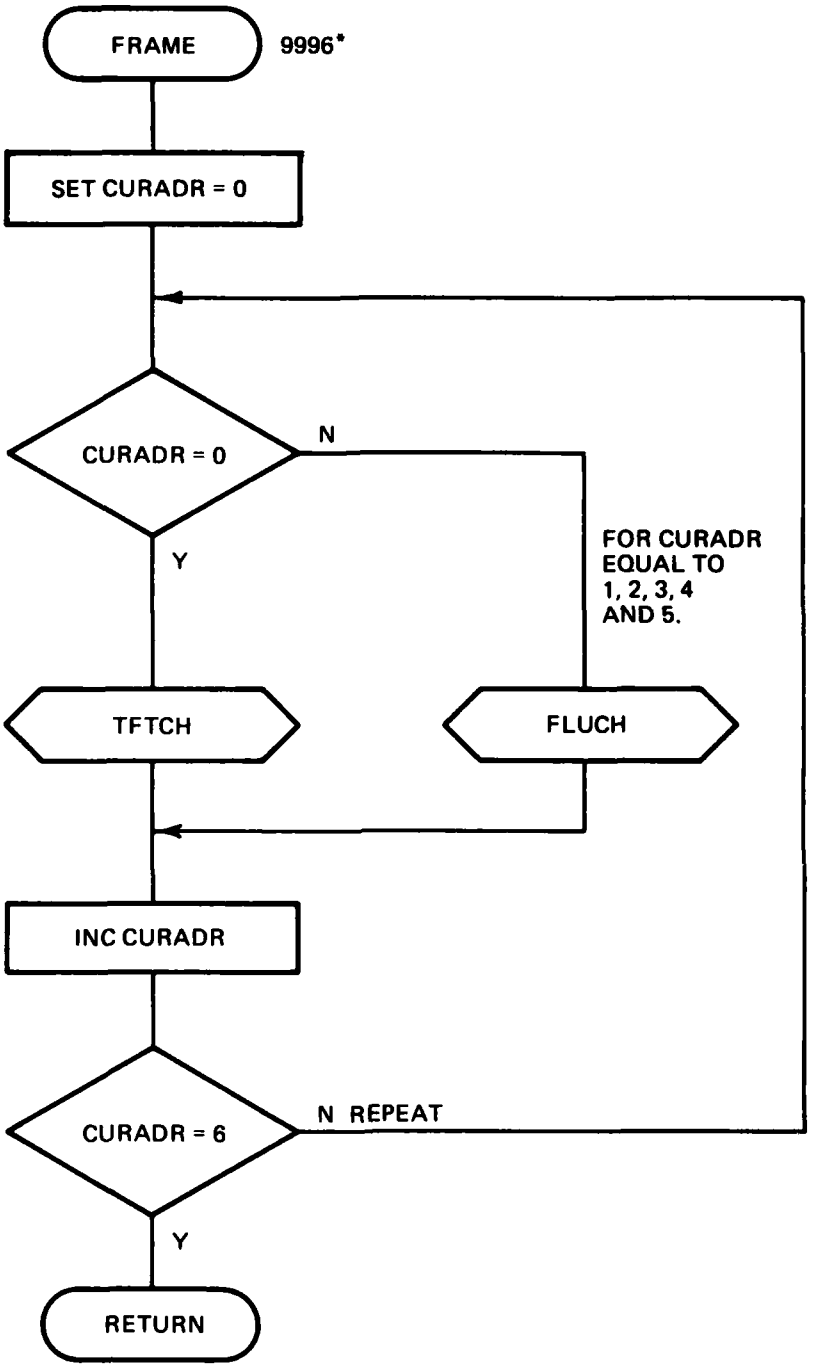

*EXECUTION TIME INCLUDING SUBROUTINE CALL

FIG. 31 FRAME SUBROUTINE FLOW CHART

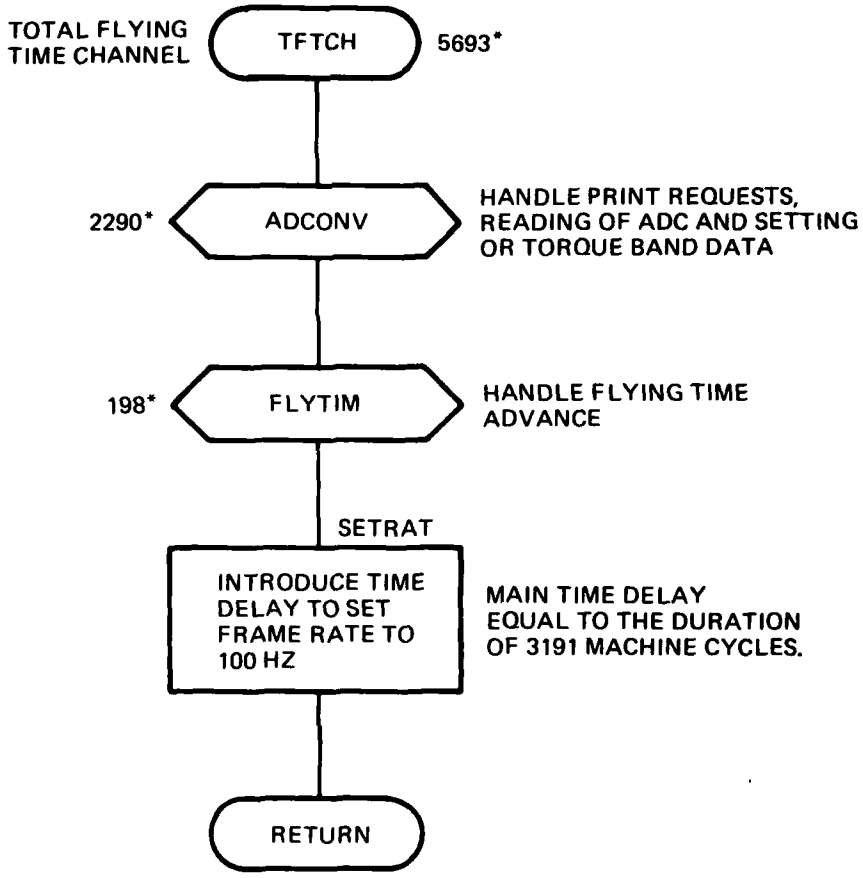

*EXECUTION TIME INCLUDING SUBROUTINE CALL

FIG. 32 TFTCH SUBROUTINE FLOW CHART

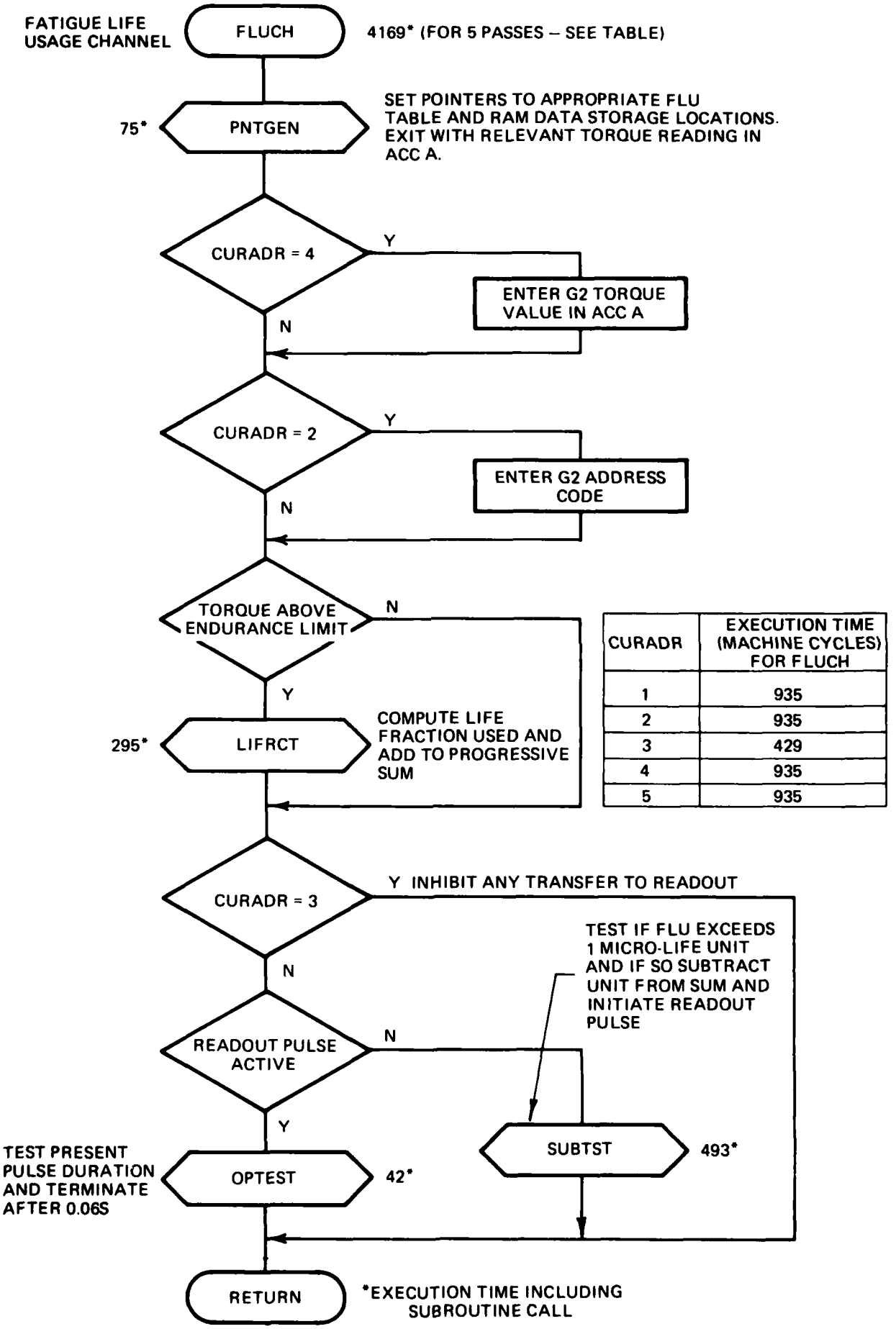

CURADR	EXECUTION TIME (MACHINE CYCLES) FOR FLUCH
1	935
2	935
3	429
4	935
5	935

FIG. 33 FLUCH SUBROUTINE FLOW CHART

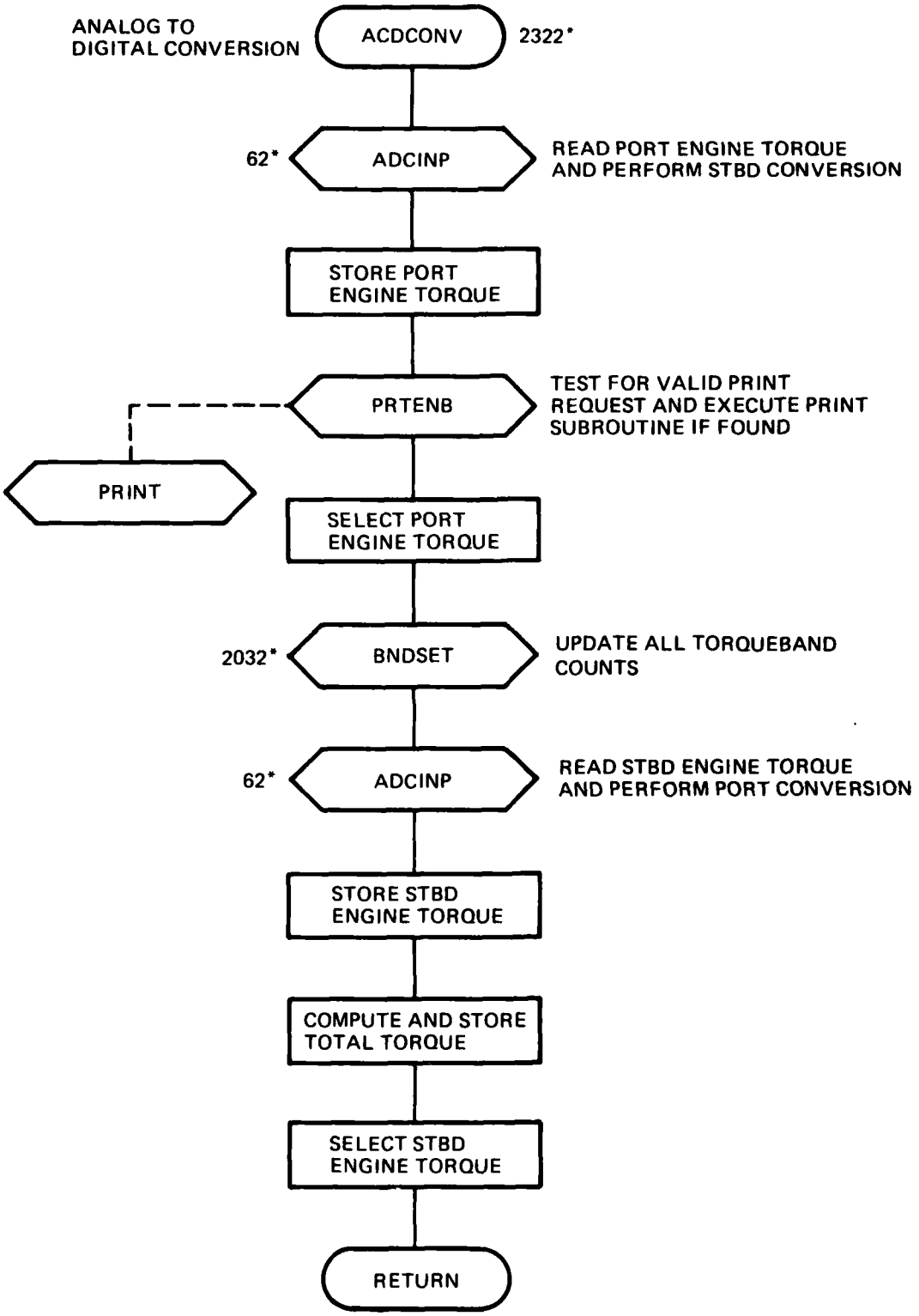

*EXECUTION TIME INCLUDING SUBROUTINE CALL

FIG. 34 ADCONV SUBROUTINE FLOW CHART

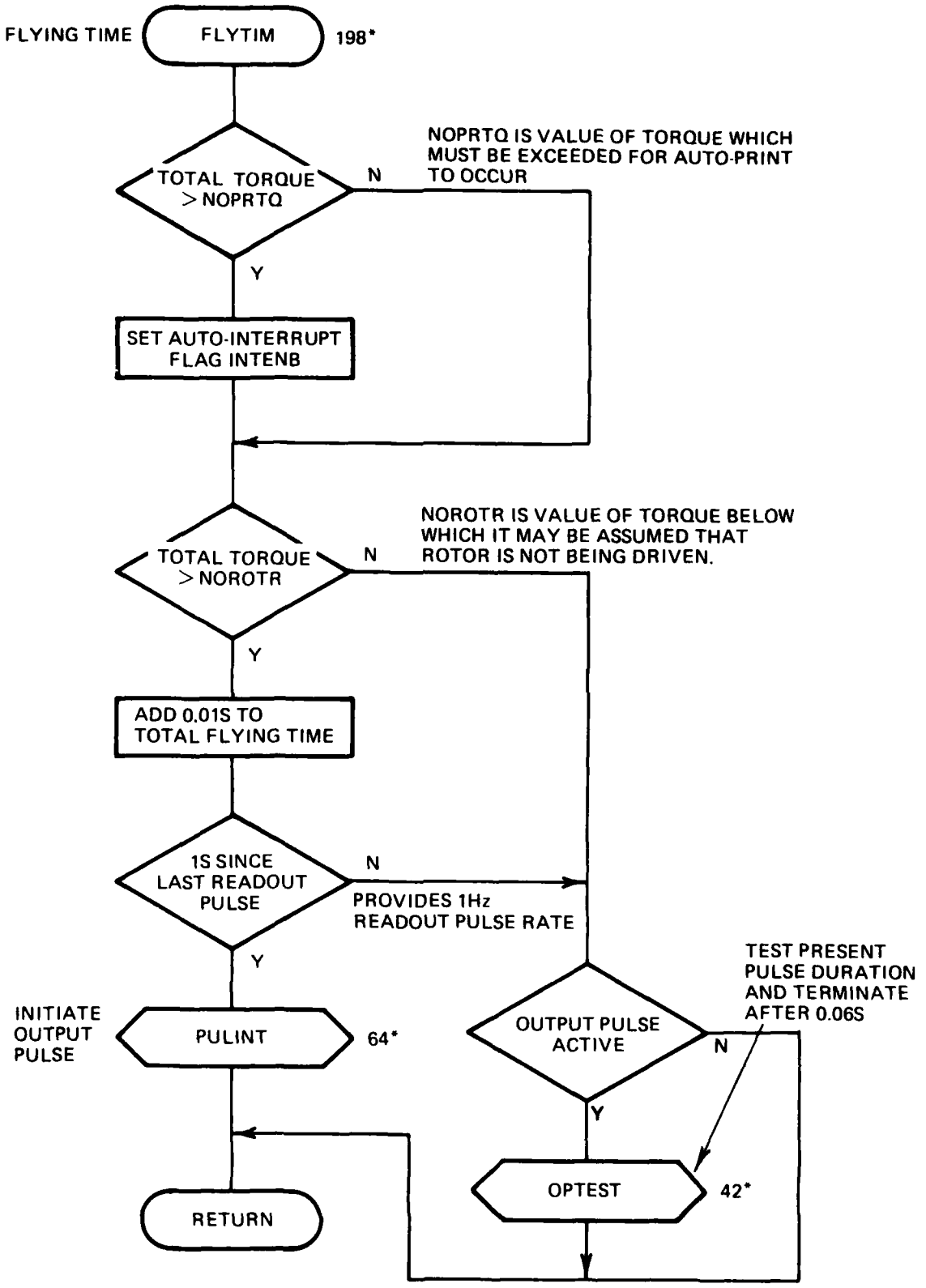

*EXECUTION TIME INCLUDING SUBROUTINE CALL.

FIG. 35 FLYTIM SUBROUTINE FLOW CHART

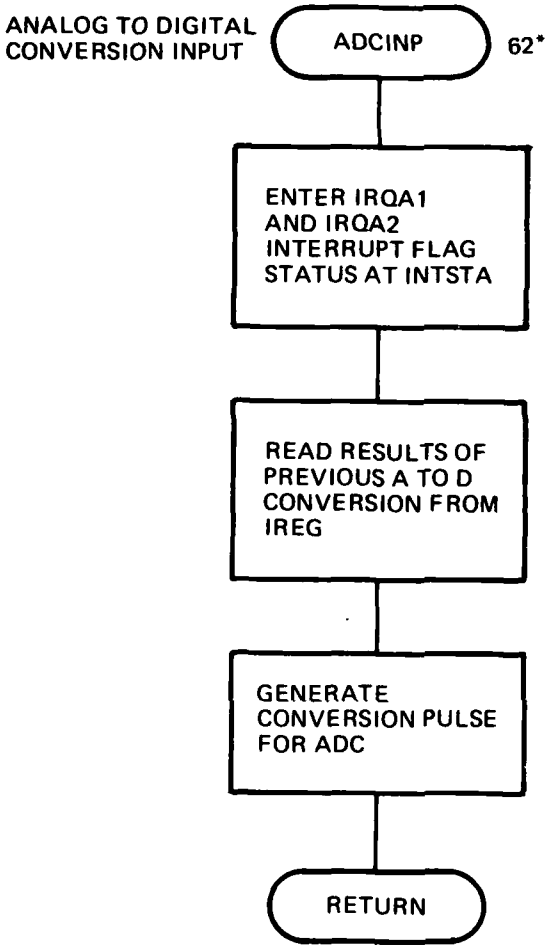

*EXECUTION TIME INCLUDING SUBROUTINE CALL

FIG. 36 ADCINP SUBROUTINE FLOW CHART

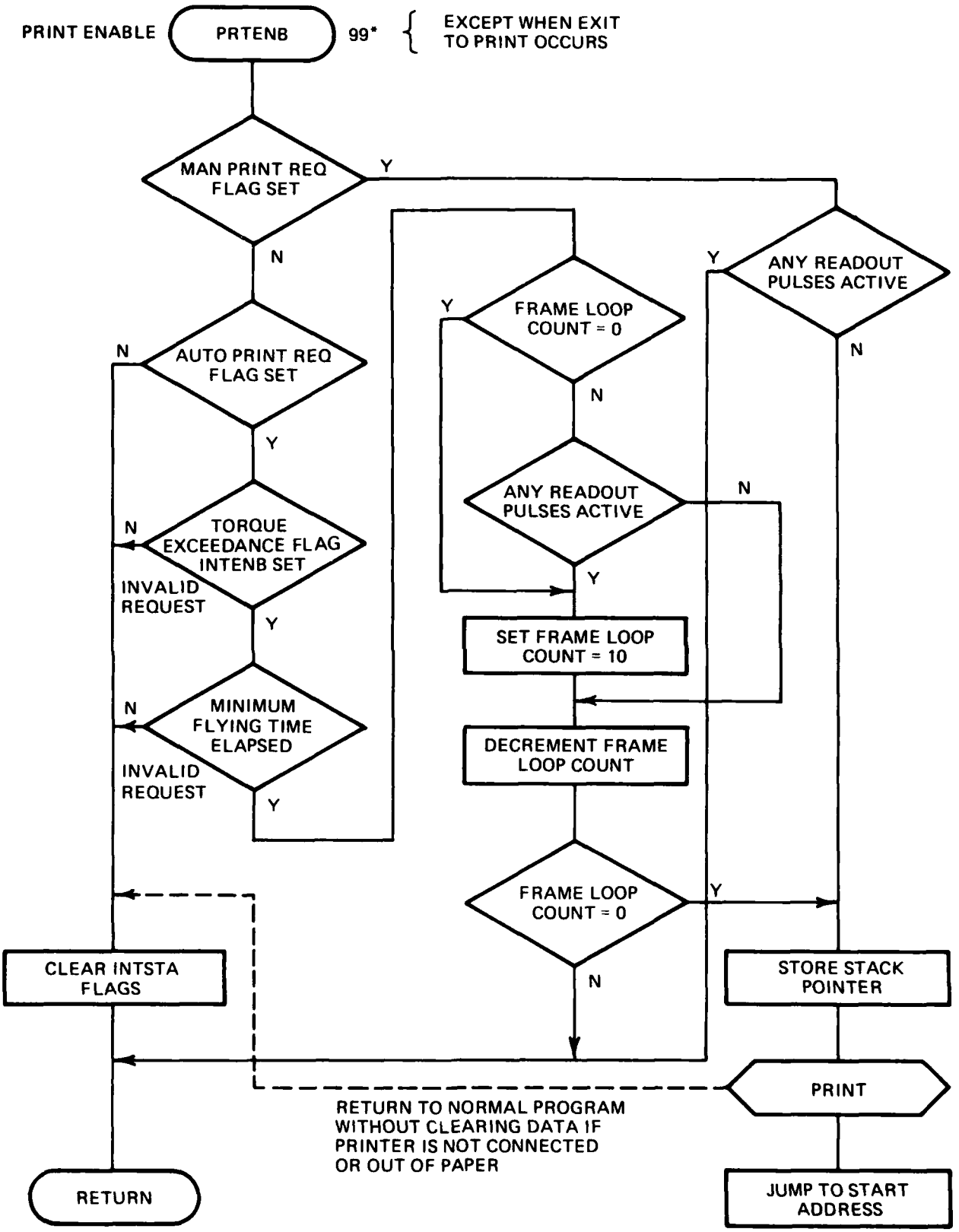

*EXECUTION TIME INCLUDING SUBROUTINE CALL

FIG. 37 PRTENB SUBROUTINE FLOW CHART

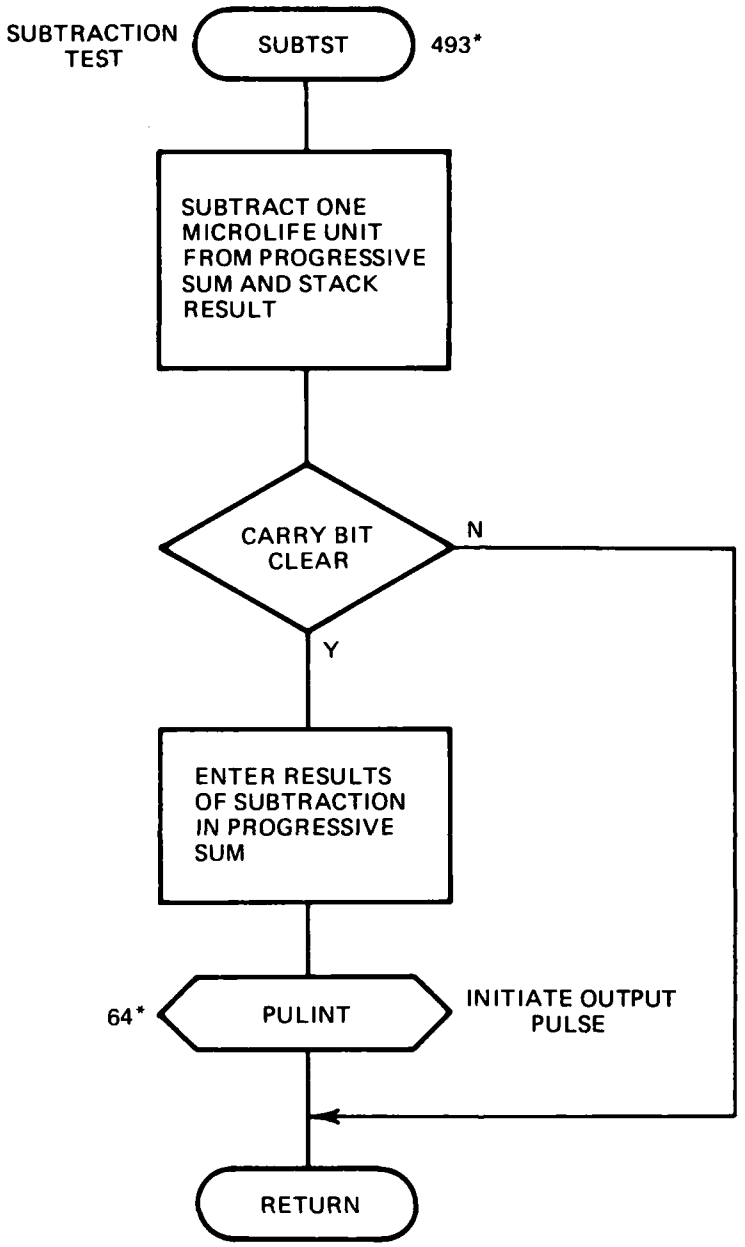

*EXECUTION TIME INCLUDING SUBROUTINE CALL

FIG. 38 SUBTST SUBROUTINE FLOW CHART

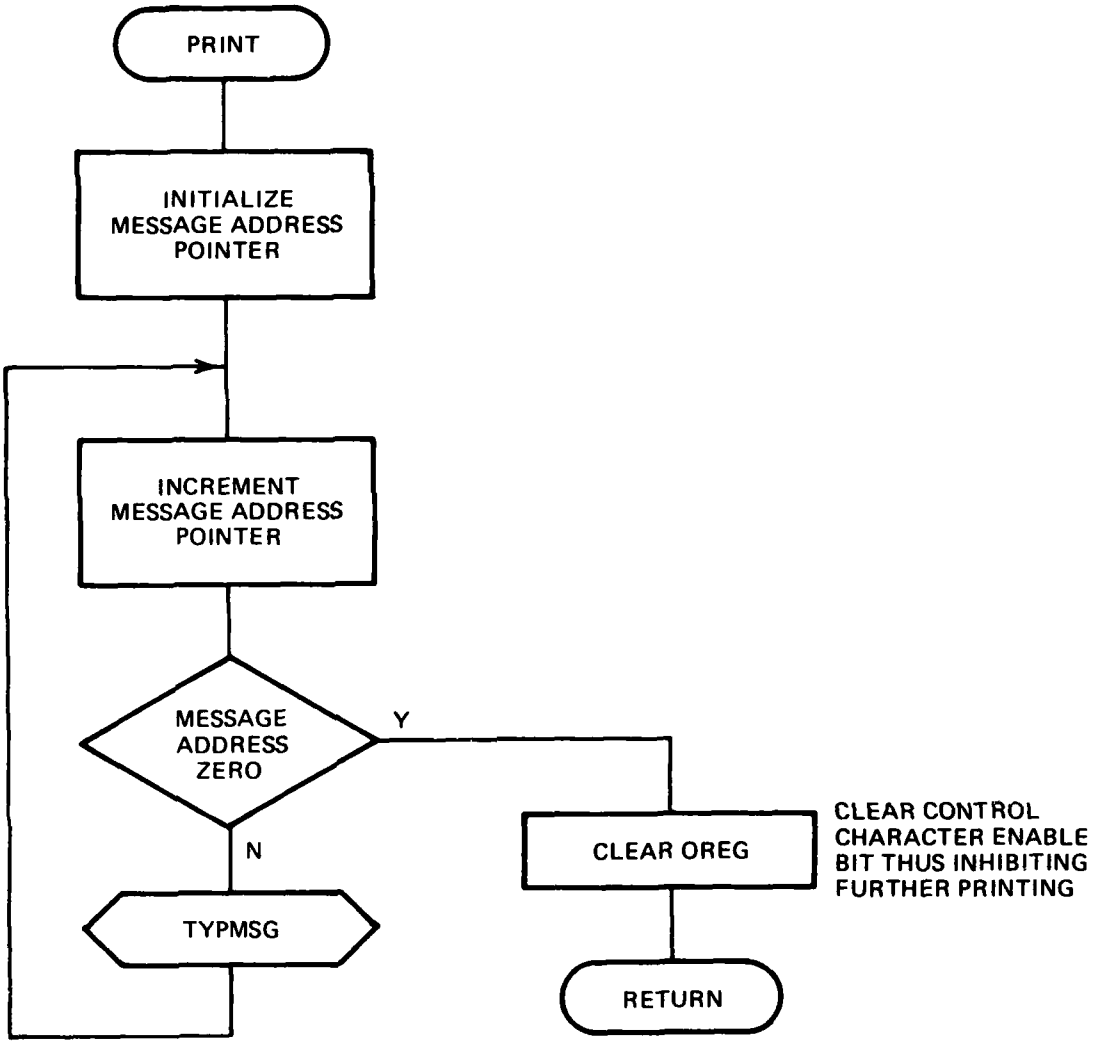

FIG. 39 PRINT SUBROUTINE FLOW CHART

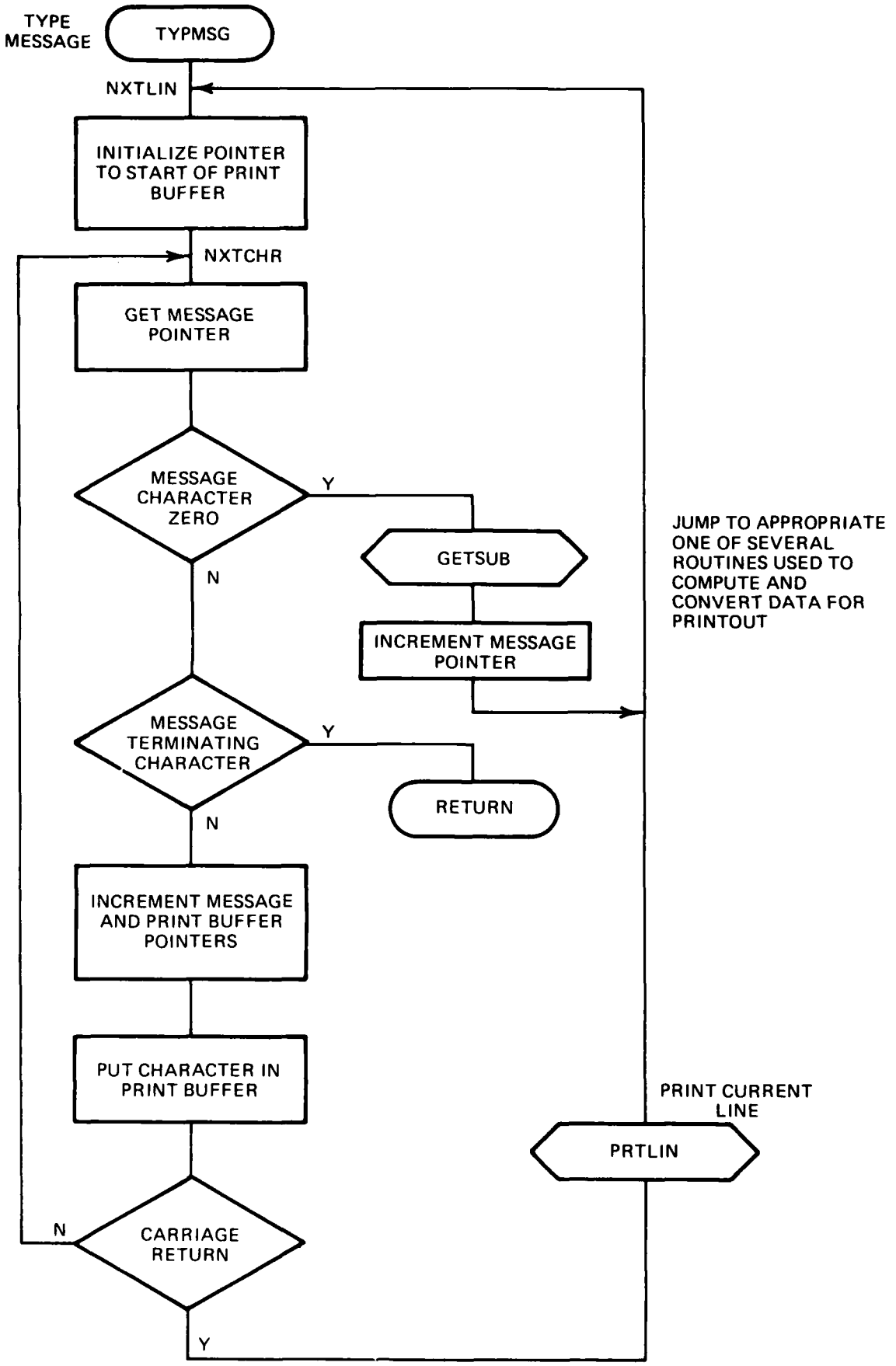

FIG. 40 TYPMSG SUBROUTINE FLOW CHART

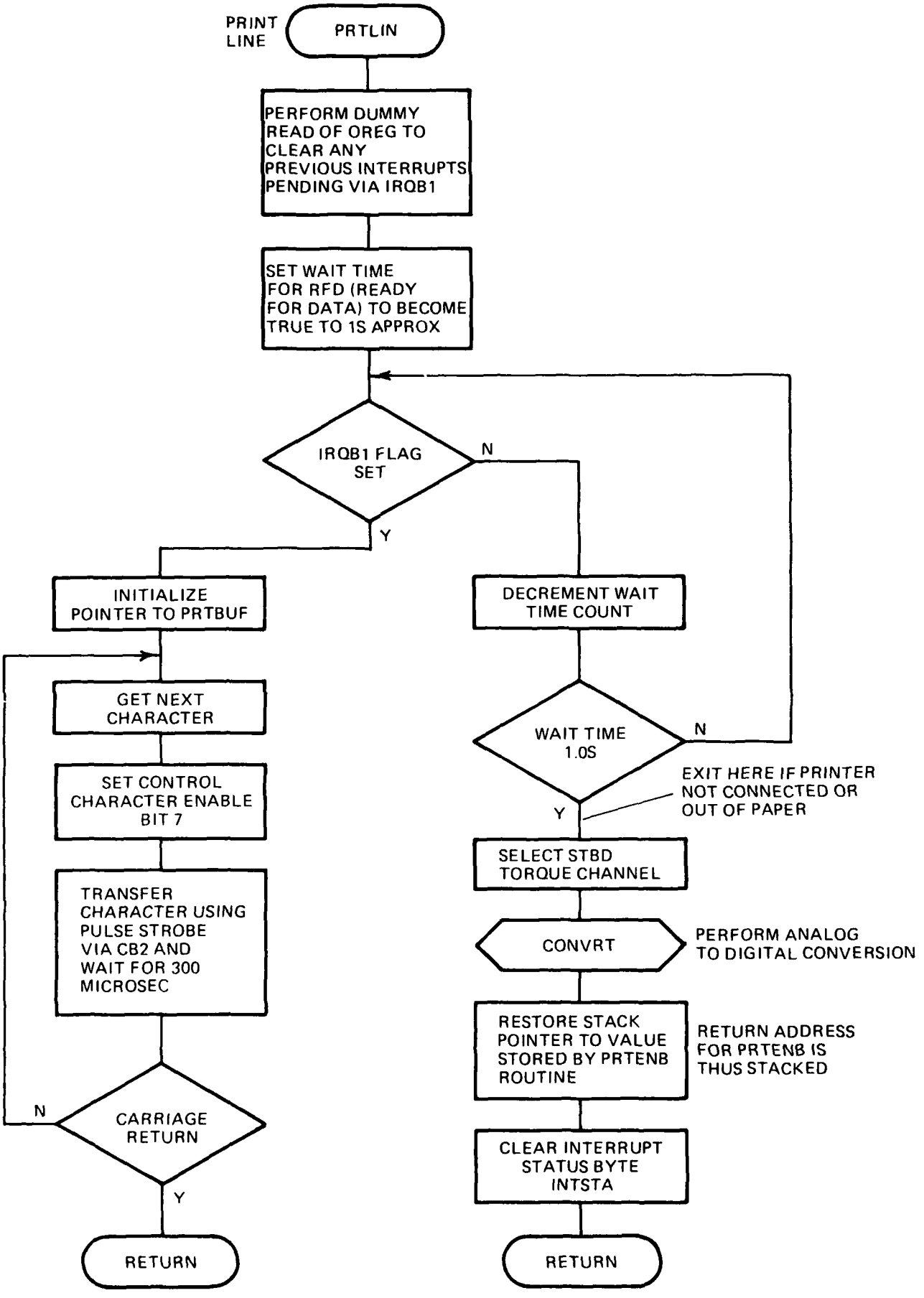

FIG 41 PRTLIN SUBROUTINE FLOW CHART

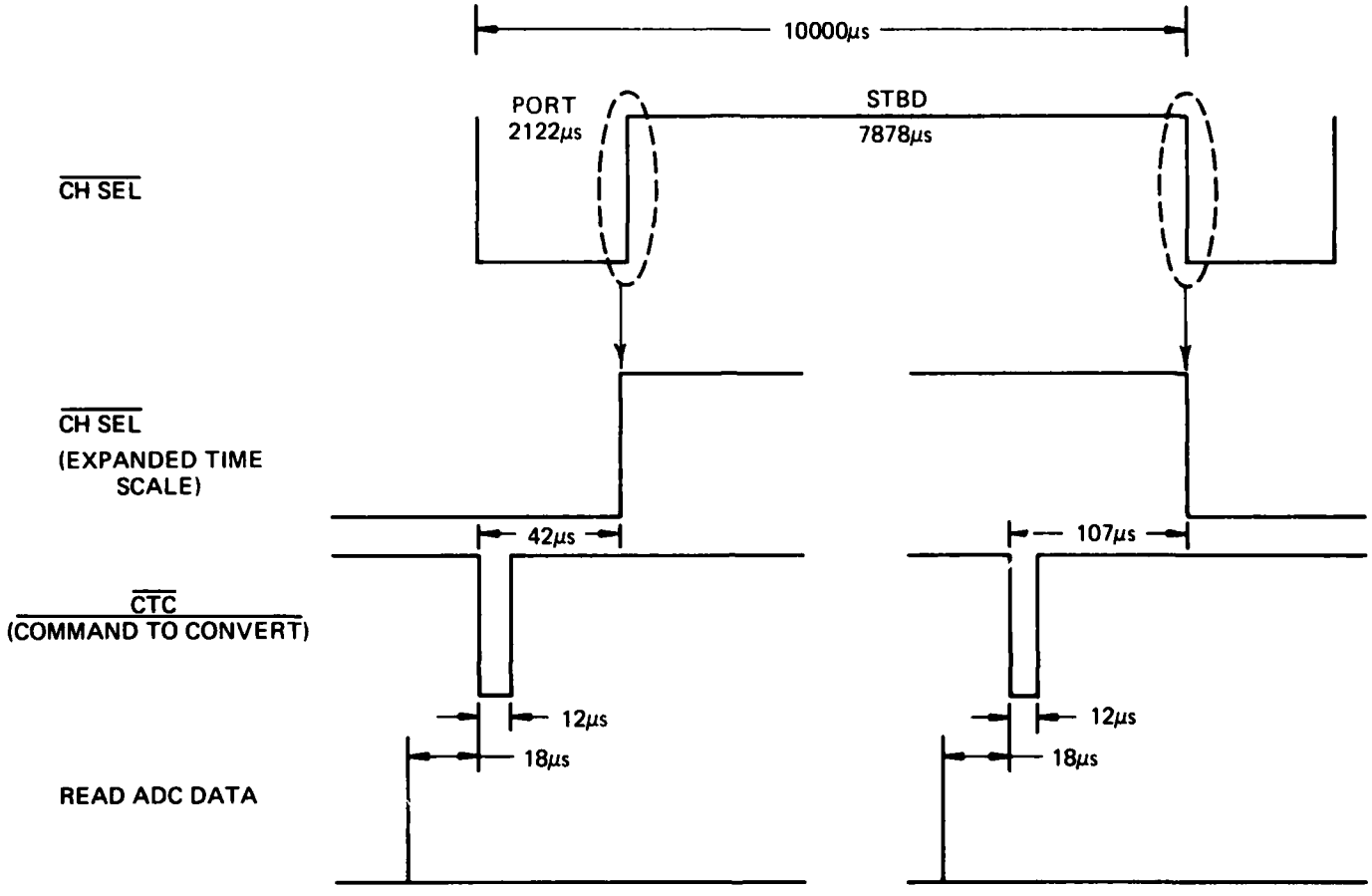

N.B. ALL THESE TIMES ARE SET BY THE SOFTWARE

FIG. 42 INPUT DATA TIMING

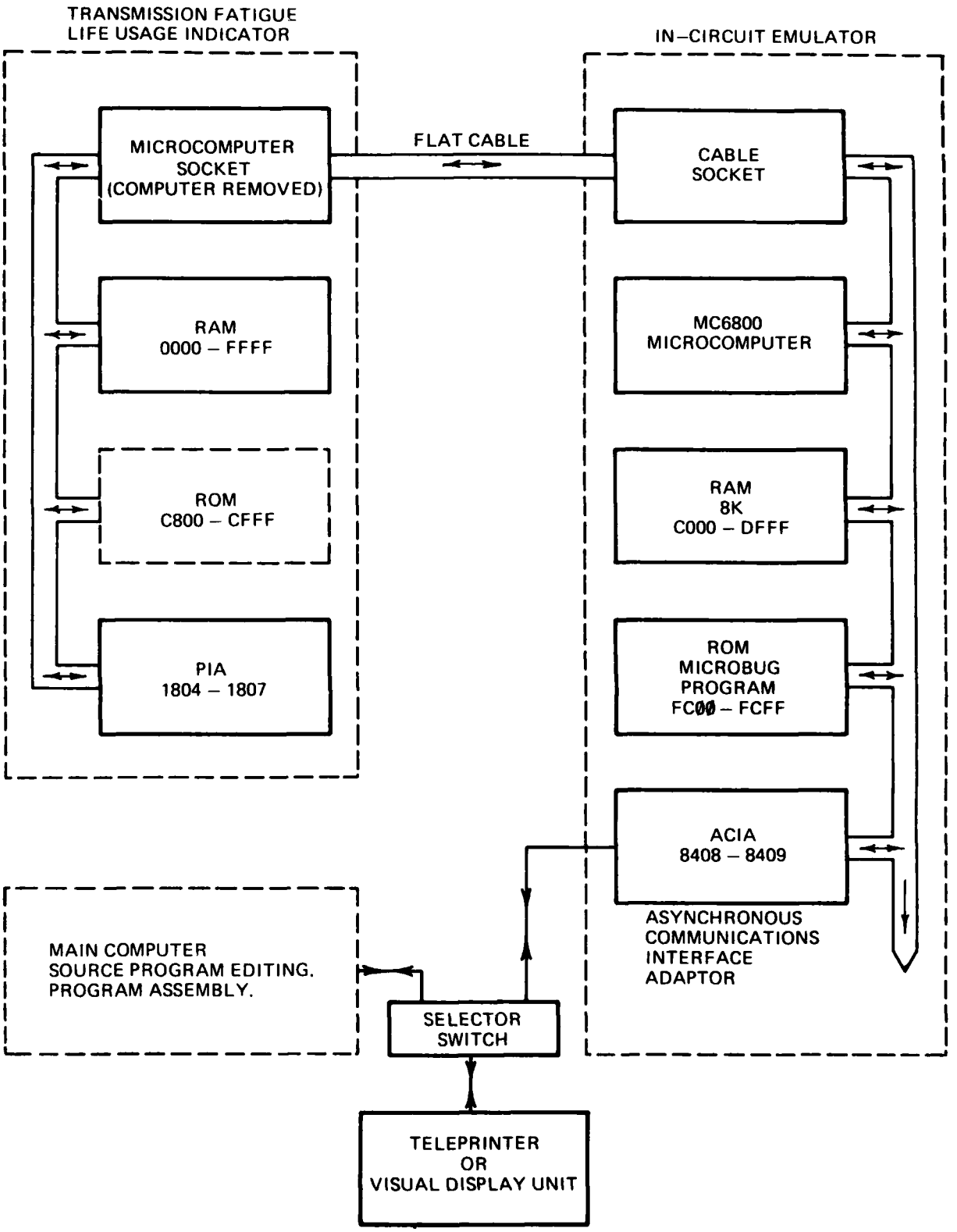

FIG. 43 SYSTEM PROGRAM TEST CONFIGURATION

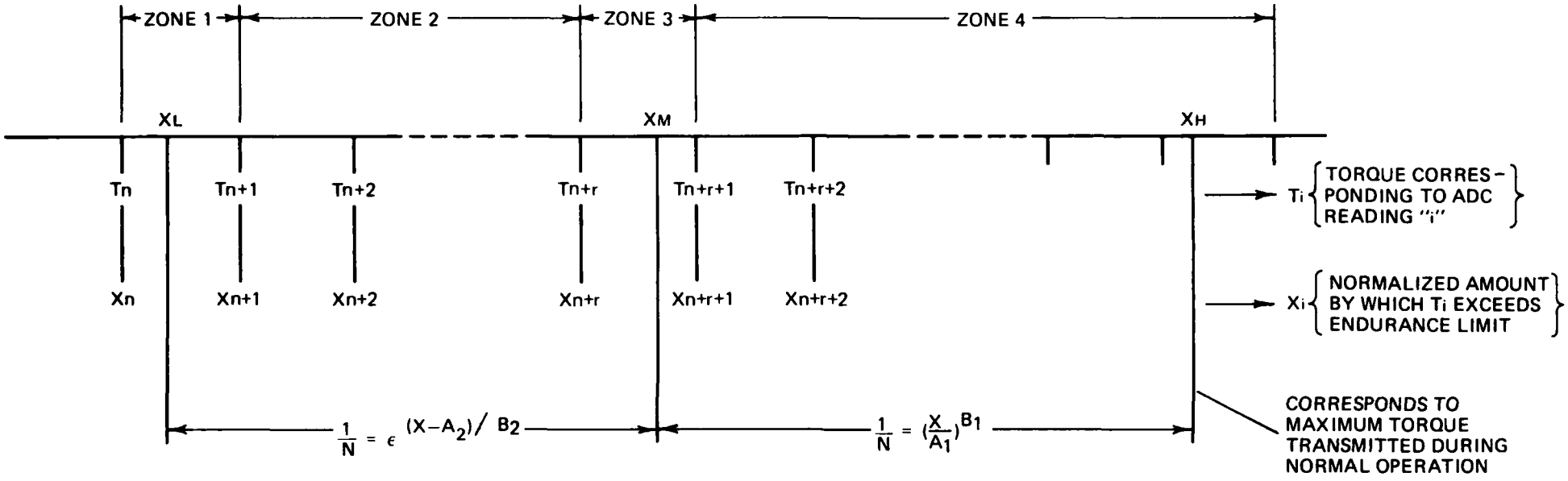

FIG. 44 GRAPHICAL REPRESENTATION OF FINITE RESOLUTION TORQUE MEASUREMENT

ADDENDUM

Contents of: ARL Mechanical Engineering Technical Memorandum 406, November 1980, U. R. Krieser.

TRANSMISSION FATIGUE LIFE USAGE INDICATING SYSTEM DETAIL

DISTRIBUTION

AUSTRALIA

DEPARTMENT OF DEFENCE

Central Office

Chief Defence Scientist
Deputy Chief Defence Scientist
Superintendent, Science and Technology Programmes
Controller, Projects and Analytical Studies Division
} (1 copy)

Defence Science Representative (U.K.) (Doc. Data only)
Counsellor, Defence Science (U.S.A.) (Doc. Data only)
Defence Central Library
Document Exchange Centre, D.I.S.B. (18 copies)
Joint Intelligence Organisation
Librarian, H Block, Victoria Barracks, Melbourne
Director General Army Development (NSO) (4 copies)
Defence Industry & Materiel Policy, FAS

Aeronautical Research Laboratories

Director
Library
Superintendent Aero Propulsion
Divisional File—Aero Propulsion
Author: K. F. Fraser (2 copies)
C. N. King
U. R. Krieser (6 copies)
K. W. Vaughan

Materials Research Laboratories

Director/Library

Defence Research Centre

Library

Navy Office

Navy Scientific Adviser
RAN Aircraft Maintenance and Flight Trials Unit
Directorate of Naval Aircraft Engineering (2 copies)
Directorate of Naval Aviation Policy
Superintendent, Aircraft Maintenance and Repair
Directorate of Naval Ship Design
AEO 817 Squadron NAS Nowra

Army Office

Army Scientific Adviser
Engineering Development Establishment, Library
Royal Military College Library
U.S. Army Research, Development and Standardisation Group

Air Force Office

Air Force Scientific Adviser
Aircraft Research & Development Unit
  Scientific Flight Group
  Library
Technical Division Library
Director General Aircraft Engineering—Air Force
Director General Operational Requirements—Air Force
HQ Operational Command (SMAINTSO)
HQ Support Command (SLENGO)
RAAF Academy, Point Cook

Central Studies Establishment

Information Centre

DEPARTMENT OF DEFENCE SUPPORT

Government Aircraft Factories

Manager
Library
Patents and Licensing Section, Mr R. Hammond (4 copies)

DEPARTMENT OF AVIATION

Library
Flying Operations and Airworthiness Division

STATUTORY & STATE AUTHORITIES AND INDUSTRY

Trans-Australia Airlines, Library
Qantas Airways Limited
Gas & Fuel Corporation of Victoria, Manager Scientific Services
SEC of Vic., Herman Research Laboratory, Library
Ansett Airlines of Australia, Library
Australian Coal Industry Research Labs Ltd., Director
B.H.P., Melbourne Research Laboratories
B.P. Australia Ltd., Library
Commonwealth Aircraft Corporation, Library
Hawker de Havilland Aust. Pty. Ltd., Bankstown, Library
Australian Institute of Petroleum Ltd.
Rolls-Royce of Australia Pty. Ltd., Mr C. G. A. Bailey

UNIVERSITIES & COLLEGES

Adelaide	Barr Smith Library
	Professor of Mechanical Engineering
Flinders	Library
Latrobe	Library

Melbourne	Engineering Library
Monash	Hargrave Library
Newcastle	Library
Sydney	Engineering Library
N.S.W.	Physical Sciences Library
	Professor R. A. A. Bryant, Mechanical Engineering
	Professor G. D. Sergeant, Fuel Technology
Queensland	Library
Tasmania	Library
Western Australia	Library
	Associate Professor J. A. Cole, Mechanical Engineering
R.M.I.T.	Library
	Dr H. Kowalski, Mech. & Production Engineering

CANADA

International Civil Aviation Organization, Library

NRC

Aeronautical & Mechanical Engineering Library
Division of Mechanical Engineering, Director
Gas Dynamics Laboratory, Mr R. A. Tyler

FRANCE

ONERA, Library

GERMANY

Fachinformationszentrum: Energie, Physic, Mathematik GMBH

INDIA

Defence Ministry, Aero Development Establishment, Library
Gas Turbine Research Establishment, Director
Hindustan Aeronautics Ltd., Library
National Aeronautical Laboratory, Information Centre

ISRAEL

Technion-Israel Institute of Technology
Professor J. Singer

ITALY

Professor Ing. Guiseppe Gabrielli

JAPAN

Institute of Space and Astronautical Science, Library

Universities

Kagawa University Professor H. Ishikawa

NETHERLANDS

National Aerospace Laboratory (NLR), Library

NEW ZEALAND

Defence Scientific Establishment, Library
RNZAF, Vice Consul (Defence Liaison)

Universities

Canterbury	Library
	Professor D. Stevenson, Mechanical Eng.
	Mr J. Stott, Chemical Engineering

SWEDEN

Aeronautical Research Institute, Library
Swedish National Defense Research Institute (FOA)

SWITZERLAND

Armament Technology and Procurement Group
F+W (Swiss Federal Aircraft Factory)

UNITED KINGDOM

CAARC, Secretary
Royal Aircraft Establishment
  Bedford, Library
Commonwealth Air Transport Council Secretariat
Admiralty Marine Technology Establishment
  St. Leonard's Hill, Superintendent
National Gas Turbine Establishment
  Director, Pyestock North
National Physical Laboratory, Library
National Engineering Laboratory, Library
British Library, Lending Division
CAARC Co-ordinator, Structures
Aircraft Research Association, Library
British Ship Research Association
National Maritime Institute, Library
Electrical Power Engineering Co. Ltd.
GEC Gas Turbines Ltd., Managing Director
Fulmer Research Institute Ltd., Research Director
Motor Industry Research Association, Director
Ricardo & Co. Engineers (1927) Ltd., Manager
Rolls-Royce Ltd.
  Aero Division Bristol, Library
British Aerospace
  Kingston-upon-Thames, Library
  Hatfield-Chester Division, Library
British Hovercraft Corporation Ltd., Library
Short Brothers Ltd., Technical Library
Westland Helicopters Ltd., Yeovil, Managing Director

Universities and Colleges

Bristol	Engineering Library
Cambridge	Library, Engineering Department
	Whittle Library
London	Professor G. J. Hancock, Aero Engineering
Manchester	Professor, Applied Mathematics
	Professor N. Johannesen, Fluid Mechanics
Nottingham	Science Library
Southampton	Library
Liverpool	Fluid Mechanics Division, Dr J. C. Gibbings
Strathclyde	Library
Cranfield Institute of Technology	Library
Imperial College	Aeronautics Library

UNITED STATES OF AMERICA

NASA Scientific and Technical Information Facility
Applied Mechanics Reviews
The John Crerar Library
Allis Chalmers Corporation, Library
Boeing Company
Mr J. C. McMillan
Kentex Research Library
United Technologies Corporation, Library
Lockheed-California Company
Lockheed Missiles and Space Company
Lockheed Georgia
McDonnell Aircraft Company, Library

Universities and Colleges

Johns Hopkins	Professor S. Corrsin, Engineering
Iowa State	Dr G. K. Serovy, Mechanical Eng.
Princeton	Professor G. L. Mellor, Mechanics
Massachusetts Institute of Tech.	M.I.T. Libraries

SPARES (10 copies)

TOTAL (172 copies)

Department of Defence

DOCUMENT CONTROL DATA

1. a. AR No.	1. b. Establishment No.	2. Document Date	3. Task No.
AR-003-013	ARL-AERO-PROP-R-164	March, 1984	NAV 80/152

4. Title	5. Security	6. No. Pages
THE IN-FLIGHT ESTIMATION AND INDICATION OF CUMULATIVE FATIGUE DAMAGE TO HELICOPTER GEARS	a. document: Unclassified b. title: U C c. abstract: U C	66 7. No. Refs: 20

8. Author(s)	9. Downgrading Instructions
K. F. Fraser	—

10. Corporate Author and Address	11. Authority (*as appropriate*)
Aeronautical Research Laboratories, P. O. Box 4331, MELBOURNE, Vic. 3001.	a. Sponsor b. Security: a) DNAE c. Downgrading d. Approval

12. Secondary Distribution (*of this document*

Approved for public release

Overseas enquirers outside stated limitations should be referred through ASDIS, Defence Information Services Branch, Department of Defence, Campbell Park, CANBERRA, ACT, 2601.

13. a. This document may be ANNOUNCED in catalogues and awareness services available to . . .

No limitations

13. b. Citation for other purposes (*i.e. casual announcement*) may be (*select*) unrestricted (*or*) as for 13 a.

14. Descriptors	15. COSATI Group
Fatigue life Gearboxes Gears Helicopters Transmissions (mechanical)	09010 01030 21050

16. Abstract

Estimates of the safe fatigue life of helicopter transmission components may be made if in-service load data together with transmission fatigue data, represented as the number of cycles to failure as a function of tooth load, are available. Instrumentation has been developed to provide in-flight estimation and indication of the proportion of safe fatigue life expended for critical gears in single or twin-engine helicopter transmission systems. In addition, basic transmission load data in the form of totalized times spent in a number of continuous torque bands are continually updated and stored during flight. The basic load data together with values of life expenditure for critical gears for the current flight can be automatically printed out after flight. This technique opens the way towards fatigue life monitoring of individual transmissions.

The special demands of the life estimating system are evaluated and in particular the very significant effects of errors in mean torque estimation are assessed.

This page is to be used to record information which is required by the Establishment for its own use but which will not be added to the DISTIS data base unless specifically requested.

16. Abstract (*Contd*)

17. Imprint

Aeronautical Research Laboratories, Melbourne.

18. Document Series and Number	19. Cost Code	20. Type of Report and Period Covered
Aero Propulsion Report 164	44 1875	

21. Computer Programs Used

22. Establishment File Ref(s)

M2/609

END

FILMED

4-85

DTIC